Geophysical Monitoring for Climatic Change

No. 7

Summary Report 1978

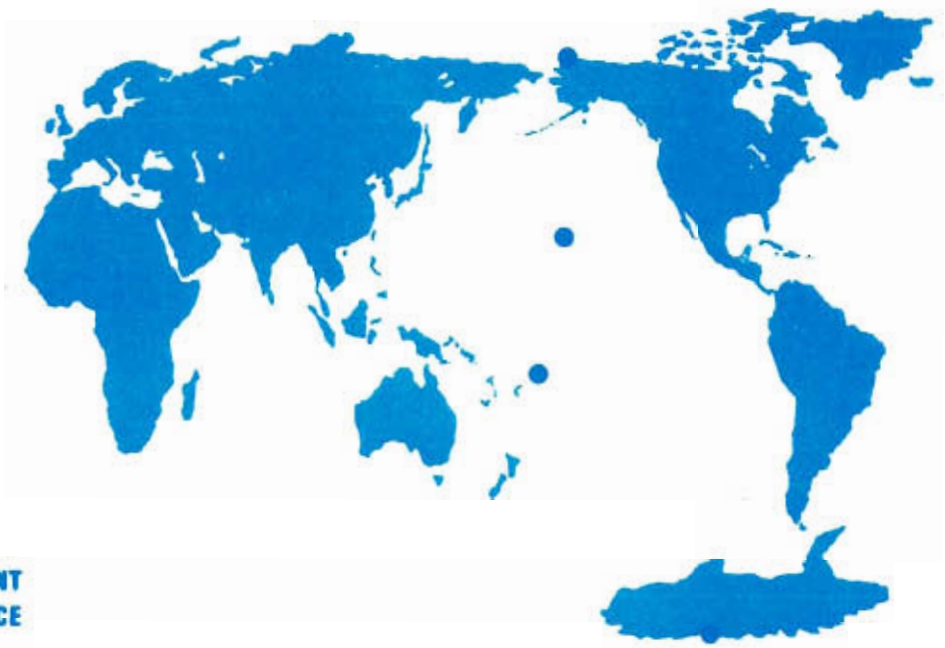

U.S. DEPARTMENT OF COMMERCE

NATIONAL OCEANIC AND ATMOSPHERIC ADMINISTRATION

ENVIRONMENTAL RESEARCH LABORATORIES

Geophysical Monitoring for Climatic Change No. 7

Summary Report 1978

Bernard G. Mendonca, Editor

December 1979

Boulder, Colorado

U.S. DEPARTMENT OF COMMERCE
Philip M. Klutznick, Secretary

National Oceanic and Atmospheric Administration
Richard A. Frank, Administrator

Environmental Research Laboratories
Wilmot Hess, Director

NOTICE

Mention of a commercial company or product does not constitute an endorsement by NOAA Environmental Research Laboratories. Use for publicity or advertising purposes of information from this publication concerning proprietary products or the tests of such products is not authorized.

CONTENTS

FOREWORD

In this seventh annual report the NOAA Geophysical Monitoring for Climatic Change (GMCC) program demonstrates that it is coming of age. In past years, this program has primarily collected data. Now that the data have accumulated, they can be analyzed, leading to valuable geophysical interpretations.

The NOAA program documented in these pages has captured world-wide attention and set a high standard for other countries to emulate. All can now recognize the benefits which these data and their analysis provide to understanding regional and global geophysical phenomena.

The success of NOAA's GMCC program is no accident. Aside from NOAA headquarters' unfailing support, the dedication of GMCC's personnel must take the greater part of the credit. In addition, NOAA is appreciative of the help of many non-GMCC scientists who have used its facilities and have guided several highly specialized programs.

The future of GMCC is promising. While the measurement programs will continue, indeed they will most likely expand, GMCC will increasingly use the data for the good of the country and mankind.

Lester Machta
Director, ARL

ACRONYMS AND ABBREVIATIONS

AL	Aeronomy Laboratory, Boulder, Colo. (NOAA)
APCL	Atmospheric Physics and Chemistry Laboratory, Boulder, Colo. (NOAA)
APO	Astrophysical Observatory, Smithsonian Institution, Washington, D.C.
ARL	Air Resources Laboratories, Washington, D.C. (NOAA)
ASRC	Atmospheric Sciences Research Center, SUNYA, Albany, N.Y.
BOSS	Basic Operating Software System
BRW	Barrow Observatory, Barrow, Alaska (GMCC)
CAF,CAQ	Clear Air Facility, Clean Air Quadrant, South Pole Observatory, Antarctica (GMCC)
CIRES	Cooperative Institute for Research on Environmental Science, Univ. of Colo., Boulder, Colo.
CNC	condensation nuclei counter
CSIRO	Commonwealth Scientific and Industrial Research Organization, Australia
DAS	Data Acquisition System
DOE	U.S. Department of Energy
ECC	electrochemical concentration cell
EML	Environmental Measurements Laboratory (DOE)
EPA	U.S. Environmental Protection Agency
ERL	Environmental Research Laboratories, Boulder, Colo. (NOAA)
GARP	Global Atmospheric Research Program
GATE	GARP Atlantic Tropical Experiment
GMCC	Geophysical Monitoring for Climatic Change (NOAA)
ICDAS	Instrument Controlled Data Acquisition System
MLO	Mauna Loa Observatory, Mauna Loa, Hawaii (GMCC)
MPI	Max-Planck Institute of Chemistry, Mainz, Germany
NARL	Naval Arctic Research Laboratory, Barrow, Alaska
NASA	National Aeronautics and Space Administration
NBS	National Bureau of Standards, U.S. Dept. of Commerce
NCAR	National Center for Atmospheric Research, Boulder, Colo.
NESS	National Environmental Satellite Service (NOAA)
NIP	normal incidence pyrheliometer
NOAA	National Oceanic and Atmospheric Administration, U.S. Dept. of Commerce
NSF	National Science Foundation, Washington, D.C.
NWS	National Weather Service (NOAA)
OGC	Oregon Graduate Center, Beaverton, Ore.
SMO	Samoa Observatory, American Samoa (GMCC)
SPO	South Pole Observatory, Antarctica (GMCC)
SRBL	Smithsonian Institution Radiation Biology Laboratory
STP	standard temperature and pressure
SUNYA	State University of New York at Albany, N.Y.
UNEP	United Nations Environmental Program, Nairobi, Kenya
URI	University of Rhode Island, Kingston, R.I.
USDA	U. S. Department of Agriculture
UV	ultraviolet
WMO	World Meteorological Organization, Geneva, Switzerland

GEOPHYSICAL MONITORING FOR CLIMATIC CHANGE

NO. 7

Summary Report - 1978

1. SUMMARY

1.1 Observatory Facilities

Minimal facility additions and modifications were made during 1978. At Samoa the Oregon Graduate Center set up a prefabricated building adjacent to the GMCC remote sampling tower on Lauagae Ridge to begin measuring fluorocarbons. Also at Samoa the GMCC emergency electrical power generator was replaced. At Barrow a 2.5-m x 2.5-m wanagan was added to the GMCC Observatory facilities in anticipation of initiating a lidar measurement program there. Six hundred cubic yards of gravel were added to the observatory road to help ensure access during all weather conditions. Although the South Pole new Clean Air Facility monitoring program was generally troublefree, modifications to the observatory power feed transformers were necessary to handle the electrical power draw when all systems were operated.

1.2 Ongoing Programs

Continuous CO_2 measurements at the South Pole were temporarily suspended during 1978. Continuous measurements at the other observatories were uninterrupted, and data processing was completed for the entire record. Monthly averages of CO_2 concentrations for Mauna Loa and Barrow are included in this report. The first CO_2-in-air calibration gases were run at Barrow and Mauna Loa. Eventually all calibration gases will be converted from CO_2-in-N_2 to CO_2-in-air. Companion CO_2 flask sampling at all the observatories was completed, and the data are included in this report.

Dobson ozone spectrophotometers at six U.S. continental stations were inspected, calibrated and refurbished in 1978. In cooperation with the World Meteorological Organization participation in the upgrading and calibration of Dobson ozone spectrophotometers continued in 1978. Dobson modifications and calibrations for four foreign countries were completed. Monthly total ozone data obtained from daily data in the GMCC Dobson network were edited and are included in this report.

Surface ozone measurements continued at the observatories. An analysis of diurnal, day-to-day, seasonal, and station-to-station ozone variations was completed and is included in this report. A stratospheric water vapor measurement program, initiated in 1978, will become an ongoing program for the GMCC. An indepth analysis of halocarbon and nitrous oxide data collected at the GMCC observatories was completed in 1978. Hemispheric concentrations, gradients, and lifetimes are given herein.

At all the GMCC observatories surface aerosol measurements of small particle concentrations and light scattering characteristics were continued. Enough data

have now been collected to begin to investigate secular trends and confirm seasonal variations. Solar radiation measurements at Barrow and Samoa were used to identify seasonal variability in atmospheric transmission.

Precipitation chemistry measurements continued at the observatories, and an analytical laboratory was established at Mauna Loa Observatory in Hilo to analyze samples from Hawaii, Barrow, and Samoa. Data showing the spatial and time variation of ph values are shown.

The reliability of the Instrumentation Control and Data Acquisition Systems (ICDAS) at the observatories improved during 1978. Noise levels in the ICDAS were reduced to improve the quality of the data collected.

1.3 Research Programs

GMCC personnel conducted several special research studies in 1978. A remote sensing technique to measure vertical ozone profiles by incorporating more Dobson wavelengths in the measurements was refined and evaluated against the older Umkehr method. An evaluation of the Robinson-Berger erythema meter measurements showed differences from the true erythemal spectrum obtained from measurements made with a double monochromater. More analysis will be done to determine the cause and significance of the differences.

A study of vertical ozone profile measurements when volcanic eruptions eject effluent into the stratosphere showed that significant errors result in the measurements. A procedure to correct the ozone profiles for perturbations in stratospheric aerosol concentrations is described herein. Variations in the isotopes of atmospheric carbon from the addition of limestone CO_2 into the atmosphere was studied. An increase in carbon-13 amounts from the addition of limestone CO_2 to the atmosphere could be significant and should be taken into account in carbon-13 to carbon-12 ratio studies determining the effects of burning fossil fuel on the total atmospheric CO_2 budget.

Two solar irradiance studies that measure urban effects on incoming radiant energy were completed. In cooperation with the U.S. Department of Energy, measurements taken in the metropolitan St. Louis area were analyzed and showed a decrease of up to 3% in solar irradiance as compared to adjacent unpolluted areas. Measurements in Voeikovo and Leningrad, U.S.S.R., were taken to assess anthropogenic effects on incoming solar energy and to compare U.S. and U.S.S.R. turbidity instruments. GMCC personnel evaluated measurements at several sites on Mt. Kenya, Africa, for the Mt. Kenya Feasibility Study. The Feasibility Study was undertaken to determine the suitability of the area for potential baseline measurement locations. The GMCC evaluation noted that background conditions may occur on Mt. Kenya and recommended that more detailed analyses of the meteorological regimes that influence CO_2 and aerosol concentrations be undertaken.

Atmospheric transmission data at Mauna Loa continued to show perturbations from explosive volcanic eruptions, the latest being Soufriere. The monthly transmission values for the 20-yr record are included in this report. Several solar-terrestrial studies were carried out to determine whether variations in the solar constant could be detected from past solar data.

1.4 Cooperative Programs

In 1978 GMCC support for cooperative programs at the observatories doubled. Twenty-seven summary reports from cooperative programs are given in this report. Investigations of aerosol chemistry at Barrow and the South Pole were the major efforts of the cooperative programs for 1978. Programs in precipitation chemistry and trace gases were also expanded through cooperative efforts. GMCC measurement programs together with university and other federal agency cooperative programs provided a multidisciplined effort in describing the trace levels of atmospheric pollutants at the GMCC observatories in 1978.

2. OBSERVATORY REPORTS

2.1 Mauna Loa

2.1.1 Facilities

The following modifications of the MLO facilities were carried out in 1978:

(1) Two strip chart recorders were acquired; a Leeds and Northrup multipoint recorder replaced an antiquated Brown recorder to record pyrheliometric data and a new dual-channel Honeywell recorder was added for use in precipitation chemistry studies.

(2) A new, improved solar tracker was purchased and installed, and the pyrheliometer and infrared hygrometer were transferred to it.

(3) Although two different pyranometer shading rings were fabricated and tested, problems with them forced acquisition of an Eppley shading disc. The disc and its Sun-following mount were used in measuring diffuse radiation.

(4) A 13-channel pyrheliometer was refurbished and put into use for measuring direct radiation.

(5) Condensation nuclei counts with the Gardner counter were discontinued, and the instrument was shipped to the mainland.

(6) Lidar system optics were changed to improve system reliability. The efforts were partially successful.

(7) The thermoscreen and precipitation collectors at Kulani Mauka were moved about 300 m northwest to avoid interference from a new telephone building.

(8) Six rainwater collection devices were installed in the volcano area for a short time as part of the Harding precipitation chemistry study.

(9) The Applied Physics carbon dioxide analyzer was modified to try to improve its stability and performance. The main modifications were as follows:

a. Replacement of vacuum tubes in the amplifier.

b. Replacement of the thermal control unit in the analyzer.

c. Replacement of the photodiode and transistor circuit in the contact and phasing adjustment assembly.

d. Replacement of strip chart recorder.

e. Replacement of alcohol bath in freezing unit and installation of a double freeze-trap arrangement.

f. Replacement of air sampling pumps.

g. General rework of electrical circuits.

h. Installation of thermal insulation for better temperature control of the device.

2.1.2 Programs

Table 1 lists the programs carried out at MLO during 1978. Brief status reports of the principal programs follow:

Carbon Dioxide

Both the AP and URAS carbon dioxide analyzers operated without significant interruptions throughout the year. Identifiable signatures in the data produced by outgassing from the volcanic caldera at the summit of Mauna Loa were detected in the CO_2 measurements. They occurred mainly between midnight and 8 a.m. local time during a downslope wind flow regime on the mountain. The frequency of occurrence of the anomalous conditions is shown for the different months of 1978 in the following tabulation:

	J	F	M	A	M	J	J	A	S	O	N	D
No. of days	9	5	4	11	6	11	13	13	10	18	8	8
Percent occurrence	29%	18%	13%	37%	19%	37%	42%	42%	33%	58%	27%	26%

Atmospheric Ozone

Total ozone in an atmospheric column was measured by the Dobson spectrophotometer on approximately 260 days of 1978, and the ozone concentration in air near the surface was measured continuously with Dasibi and EEC ozone meters. All three measurement programs operated satisfactorily, although a few problems were encountered in maintaining the chemical solution in the EEC meter.

Sulfur Dioxide

The SO_2 meter operated well after installation in January 1978, although some data were lost because of strip chart recorder problems. The SO_2 data show the episodes of fuming from the Mauna Loa volcano.

Carbon Monoxide

Except for short periods in early January and November, the carbon monoxide measurements continued throughout the year. The record continued to show interesting variations that appear to be related to the changing of air mass types over the Pacific area.

Atmospheric Aerosols

The aerosol measurement program operated successfully throughout 1978. After minor repairs at the University of Washington, the nephelometer was reinstalled in late January and gave reliable measurements during the rest of the year. Faulty lamps forced termination of Aitken nuclei measurements by the Gardner counter, but equivalent data were obtained on a routine basis with the Pollak counter. The least reliable instrument in the aerosol program, the G.E. counter, required realignment and voltage adjustments but provided adequate continuous measurements of nuclei concentration.

Table 1.--Summary of monitoring programs at MLO in 1978

Program	Instrument	Sampling frequency	Remarks
Gases			
Carbon dioxide	URAS-2 infrared gas analyzer	Continuous	
	Evacuated glass flasks	Weekly	Mountain and seacoast
	Evacuated flasks	Weekly	For Okayama Univ., Japan
Surface ozone	Electrochemical concentration cell	Continuous	
	Dasibi ozone meter	Continuous	
Total ozone	Dobson spectrophotometer	Discrete	3 meas. weekdays; 0 weekends
Fluorocarbons	Pressurized flasks	Weekly	
Aerosols			
Stratospheric aerosols	Lidar	Weekly	694.3 nm, 1 J
Condensation nuclei	Pollak CN counter	Discrete	5 meas. weekdays; 0 weekends
	G.E. CN counter	Continuous	
Optical properties	4-wavelength nephelometer	Continuous	Wavelengths 450, 550, 700, 850 nm
Solar radiation			
Global irradiance	4 Eppley pyranometers	Continuous	Cutoff filters at 280, 390, 530, 695 nm
Ultraviolet irradiance	Eppley ultraviolet pyranometer	Continuous	Wavelength range 295 to 385 nm
Direct beam irradiance	Eppley pyrheliometer	Continuous	Wavelength range 280 to 3000 nm
	Eppley pyrheliometer with filters	Discrete	Cutoff filters at 280, 530, 630, 695 nm
	Eppley 13-channel pyheliometer	Intermittent	
Meteorology			
Maximum temperature	Maximum thermometer	Daily	
Minimum temperature	Minimum thermometer	Daily	
Ambient temperature	Thermistor	Continuous	Combined with dew point hygrometer
	Hygrothermograph	Continuous	At MLO and Kulani Mauka
Dewpoint temperature	Dewpoint hygrometer	Continuous	
Relative humidity	Hygrothermograph	Continuous	At MLO and Kulani Mauka
Total precipitable water	Faskett infrared hygrometer	Continuous	
Pressure	Electronic pressure transducer	Continuous	
	Microbarograph	Continuous	Checked with mercurial barometer
Precipitation	Rain gauge, 8 ft	Weekly	At MLO and Kulani Mauka
	Rain gauge, tipping bucket	Continuous	
Wind speed	Anemometer	Continuous	
Wind direction	Wind vane	Continuous	
Precipitation chemistry			
Acidity of rainwater	pH meter	Discrete	Rainwater collect. at 6 sites
Conductivity of water	Conductivity bridge	Discrete	
Chemical components	Ion chromatograph	Discrete	
Cooperative programs			
Carbon dioxide (Scripps Inst.)	Infrared analyzer (Applied Physics)	Continuous	
	Evacuated flasks	2 mo^{-1}	Mountain and seacoast
Carbon monoxide (Max Planck Inst.)	Special	Continuous	Chemical reaction with HgO
Total nitrogen dioxide (Aeronomy Lab/NOAA)	Spectrometer	Continuous	
Surface SO_2 (EPA)	Chemical bubbler system	1 every 12 days	
Total surface particulates (DOE)	High-volume filter	Continuous	Dependent on wind direction
Total surface particulates (EPA)	High-volume filter	1 every 12 days	
Atmospheric electricity (APCL/NOAA)	Field mill, air conductivity meter, surface antenna	Continuous	
Stratospheric aerosols (AFGL)	Twilight photometer	Continuous	
Ultraviolet radiation (Temple Univ.)	Ultraviolet radiometer	Continuous	Radiation responsible for sunburning of skin
Precipitation collection (DOE)	Wet-dry Health & Safety Lab collector	Continuous	
Precipitation collection (EPA)	Misco model 93	Continuous	
Precipitation collection (Univ. of Paris)	Likens funnel collector	2 wk^{-1}	
Precipitation collection (IAEA, Vienna, Austria)	Likens funnel collector	2 wk^{-1}	
Cloud water collection (SUNYA)	Cloud and fog collector	Continuous	

Lidar

Some equipment failures occurred during 1978 in the MLO lidar program. Measurements were made on a weekly schedule, but electronic malfunctions prevented complete measurements on some occasions. Optical components, flash lamps, and the cooling system were replaced to improve the measurements.

Solar Radiation

The solar radiation program was relatively troublefree, and many reliable data were obtained. The acquisition of a new equatorial mount and a new shading disc improved the overall quality of the data, and calibration checks reaffirmed the basic stability of instrument responses. Efforts to use the 13-channel pyrheliometer were initiated late in the year.

Meteorological Parameters

Temperature, pressure, wind, and other meteorological parameters were measured routinely with few problems. The dew cell installed for dew point measurements was inoperable for the entire year, but humidity data were obtained by using the hygrothermograph records.

Precipitation Chemistry

Precipitation samples from Barrow, Samoa, South Pole, and several sites in Hawaii were routinely analyzed. Vandalism at collection sites continued, and the unavailability of ultraclean water caused some interruptions in the analyses.

A special study of precipitation in the vicinity of the Kilauea Volcano was carried out by D. Harding. This program was quite successful; the details are discussed in section 3.11 of this report.

Fluorocarbons (Halocarbons)

This discrete sampling program continued without difficulty in 1978. Weekly air samples were taken at the observatory and shipped to Boulder for analysis.

Cooperative Programs

The observatory cooperated with several agencies and organizations in measuring environmental parameters during 1978. The main studies are the following:

a. Measurements of sulfur dioxide - EPA. Changes in the operational procedures during 1978 included lengthening the sampling duration from 6 to 12 days, shifting the cognizant laboratory from the mainland to Honolulu, and instituting quarterly calibration and maintenance visits by EPA personnel.

b. Collections of atmospheric particulates - EPA. High-volume samplers were run continuously to collect total particulates. The only modification in 1978 was the provision of a backup sampler unit.

c. Precipitation chemistry - EPA. Monthly precipitation samples were routinely sent to the EPA laboratory in North Carolina. The small quantity of water available for the samples was a problem; a different type of collector unit could eventually solve this.

d. Precipitation chemistry - DOE. The automatic collector used in this program separates wet from dry fallout, and samples are sent monthly to the central laboratory. A second part of this project is to intercompare the DOE monthly collections and MLO's shorter term collections to assess the effects of time lags in the analysis. No particular problems were encountered.

e. Collection of atmospheric particulates - DOE. This project uses two high-volume samplers, one operated at night and the other during the day to distinguish the particulate loading of upslope versus downslope wind flows. No problems were encountered during the year. An interesting result of the measurements is that the "down-slope" filters sometimes appeared darker than the "upslope" filters since fuming from the Mauna Loa summit has become evident.

ICDAS Computer Operation

The MLO computer experienced some hardware difficulties in 1978; however, the actual data loss was kept to a minimum. Malfunctions of connectors, switches, and sockets in the tape unit and Chronolog clock resulted in intermittent computer failures from January through May. The tape unit connectors were replaced, and a new, improved clock was received and installed. A noise problem manifested by drifts of the zero offset and 5-V reference was traced to the multiplexer cabinet and improved by strapping the system units together and eliminating some spare cables. The multiplexer was believed to be out of alignment, and a replacement was received in June. A bad address register board and a failure in the computer CPU board required repairs in June. Some drifting of the zero offset and 5-V reference was experienced during the latter half of 1978, but several grounding straps, line filters, and a replacement 5-V reference card improved the situation in October.

2.2 Barrow

2.2.1 Facilities

A standard 8 ft x 8 ft wanagan from NARL was added to the GMCC Barrow Observatory's facilities during 1978. Work was begun to convert the wanagan into a lidar observatory. Since some lidar observations were to be made after normal working hours during part of the year, it was decided to locate the observatory within the NARL camp area, in walking distance of the GMCC staff's housing.

Six hundred cubic yards of gravel were added to the most needy sections of the observatory's access road. Additional gravel and clay will be required as a binder during summer 1979 to stabilize the road's surface. This work should significantly improve the road's surface and extend its life.

2.2.2 Programs

1978 sampling programs for the BRW Observatory are summarized in table 2.

In September, T. Harris visited the BRW Observatory to exchange the station's UNOR CO_2 analyser with a URAS-2T analyser and to intercompare both analysers by using GMCC's CO_2-in-air reference tanks. Beginning in August, as an additional check on the CO_2 sampling system, hand-aspirated CO_2 flasks were exposed on alternate weeks as opposed to the pressurized flask pairs, which are exposed at the analyser.

Table 2.--Summary of sampling programs at Barrow during 1978

Monitoring programs	Instrument	Sampling frequency	Data record
Gases			
Carbon dioxide	UNOR infrared analyzer	Continuous	Mar 73-Sep 78
	URAS-2T infrared analyzer	Continuous	Sep 78-present
	Glass flask pairs	1 pair wk^{-1}	Apr 71-present
Surface ozone	Electrochemical concentration cell (ECC)	Continuous	Mar 73-present
	Dasibi ozone meter	Continuous	Jul 75-present
Halocarbons	Flask samples	1 pair wk^{-1}	Sep 73-present
Total ozone	Dobson spectrophotometer	Discrete	Aug 73-present
Aerosols			
Condensation nuclei	G.E. CN counter	Continuous	May 73-Nov 74 Apr 76-present
	Pollak CN counter	Discrete	Jul 73-present
Optical properties	4-wavelength nephelometer	Continuous	Apr 76-present
Solar radiation			
Global spectral irradiance	4 Eppley pyranometers with Q1, GG22, OG1, & RG8 filters	Continuous	Jun 74-present
	Eppley UV radiometer	Continuous	Jun 74-present
Direct spectral irradiance	Eppley normal incidence pyrheliometer with filter wheel	Discrete	Apr-77-present
Turbidity	Eppley sunphotometer	Discrete	Apr 78-present
Meteorology			
Air temperature	Thermistor	Continuous	Nov 75-present
	Hygrothermograph	Continuous	Feb 73- ? Nov 77-present
Relative humidity	Dew point hygrometer	Continuous	? - ? Nov 78-present
	Hygrothermograph	Continuous	Feb 73- ? Sep 78-present
Air pressure	Transducer	Continuous	Nov 75-present
	Microbarograph	Continuous	Feb 73-present
	Mercurial barometer	Discrete	May 74-present
Wind speed & direction	Bendix Aerovane	Continuous	Feb 73-present
Ground temperature	Thermistor	Continuous	Nov 75-present
Precipitation chemistry			
pH and conductivity	Wide-mouth polyethylene collector (samples analyzed at MLO)	Discrete	Sep 77-present
	Collection of snow on tundra at old east precip. sampling site (samples analyzed at MLO)	2 times mo^{-1}	? - ? Oct 78-present
Cooperative programs			
Total surface particulates (DOE/ELM)	High-volume sampler	Continuous	Aug 75-present
Arctic haze particulates (URI)	High-volume sampler	Continuous	Sep 76-present
Global radiation (SRBL)	Eppley pyranometers	Continuous	Apr 73-present
	Scanning UV radiometer	Continuous	May 75-present
	Temple Univ. sunburning meter	Continuous	Sep 78-present
NO_2 (Aeronomy Lab/NOAA)	NO_2 spectrometer	Discrete	Aug 75-Feb 77
CO_2 sampling (SIO)	Evacuated flask	2 sets mo^{-1}	Jan 74-present
Icc nuclei sampling (Univ. of Alaska)	Low-volume sampler, membrane filters	1 set day^{-1}	Sep 78-present
Soil Conservation Service's precipitation gauge (USDA)	Wyoming shielded precipitation gauge	2 times mo^{-1}	Mar 78-present

In November BRW's surface O_3 equipment, ECC #005-06, Dasibi #1323, and MacMillan 1000 ozone generator #313 were compared against GMCC's standard Dasibi.

Beginning in April, turbidity observations were resumed. These data will be used in the study of the Arctic haze phenomenon.

In May the air temperature thermistor was moved from the instrument shelter, placed in an aspirated shield, and installed on the meteorological tower approximately 2.5 m above the tundra. In July, the ground temperature thermistor was moved from near the tower (depth 5 cm) to approximately 18 m east of the tower (depth 30 cm). The observatory's mercurial barometer was returned to Boulder for a replacement after a second yearly calibration by NWS indicated an unacceptable drift in the barometer's calibration. After extensive repairs and modifications the dew point hygrometer was made to operate on the data acquisition system (DAS) and since November has been taking good data.

Because of renewed interest in the chemistry of the Barrow area precipitation, it was decided to start taking precipitation samples off the tundra surface twice a month to supplement the falling precipitation collection started in 1977. The old precipitation chemistry station approximately 50 m east of the observatory was selected as the sampling site.

A Temple University sunburning UV meter was added to SRBL's cooperative program in September. A new cooperative program with the University of Alaska's Geophysical Institute to sample ice nuclei was started in June. Ice nuclei filters were also exposed for a 2-wk period in April and May for the URI. Beginning in March BRW personnel took over the servicing of the USDA Soil Conservation Service's Wyoming shielded precipitation gauge.

2.3 Samoa

2.3.1 Facilities

No major GMCC-originated scientific facilities were added during 1978. An addition was made, however, by the Oregon Graduate Center, Beaverton, Ore., as part of the Atmospheric Lifetime Experiment (ALE) for fluorocarbons. The facility addition consisted of a small prefab building erected adjacent to the GMCC remote sampling tower on Lauagae Ridge. R. Rasmusson of the OGC is responsible for the ALE operations in Samoa.

Some facility replacement activity was required at Samoa. A serious problem was caused by failure of the Samoa Station emergency generator set in March. Lack of emergency power effectively destroys the day-to-day data continuity because of frequent power outages, which are not necessarily long, but which put the ICDAS offline until an operator can restart the system. A replacement generator set (Kato) was purchased and sent to Samoa soon after the failure, and was mounted to the engine after removal of the defective generator. Emergency power was restored on May 13.

A factor that may have contributed to the original generator failure was moisture absorption by its windings. This problem should be effectively eliminated in the replacement unit by factory-installed resistance heaters which run continuously and keep the unit always warmer than its surroundings when not in use, thus slowing down corrosion processes and preventing moisture buildup.

Other equipment problems involved air conditioner failures including the primary central unit for the main building, the unit for our remote sampling building, and the unit for the Ash dome, which houses the Dobson #42.

2.3.2 Programs

1978 is the first full year of operation for the present complement of GMCC monitoring instrumentation in Samoa's Southern Hemisphere tropical location. Installations of equipment were completed in July 1977 with the aerosol program equipment the last major addition. Table 3 summarizes the 1978 sampling programs at the Samoa station.

Although certain programs had difficulties during the year, overall continuity of the data record was not seriously affected. For purposes of discussion difficulties may be classed in four categories: (1) island a.c. supply problems and station emergency a.c. power supply problems, (2) instrument problems, (3) sampling problems, and (4) human errors. The first category, a.c. power supply, was the primary source of continuity problems, and has been during the 3 years of operation in Samoa. Instrument problems are intermittent and usually short, and when longer periods of downtime are probable, interim substitution equipment is sent from Boulder.

Samoan sampling problems are compounded by the humid tropical environment. The most serious 1978 sampling problem was encountered in the continuous CO_2 program which used a rather long sample line of polyethylene tubing. The problem of apparently elevated CO_2 index values obtained after sampling through a poly line was addressed by installing a liquid water condensation trap ahead of the normal freezer trap system as near the line inlet as possible. The trap should prevent the humid sample air from condensing in the long sample line and causing water buildup. During the year various line lengths and line replacements were used. Air samples were taken from two locations: Lauagae Ridge, where the GMCC remote sampling tower is located, and Matatula Point, where the remnant URI tower and building are located. Sample line lengths are approximately 120 m and 350 m, respectively.

A modified flask sampling schedule was also instituted; hand-aspirated flasks exposed at Matatula Point were alternated with through-the-analyzer samples to check on sample line effects.

During 1978, R. Williams completed a series of reports on ICDAS performance in general areas of reliability, noise characteristics of the system, and analysis of the kinds of system failures experienced.

2.3.3 Cooperative Programs

T. Fogg, URI Graduate School of Oceanography, arrived in Samoa on the Woods Hole research vessel Knorr during August. He spent about 2 weeks sampling at Matatula Point as part of his graduate research.

Other individuals from the Knorr also visited the observatory, and preliminary discussions were held concerning use of Samoa GMCC site for Southern Hemisphere SEAREX work in 1980-81.

Table 3.--Summary of sampling programs at Samoa in 1978

Monitoring programs (GMCC)	Instrument	Sampling frequency
Gases		
Carbon dioxide	URAS-2T NDIR analyzer	Continuous
	Evacuated glass flasks	Discrete
Surface ozone	Electrochemical concentration cell	Continuous
	Dasibi ozone meter	Continuous
Total ozone	Dobson spectrophotometer #42	Discrete
Fluorocarbons	Flask sampling	1 wk^{-1}
Aerosols		
Condensation nuclei	G.E. CN counter	Continuous
	Pollak CN counter	Discrete
Scattering properties (surface air)	4-wavelength nephelometer	Continuous
Atmospheric turbidity	Volz sunphotometer	Discrete
Solar radiation		
Global spectral irradiance	4 Eppley pyranometers with quartz, GG22, OG1, RG8 filters	Continuous
Direct spectral irradiance	Eppley NIP with filter wheel (OG1, RG2, RG8)	Discrete
	Eppley NIP/equatorial mount combination	Continuous
Meteorology		
Temperature (air)	Thermistor	Continuous
	Thermograph	Continuous
	Psychrometer	Discrete
	Max/min thermometers	Discrete
Temperature (soil)	Thermistor	Continuous
Temperature (dew point)	Thermistor with LiCl dew cell	Continuous
Relative humidity	Hygrothermograph	Continuous
Wind (speed/direction)	Bendix aerovane	Continuous
Pressure	Transducer (capacitance type)	Continuous
	Microbarograph	Continuous
	Mercurial barometer	Discrete
Precipitation chemistry		
pH and conductivity	Orion ph meter	Discrete
	Beckman conductivity bridge	
	Samples sent to MLO for further analysis on ion chromatograph	
Cooperative programs		
NO_2 (Aeronomy Lab/NOAA)	NO_2 spectrometer	Discrete 2 day^{-1}
Atmospheric Lifetime Experiment fluorocarbon program (OGC)	H-P 5840A gas chromatograph	Discrete 1 h^{-1}
Rain collection (DOE/EML)	Wet/dry collectors	Continuous
Rain collection (EPA)	Misco collector	Continuous

2.4 South Pole

2.4.1 Facilities

All GMCC South Pole measurement programs for 1978 were carried out from the Clean Air Facility (CAF). Figure 1 shows CAF exterior design, and fig. 2 shows the South Pole station layout and CAF and sensor locations. The CAF is off the snow surface, and drifting around the base poles is nonexistent. However, a ridge of drifted snow has been compressed by foot traffic, 15 m downwind from the grid southwest corner. It posed no threat to the CAF or GMCC operations.

The interior of the CAF consists of four isolated rooms and two common areas for short-term projects and storage. Figure 3 shows the building's interior layout and space allocations. GMCC occupies rooms 1 and 4, and portions of rooms 5 and 7. Figure 4 shows the layout of sensors and equipment on the CAF roof.

Ambient air for continuous measurement instrumentation is obtained through two sampling stacks (see figs. 1 and 3). One is for gas sampling and has six taps inside GMCC room 1 to which lines are attached that run to the instrumentation. Flows are adjusted at the instruments. The other is for aerosols and maintains laminar flow to prevent aerosol destruction. Three isokinetic taps are located inside room 1 with lines to the aerosol measuring instruments. The stacks are 14 m above the snow surface. Except for a slight buildup of snow at both intakes, discovered during a visual inspection in September, the stacks were free of obstruction and the interiors were in excellent shape. No other problems were encountered with the system during the year.

One CAF problem was localized contamination of sampled air. Four ways by which locally contaminated air can reach GMCC instrumentation were evident during the year: (1) contamination from the CAF, (2) station contamination in winds from 225° to 270°, (3) station contamination during periods of calm in strong temperature inversions, and (4) violations of the integrity of the CAQ. These instances were isolated, however, since the predominant polar winds eliminated (2) and (3), and regular inspection and scrutiny eliminated (1) and (4). Little if any data loss resulted from contamination.

The major problem encountered in the CAF during 1978 was the inadequate power supply from the station power plant. A greater than anticipated amperage draw by air sampling pumps of another CAF project (Univ. of Maryland, S-250) was noticed in February. This caused the transformers in the power plant and CAF to

Figure 1.--New South Pole CAF constructed during summer 1976-1977.

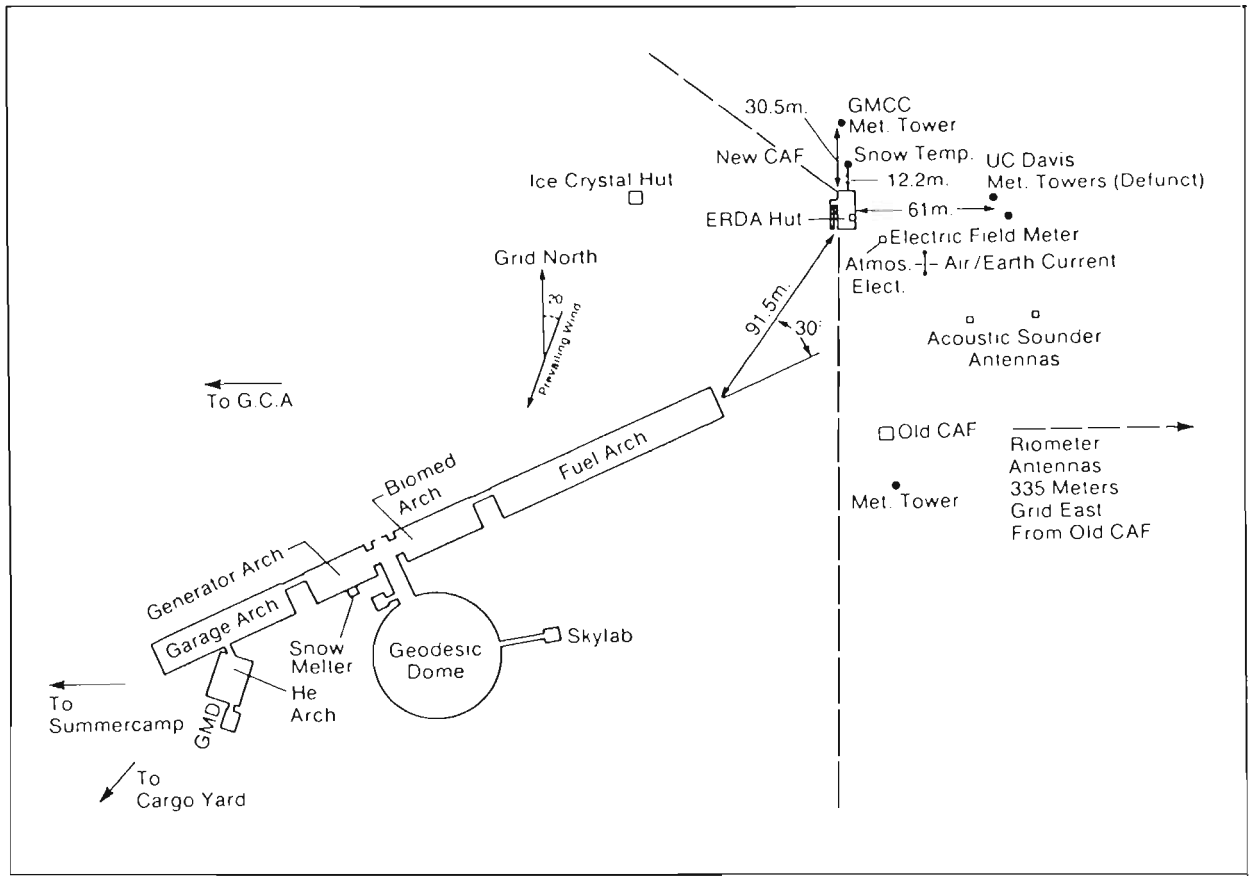

Figure 2.--Amundson-Scott Station, South Pole, Antarctica, 1978.

overheat and reach a core temperature of 170° F, burning insulation, and causing deterioration. Stopgap measures to alleviate this situation proved inconclusive. Finally, in April, a larger capacity transformer to service the CAF was installed in the power plant and a separate transformer for the S-250 pumps was junctioned in at the CAF. All other CAF programs, including GMCC, were left on the original transformer. This solution was adequate but left the CAF without backup transformer capabilities for the winter.

2.4.2 GMCC Programs

ICDAS

ICDAS performed excellently throughout 1978. No difficulties were encountered with the NOVA, Xerox multiplexor-digitizer, TTY, or Chronolog clock. Printed circuit board edge connector cleaning, digitizer zeroing, and TTY lubrication were the only preventive maintenance required.

Two small problems were encountered with the magnetic tape drive during the year. From January to March 1978, EOF's being left on tape were traced to a loose pin on the transport control board. In August, the BOT was not sensed during a tape rewind, causing damage to transport control board components. Repairs were effected by installing the spare board with new components and modified jumpers to match the NOVA interface.

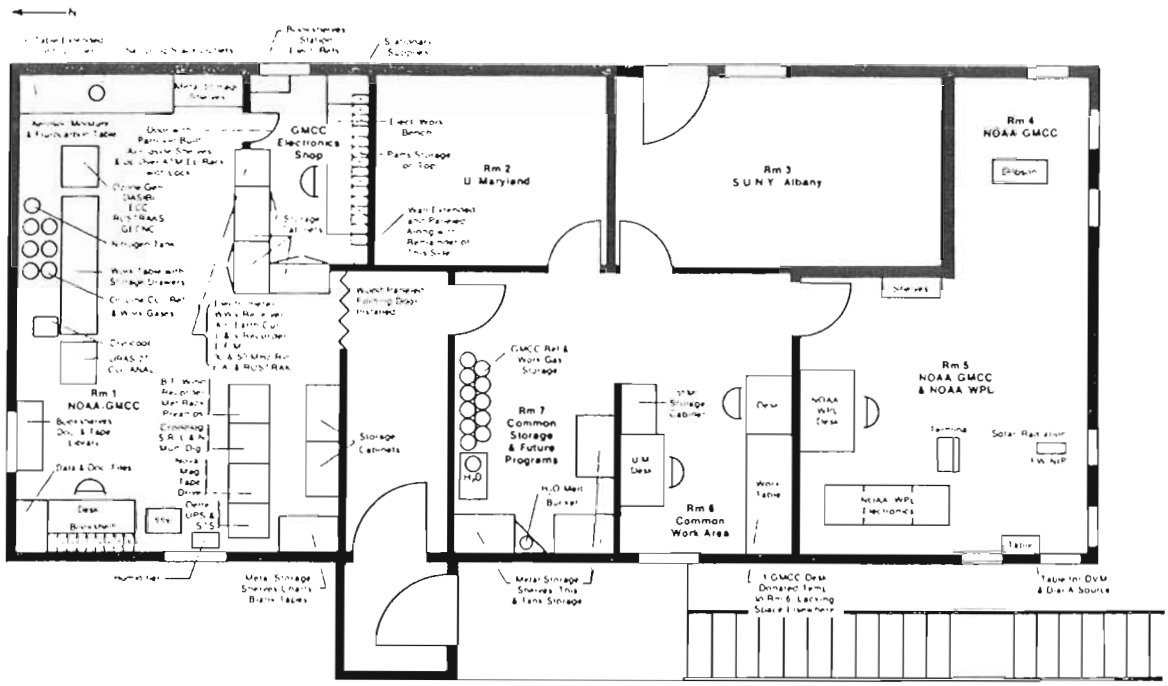

Figure 3.--Interior plan of new CAF, South Pole, Antarctica, 1978.

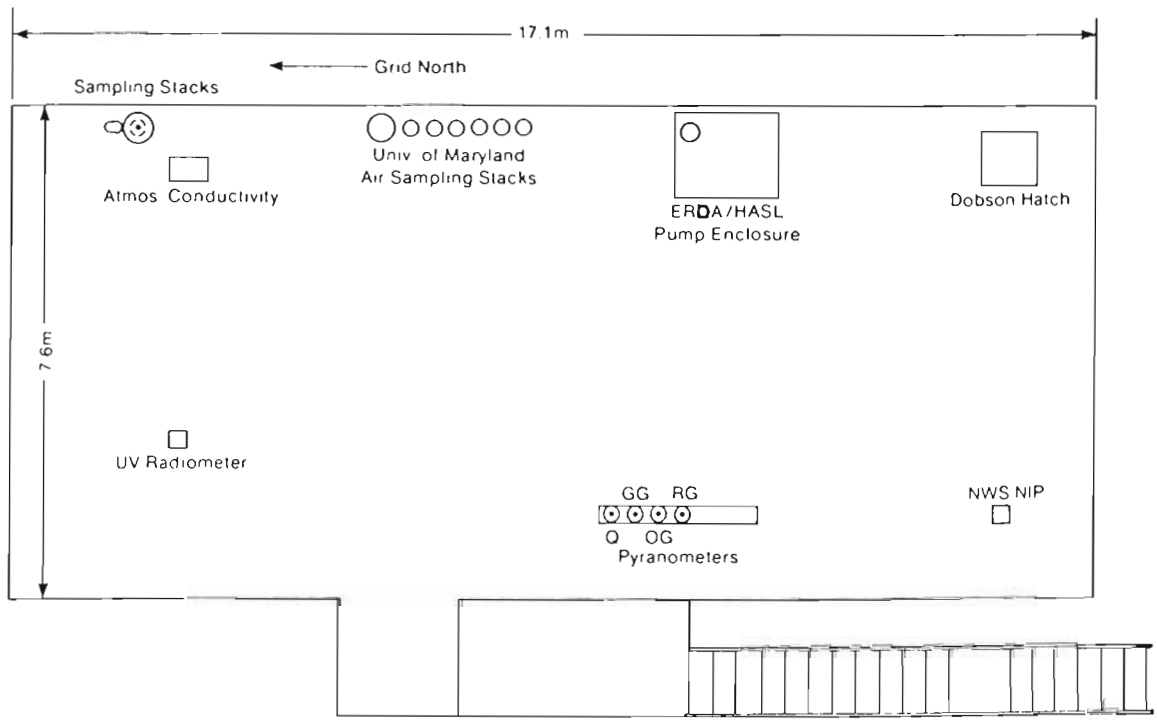

Figure 4.--Roof plan of new CAF, South Pole, Antarctica, 1978.

Because of acceptable steadiness of station power and the lack of correct schematics and components necessary to construct a phase-locked loop driver board for the static transfer switch, the Deltec U.P.S. was not used for most of the year.

No software problems were encountered. BOSS 76186 was used from November 3, 1977, to December 14, 1977, when BOSS 77280 was put on line and run for the remainder of the year. Major improvements to the new version include a simplified startup sequence, TTY output for CO_2 calibration sequence, and a revised method for ECC surface ozone data collecting and calibration.

Carbon Dioxide

Continuous sampling was performed throughout the year using the URAS-2T analyser, plus Cryo-cool refrigeration unit, solenoid switching valves, and the working calibration, and zero gases. For discrete sampling a pair of glass 0.5-ℓ flasks were exposed twice monthly by diverting air from the analyzer's sampling line during the working gas cycle. Working gases were changed twice during the year, calibration and zero gases once. New IR sources were installed in March. Noise was minimal for most of the year, especially after the new sources stabilized. Slow downscale output drift was seen sporadically during the year, necessitating regular zero adjustments and analyzer realignments.

Surface Ozone

BOSS 77280 brought new methods for data handling and calibration. The Dasibi used a self-scaling routine written in the software. The ECC low calibration routine was relay controlled and TTY initiated. Zero ozone voltages for 7 minutes were automatically transferred to the offset D-array registers. The scale factor was computed and entered by SR and TTY.

All ECC problems centered on the cell. Those on line were recharged regularly, and one previously thought bad was washed in a mild nitric acid solution to clean the platinum screen and sensing chambers. As a result the output was increased and steadier. The Dasibi UV light source caused the most trouble. Power surges due to restoration after outages cracked the sources and diminished their stability. Sources were changed fairly frequently to try to keep the strongest and steadiest on line and to maintain maximum instrument reliability.

Aerosols

The aerosol program depended on three measuring instruments. A Pollak CNC and a long tube Gardner counter were used for discrete measurements, and a G.E. CNC provided a continuous record for the year.

After extensive mechanical and electronic overhauling in November 1977, requiring a 1-mo down period to await replacement partial main board and spare transistors from Boulder, the G.E. performed excellently for the year. Regular calibration and routine maintenance were all that were required for optimum performance.

Pollak observations were taken three times every 24 h, throughout most of the year. One observation always corresponded to the daily SPO Meteorological

Office radiosonde flight. Cleaning and preventive maintenance were performed regularly. No problems were encountered with instrument operation. Concentrations below 10 cm^{-3} were seen throughout the winter. One Gardner observation was made daily, corresponding to a Pollak observation. Preventive maintenance was required every 10 days, and deflections corresponding to concentrations as low as 12 cm^{-3} were obtainable.

Solar Radiation

The program consisted of discrete measurements of normal incidence and continuous measurements of both global spectral irradiance and normal incidence irradiance. The standard instrumentation (table 4) was used. In December 1977 and January 1978, a series of special observations was made using the station filter wheel NIP and the traveling standard NIP and filter wheel to generate an intercomparison between the station and standard NIP both on the clear filter, and a correlative factor between the station and standard filter wheel, when both were on the standard NIP. Between November 1977 and January 1978, the traveling standard quartz pyranometer was installed and placed on line to provide an intercomparison between it and the station quartz pyranometer.

Ice crystal buildup on the domes was the major problem during the year. A new type of ring blower was installed in November. This ring clamps to the perimeter of the guard disc, and warmed air from the Thomas pump is forced out small holes in the ring. The old system forces the air up next to the dome through a ring under the disc. After intercomparing the two, it was decided that the newer rings were less efficient, and the old system was reinstalled on all pyranometers.

Meteorology

The six recorded parameters in table 4 make up the meteorology program. The only problem with recorded wind directions was related to some type of 360° to 540° scale expander card instability in winds from grid north (000°). Card modifications proved inconclusive, and because it was a sporadic problem and did not affect the resultant wind calculation, no further attempts were made to alleviate the instability. Low wind speeds when compared against station Meteorology Office values proved a puzzle for the first part of the year. Eliminating excess resistance from the signal receiving unit reduced the difference. In late November 1977 a new generator with newer bearings and brushes was installed in the aerovane. This further reduced, but did not eliminate, the difference. The problem was traced to excess capacitance across the input terminals acting like a resistor. Removal of this, however, fed the reference voltage onto the signal line, giving intermittent speeds around 35 m s^{-1}. Card modifications in January and February 1978 reduced this to a sporadic occurrence only when wind speeds were high and gusty. After these modifications, GMCC wind speeds were still 10% lower than those of the station Meteorology Office. However, when the voltage output of the Meteorology Office aerovane was checked against Bendix-Friez documentation, its speed was fast by 1.5 kt over a range from 5 to 20 kt. This could account for the difference.

A daily intercomparison between GMCC pressure values and the station Hg barometer, begun in March 1978, was stopped when the barometer was found to need repairs. The pressure transducer and temperature sensors operated for the year with no problems.

Table 4.--Summary of sampling programs at South Pole in 1978

Monitoring programs	Instrument	Sampling frequency	Data record
Gases			
Carbon dioxide	URAS-2T NDIR gas analyser	Continuous	Jan 75-Nov 78
	0.5-ℓ evacuated glass flasks	2 pairs mo^{-1}	Jan 75-Nov 78
		1 pair wk^{-1}	Dec 78
Surface ozone	Electrochemical concentration cell	Continuous	Dec 71-Jan 79
	Dasibi ozone meter	Continuous	Jan 76-present
Total ozone	Dobson spectrophotometer	Discrete	Dec 63-present
Fluorocarbons	300-ml stainless steel sampling cylinders	2 pairs mo^{-1} summer 1 pair mo^{-1} winter	Jan 77-Dec 78
Aerosols			
Condensation nuclei	G.E. CN counter	Continuous	Jan 74-present
	Pollak CN counter	Discrete, 2-4 day^{-1}	Jan 74-present
	Long-tubed Gardner CN counter	Discrete, 1 day^{-1}	Jan 74-present
Optical properties	4-wavelength nephelometer	Continuous	Jan 79-present
Solar radiation			
Global spectral irradiance	4 Eppley pyranometers with quartz, G6-22, OG-1, and RG-8 filters	Continuous during austral summer	Feb 74-present
	Ultraviolet radiometer	Continuous during austral summer	Feb 74-present
Direct spectral irradiance	NIP on meridional tracker	Continuous during austral summer	Oct 75-present
	Filter wheel normal incidence pyrheliometer with quartz, OG-1, RG-2, and RG-8 filters	Discrete during austral summer	Jan 77-present
Meteorology			
Air temperature	Thermistor (aspirated shield)	Continuous during austral summer	Dec 75-Jan 78
Air temperature	Thermistor (naturally ventilated shield)	Continuous	Mar 77-present
Snow temperature	Thermistor	Continuous during austral summer	Dec 75-Jan 78
Snow temperature	Thermistor	Continuous	Jul 77-present
Pressure	Transducer	Continuous	Dec 75-present
Wind speed and direction	Bendix-Friez aerovane and recording system	Continuous	Dec 75-present
Atmosphere moisture content	Dupont 303 moisture monitor	Continuous	Mar 77-present
Miscellaneous			
Room temperature	Thermistor	Continuous	Jul 78-present
Cooperative programs			
Carbon dioxide (SIO)	5-ℓ evacuated glass flasks	2 mo^{-1} (3 flasks per sample)	1957-present
Total surface particulates (Atmosphere trace metals) (DOE/ERDA/HASL)	Motor driven rotary lobe blower (high-volume air sampling through filters)	Continuous (filters changed 4 times mo^{-1})	May 70-present
Turbidity (NOAA/ARL)	Dual wavelength sunphotometer	Discrete during austral summer	Jan 74-present
Carbon-14 sampling (NOAA/ARL)	Pressurized steel spheres	500 P.S.I. ambient air day^{-1}, for 6 days	Jan 74-present
Atmospheric electricity (NOAA/APCL)	Atmospheric conductivity meter, electric field mill, air/earth current antenna	Continuous	1973-Nov 78
Thermal radiation budget (NOAA/APCL)	Net infrared radiometer	Continuous	Terminated Feb 78
Acoustic echo sounding of planetary boundary layer (NOAA/WPL)	Monostatic and bistatic echo sounding system	Continuous	Turned over to WPL personnel Jan 78
Ionospheric opacity (Univ. of Calif., San Diego; NOAA/EDIS)	30- and 50-MHz riometers	Continuous	1974-present

The Dupont moisture monitor dynapump was replaced in late December 1977 with a smoother and less noisy metal bellows pump. The only operational problem during the year was shorting of phosphorus pentoxide sensing cells because of moisture buildup in the pump being injected rapidly into the cell after power restorations. The shorting was eliminated by allowing the pump to flush for 10 minutes before reattaching to the instrument.

Fluorocarbons

The revised sampling system (see GMCC Summary Report 1977) was used throughout 1978. Winter samples were mailed to Boulder immediately after the station opened. No leaks in the system or problems of any type were encountered.

Total Atmospheric Ozone

Dobson spectrophotometer observations were made from the CAF for the entire year. In early November, the times of the 2200 and 0200 CUT observations were altered by as much as one hour. This was done to provide ground truth for, and match the predicted times of, the solar overpass of the F_2 satellite MFT ozone sensor, at the request of J. Lovill, Satellite Ozone Analysis Center, Lawrence Livermore Laboratory, Univ. of Calif. A bad photomultiplier tube, discovered and replaced in December 1977, was the only malfunction during the year.

Cooperative Programs

As a part of CAF operations, GMCC maintained cooperative programs for the institutions listed in table 4. No strain on GMCC personnel or equipment occurred, and the quality and quantity of GMCC data were not affected. Cooperative programs enhanced GMCC's polar presence and the functioning of the CAF.

3. CONTINUING GMCC PROGRAMS

3.1 Carbon Dioxide

3.1.1 Analyzer CO_2 Measurements

During 1978, atmospheric CO_2 concentrations were continuously monitored by nondispersive infrared gas analyzers at the four GMCC observatories. Analyzer measurements at South Pole were discontinued on November 19, 1978.

The output from each analyzer was simultaneously recorded digitally by ICDAS and in an analog form by a strip chart recorder. Hourly CO_2 values were obtained by using data processing procedures described in GMCC Summary Report 1977.

Editing the hourly CO_2 data collected since the beginning of the GMCC monitoring program at Barrow (July 1973) and Mauna Loa (May 1974) has been completed. Mauna Loa Observatory CO_2 data bases for the first four years (May 1974 through June 1978) have also been updated by using revised values for the working reference gases.

Special calibrations, which used CO_2-in-air standard mixtures, were carried out at Barrow during August 1978 and at Mauna Loa during September 1978 to obtain data for calculating pressure broadening corrections. These corrections are necessary when CO_2-in-N_2 standards have been used with an infrared gas analyzer to determine atmospheric CO_2 concentrations. Pressure broadening (sometimes called carrier gas effect) errors result when the proportions of N_2 and O_2 in the reference gas mixtures differ markedly from those in natural air. The sensitivities of different analyzers to pressure broadening errors vary, and apparent measured CO_2 concentrations may be greater or smaller than when calibrated mixtures of air are used as reference standards.

Since inception of the GMCC CO_2 monitoring program at Barrow, three different infrared analyzers have been used during the following time periods:

Analyzer	Serial no.	Period of use
UNOR-2	631521	July 73 - Aug 12, 75 Aug 1, 76 - Aug 14, 78
UNOR-2	631268	Aug 12, 75 - Aug 1, 76
URAS-2T	0111	Aug 14, 78 -

At Mauna Loa Observatory, only one analyzer, a URAS-2 (serial no. 37626682), has been in use since the beginning of the measurement program in May 1974.

Monthly mean CO_2 concentrations have been computed from edited hourly CO_2 values for Barrow for July 1973 to December 1978, and for Mauna Loa for May 1974 to December 1978. The data are shown in tables 5 and 6. Values in column a are expressed in the Scripps 1959 adjusted index scale, whereas those in column b are given in the 1974 WMO CO_2-in-air mole fraction scale with tentative pressure

Table 5.--Barrow Observatory monthly mean CO_2 concentrations*

Month	1973 a	1973 b	1974 a	1974 b	1975 a	1975 b	1976 a	1976 b	1977 a	1977 b	1978 a	1978 b
Jan			340.93	339.06	340.35	338.45	339.46	337.51	338.64	336.63	341.18	339.34
Feb			338.77	336.77	340.57	338.68	339.70	337.75	338.84	336.85	342.00	340.20
Mar			339.48	337.52	340.09	338.17	340.61	338.72	340.06	338.15	343.40	341.69
Apr			340.71	338.83	340.38	338.48	340.73	338.85	340.91	339.04	342.77	341.02
May			339.27	337.31	341.41	339.58	340.11	338.30	341.06	339.20	342.55	340.78
Jun			338.38	336.36	338.06	336.02	339.05	337.07	339.67	337.73	341.37	339.53
Jul	327.13	324.42	333.30	330.97	332.30	329.91	333.54	331.23	332.48	330.10	334.25	331.98
Aug	325.49	322.65	328.14	325.49	327.41	324.71	326.51	323.75	329.34	326.76	327.23	328.28
Sep	328.29	325.64	328.95	326.35	328.38	325.75	327.74	325.06	330.51	328.00	324.44	328.64
Oct	332.63	330.26	332.41	330.03	332.52	330.17	332.41	330.03	334.40	332.14	327.73	332.29
Nov	336.19	334.03	335.43	333.23	337.36	335.27	336.27	334.13	336.98	335.84	333.19	338.10
Dec	336.56	334.43	338.61	336.61	338.95	336.96	338.43	336.41	340.62	338.74	333.63	338.59

*Values expressed in ppm.

broadening corrections applied. Figure 5 shows plots of the data in the 1974 WMO mole fraction scale.

The data presented are preliminary; e.g., all Barrow data must yet be updated with revised CO_2 concentration values for the working reference gases. Estimates of the pressure broadening corrections will be improved. Pressure broadening corrections for UNOR-2 instrument (serial no. 631268), operated at Barrow from August 12, 1975, to August 1, 1976, have not yet been determined; instead, corrections derived for the UNOR-2 (serial no. 631521) instrument have been used. The pressure broadening characteristics of the two instruments are believed to be sufficiently similar (Pearman, 1977) to warrant application of this initial data adjustment procedure. Relative errors in the data sets plotted

Table 6.--Mauna Loa Observatory monthly mean CO_2 concentrations*

Month	1974 a	1974 b	1975 a	1975 b	1976 a	1976 b	1977 a	1977 b	1978 a	1978 b
Jan			326.62	330.42	327.68	331.55	328.77	332.71	330.96	335.05
Feb			327.34	331.19	328.59	332.52	329.14	333.11	331.17	335.27
Mar			327.95	331.84	329.28	333.25	330.62	334.68	332.18	336.35
Apr			329.02	332.98	330.52	334.58	331.78	335.92	333.49	337.75
May	328.92	332.87	329.59	333.58	330.73	334.80	332.41	336.59	333.64	337.91
Jun	327.88	331.76	329.06	333.02	330.19	334.22	331.84	335.98	333.60	337.86
Jul	326.68	330.49	327.41	331.26	328.57	332.50	330.29	334.33	332.10	336.26
Aug	324.76	328.44	325.66	329.40	326.49	330.28	328.36	332.27	330.13	334.16
Sep	323.29	326.88	324.40	328.06	325.10	328.81	327.21	331.05	328.07	331.97
Oct	323.15	326.73	324.72	328.40	324.91	328.60	327.36	331.21	328.42	332.34
Nov	324.28	327.93	325.60	329.34	326.12	329.89	328.61	332.54	329.63	333.63
Dec	325.55	329.28	326.85	330.67	326.57	330.37	329.83	333.84	330.69	334.76

*Values expressed in ppm.

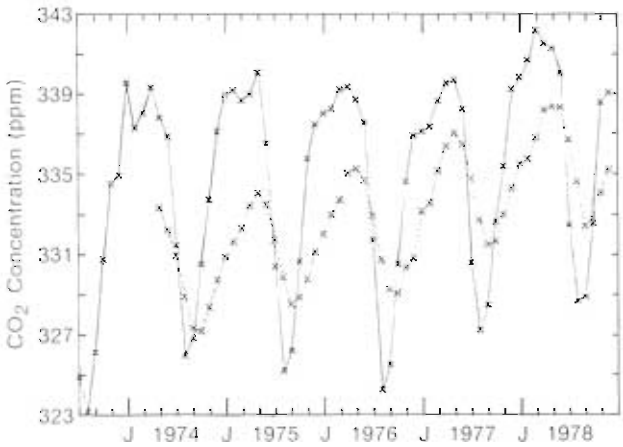

Figure 5.--Mean monthly CO_2 mixing ratios for Barrow, Alaska (solid line) and Mauna Loa, Hawaii (dashed line) plotted in SIO 1974 mole fraction CO_2-in-air scale.

in fig. 5 are estimated to be <1 ppm for the Barrow data and <0.5 ppm for the MLO data. Systematic errors for both data sets are believed to be less than ±1 ppm when referred to an absolute CO_2 mole fraction calibration scale.

CO_2 analyzer data for South Pole and Samoa stations are not presented in this report since an analyzer problem was experienced at South Pole and an air-intake line problem was encountered in Samoa during 1978. Final data processing from these stations has been postponed pending receipt of more CO_2 data and additional information about the performance of the analyzer system at these two stations.

3.1.2 Flask Sample CO_2 Measurements

Collection of pairs of atmospheric air samples in 500 cm^3 double-stop-cock glass flasks continued at the four GMCC observatories and other sites during 1978. Full-year data are available from eight stations shown below:

Station	Sampling frequency	Analytical standards
Barrow, Alaska	1 pr wk^{-1}	CO_2-in-N_2
Niwot Ridge, Colo.	1 pr wk^{-1}	CO_2-in-N_2
Key Biscayne, Fla.	2-3 pr mo^{-1}	CO_2-in-N_2
Mauna Loa, Hawaii	1 pr wk^{-1}	CO_2-in-N_2
Cape Kumukahi, Hawaii	1 pr wk^{-1}	CO_2-in-N_2
Cape Matatula, Am. Samoa	1 pr wk^{-1}	CO_2-in-N_2
Palmer Station, Antarctica	1 pr wk^{-1}	CO_2-in-air
South Pole, Antarctica	2 pr mo^{-1}	CO_2-in-air

Two methods were used to collect the Barrow, Mauna Loa, and Samoa samples. The practice of filling the flasks by flushing with air from the CO_2 analyzer air intake system was alternated at weekly intervals with hand aspirating air

into the flasks outdoors while facing into the wind. The South Pole samples were collected by the CO_2 analyzer air-intake system, except after November 7 when the manual aspiration technique was employed. Flask air samples at all other stations were collected by the hand-aspiration technique. All flask samples were analyzed with a Lira (Mine Safety Appliance) infrared analyzer, model 202, (serial no. 20719). Samples from the first six stations were returned to Boulder as soon as practical after collection (usually within 1 to 2 weeks), and analyzed within a few days to a month thereafter. The Palmer, Antarctica, and South Pole samples were received in Boulder early in 1979 and were analyzed during the period of March 1 to April 12, 1979.

Flask data in this report are presented in the Scripps 1959 adjusted index scale. All data are provisional. The data from the first six stations were obtained by using CO_2-in-N_2 calibration gas standards, and must be corrected for pressure broadening after conversion to the 1974 WMO CO_2-in-N_2 mole fraction scale. All data are subject to corrections when final concentration values are determined for the calibration gas standards.

Mean monthly CO_2 mole fractions expressed in parts per million (ppm) Scripps 1959 adjusted index scale are presented in table 7 for Barrow, Niwot Ridge, Key Biscayne, Mauna Loa, Cape Kumukahi, Cape Matatula, Palmer, and South Pole. Plots of the data are shown in fig. 6. Sample values enclosed in brackets in the plots have been visually judged to be outliers and have not been used in computing the monthly mean CO_2 concentrations. In addition, a small number of outliers lying outside the range of the plots have been excluded from the monthly mean value computations. The monthly mean CO_2 mole fractions in table 7 have been determined from CO_2 measurement values where analysis values of two flask samples collected quasi-simultaneously represent one measurement result; also, a single sample value represents a measurement result in instances where its pair value is unavailable (e.g., because of a broken flask) or is deemed to be an outlier. The number of measurements made per month, the number of flask samples collected each month, and the number of sample values judged to be outliers per month at each station are indicated in table 7.

3.2 Total Ozone

3.2.1 Routine Observing Program

Routine total ozone observations were continued in 1978 at the four GMCC stations, one foreign cooperative station, three domestic cooperative stations, three NWS stations, and GMCC headquarters, Boulder.

Figure 7 lists the 12 stations of the U. S. Dobson ozone spectrophotometer network, the instrument numbers, the agencies responsible for taking observations, and the periods of record when observations were made.

Other instruments under NOAA/GMCC control are: no. 94, to be installed at a U.S. West Coast station in California; no. 83, the world standard Dobson ozone spectrophotometer; no. 65, on loan to the University of Michigan; no. 93, loaned to Brazil; no. 81, loaned to Australia; and no. 38 in Boulder, a secondary standard instrument.

Table 7.--1978 provisional mean monthly CO_2 concentrations from flask sampling

Month	Barrow				Niwot Ridge				Key Biscayne				Mauna Loa			
	Mean conc.	No. of meas.	No. of flasks	No. of outliers	Mean conc.	No. of meas.	No. of flasks	No. of outliers	Mean conc.	No. of meas.	No. of flasks	No. of outliers	Mean conc.	No. of meas.	No. of flasks	No. of outliers
Jan	336.40	4	8		334.56	3	6	1	334.87	3	4	2	331.56	3	6	
Feb	337.76	5	10		334.44	1	1	3	334.90	1	2		332.37	4	8	
Mar	340.12	2	3		335.12	2	4		335.54	3	5	1	333.40	4	8	
Apr	338.57	4	8		338.22	1	2		338.00	2	4		334.46	4	8	
May	337.34	3	6	4	336.40	3	5	1	336.73	3	6		335.21	2	6	2
Jun	337.02	5	12		334.24	4	7	1	334.45	2	4		333.86	4	8	
Jul	330.72	5	9		331.82	3	6	4	332.40	2	4		332.56	3	5	1
Aug	327.00	4	8		328.61	3	6		330.48	3	5	1	330.54	4	7	1
Sep	326.83	4	8		329.14	3	6		330.33	1	2		329.54	5	10	
Oct	332.20	4	8		330.69	3	5	1	330.76	2	4	2	329.15	4	6	2
Nov	335.13	4	4		332.12	5	10	2	333.43	3	6		330.50	4	10	
Dec	335.29	5	9	1	334.32	1	2		333.36	2	4		331.28	5	10	
Total		49	93	5		32	60	13		27	50	6		46	92	6

Month	Cape Kumukahi				Cape Matatula				Palmer Station				South Pole			
	Mean conc.	No. of meas.	No. of flasks	No. of outliers	Mean conc.	No. of meas.	No. of flasks	No. of outliers	Mean conc.	No. of meas.	No. of flasks	No. of outliers	Mean conc.	No. of meas.	No. of flasks	No. of outliers
Jan	333.69	2	4	4	331.30	2	4		328.06	2	4		329.01	3	6	
Feb	333.74	5	10		331.06	1	2	2	327.98	3	6		329.06	1	2	
Mar	334.16	3	6		331.93	4	6	5	329.69	5	9	1	328.41	2	4	
Apr	334.50	4	7	1	331.40	4	8		330.50	3	6		328.58	2	4	
May	335.62	5	9	1	331.88	3	6	2	330.19	4	8		328.78	2	2	2
Jun	336.07	3	6		332.06	3	6		331.47	5	9		329.08	2	2	2
Jul	331.96	4	8		331.98	4	7	1	330.40	4	7	1	329.42	2	4	
Aug	330.21	5	9	1	331.17	2	4		330.63	5	10		330.13	2	4	
Sep	327.44	4	8		331.26	4	8		331.02	3	5	2	330.35	2	2	2
Oct	329.58	5	10		332.11	3	6		330.55	3	6	2	330.91	2	3	1
Nov	332.15	4	8		331.14	1	2		331.18	4	7	1	331.05	1	2	
Dec	332.66	3	6		332.61	7	14		330.17	4	8		330.33	2	4	
Total		47	91	7		38	73	10		45	85	7		23	39	7

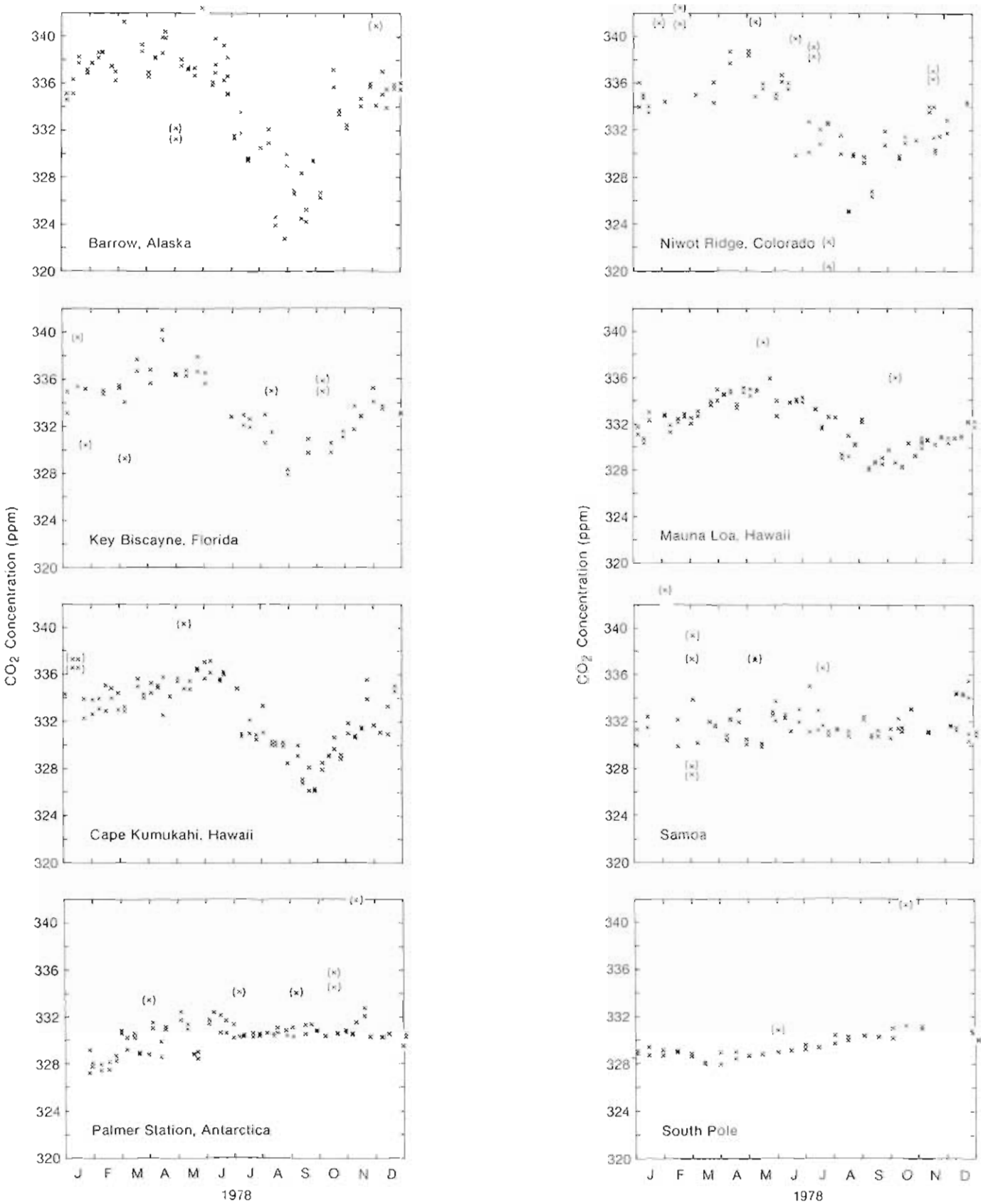

Figure 6.--Plots of 1978 CO_2 flask sample data. CO_2 mixing ratios are expressed in SIO 1959 adjusted index scale.

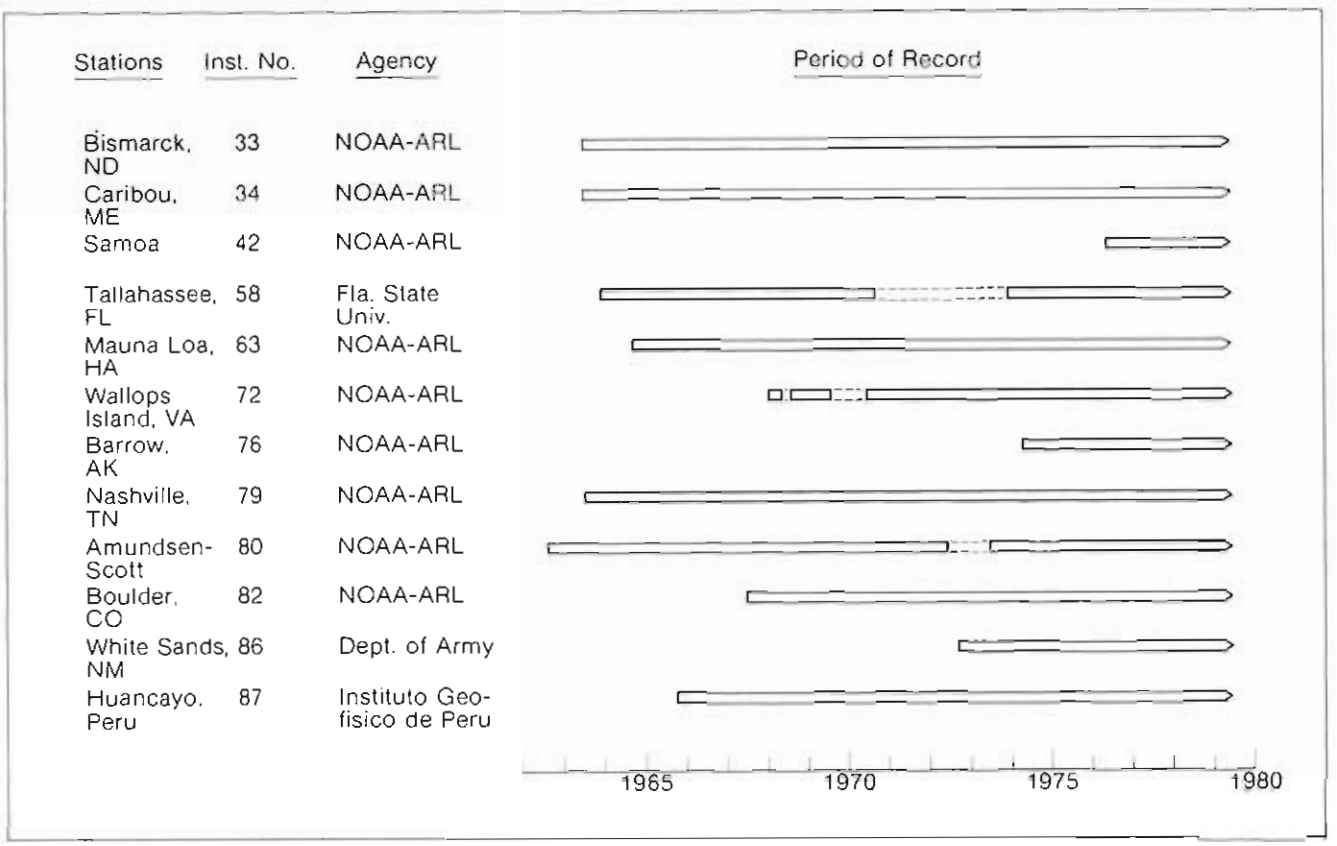

Figure 7.--U.S. Dobson spectrophotometer station network, including cooperative stations.

During 1978, the six continental Dobson instrument stations were visited to conduct instrument inspections, perform instrument calibration tests, and train observers. No major problems were found, but some instrument components showed wear from years of continuous service. At Samoa and South Pole, Dobson instrument optical wedge calibrations were performed but because of the shortage of time and a logistics problem, the instruments were calibrated with standard lamp UQ2 rather than compared directly with the world standard Dobson spectrophotometer. (Results of the Boulder 1977 International Intercomparison of Dobson Ozone Spectrophotometers show that a Dobson instrument can be calibrated, by using standard lamps, to within an accuracy of ± 0.5 N units, or about ± 1%. The Samoa and South Pole instruments had both maintained their previous calibrations to within ± 1%.)

3.2.2 Modernization and Calibration of Dobson Spectrophotometers

During 1978 GMCC personnel continued to participate in the WMO Global Ozone Monitoring and Research Project to upgrade the quality of Dobson spectrophotometers throughout the world. Table 8 lists the instruments that were reconditioned. New electronic systems that use miniature solid-state high-voltage converters, modern amplifier circuitry, and electromechanical phase-sensitive rectifiers were installed in these instruments. After the alignments of optical components were checked and adjusted, the instruments were calibrated by direct comparison with the world standard Dobson instrument no. 83.

Table 8.--Dobson instruments modernized and calibrated during 1978

Location	Instrument no.
Mexico City, Mexico	98
Natal, Brazil	93
Leningrad, U.S.S.R.	108
Manila, Philippines	52
Boulder, Colo., U.S.A.	38

Dobson instrument no. 93, now located at Natal, Brazil, was operated at Puerto Montt, Chile, in 1965. The instrument belongs to the United States and has been loaned indefinitely to the Instituto de Perquisas, Espaciais at San Jose dos Campos, Brazil, where it will be operated daily by the Institute at Natal. Data from the station will be used for ground truth information to support a rocket ozonesonde program being conducted at Natal by NASA, Wallops Island, Va.

Dobson instrument no. 52, a surplus Japanese instrument given to the WMO, is located at Manila, Philippines, and was put into operation on December 6, 1978. It is operated on a routine daily basis by the Philippine Atmospheric Geophysical and Astronomical Service Administration at the Manila Observatory.

Dobson instrument no. 38 was in operation at Green Bay, Wis., for a number of years before observations were terminated in 1975. It has been modified, optically aligned, and recalibrated, and is now used as a secondary standard instrument for total ozone measurements at Boulder, Colo.

3.2.3 Data

Daily 1978 total ozone values (applicable to local apparent noon) for all stations in the U.S. network have been submitted to and are available from the World Ozone Data Center, Atmospheric Environment Service, 4905 Dufferin Street, Downsview, Ontario M3H5T4. Table 9 lists mean monthly 1978 total ozone amounts for the NOAA observatories and cooperative stations.

3.3 Surface Ozone

3.3.1 Operations

At the end of 1978, the Dasibi ozone photometer at the South Pole was replaced with an updated, recalibrated version and use of the ECC meter was discontinued. Surface ozone measurements were discontinued at Fritz Peak Observatory west of Boulder because pollution from the Denver urban area prevented this site from providing data representative of clean air at midlatitudes in the Northern Hemisphere.

Table 9.--1978 provisional mean monthly total ozone amounts (milli-atmo-cm)

Location	Jan	Feb	Mar	Apr	May	Jun	Jul	Aug	Sep	Oct	Nov	Dec
Bismarck, N. Dak.	374	386	367	373	369	340	322	313	291	289	305	332
Caribou, Maine	378	431	428	412	373	359	349	322	318	317	296	343
Tutuila Is., Samoa	261	262	262	259	263	267	271	266	271	268	265	268
Tallahassee, Fla.	291	293	312	307	326	318	325	316	306	288	285	276
Mauna Loa, Hawaii	238	234	254	281	284	269	271	264	261	251	256	258
Barrow, Alaska	--	--	425	426	398	366	317	295	309	307	--	--
Wallops Is., Va.	333	340	342	338	348	331	323	308	300	294	278	296
Nashville, Tenn.	323	332	334	345	360	350	328	321	302	298	282	295
Boulder, Colo.	322	325	340	337	349	323	315	310	297	283	282	291
White Sands, N. Mex.	287	306	308	314	331	310	308	307	294	288	284	280
Huancayo, Peru	258	264	264	258	263	266	266	269	269	270	271	260
Amundsen-Scott, Antarctica	329	301	--	276	280	288	288	293	--	297	369	328

3.3.2 Data Analysis

Research on the chemistry of the unpolluted troposphere requires continuous monitoring of the surface ozone content of the troposphere. The distribution of ozone in clean air must be studied before a determination can be made of whether or not the tropospheric ozone distribution results from photochemical or transport processes, or both. Since the four baseline stations of the GMCC network are far removed from major local sources of ozone producing or destroying contamination, samples taken there represent ozone behavior in the clean troposphere.

Measurements of surface ozone have been made by the ECC meter and Dasibi ozone photometer since 1973. Before the 1977 Summary Report, data were published with the assumption that the instruments were self-calibrating, i.e., that ozone amounts could be calculated from the basic instrument equations. Comparisons existed, however, between field instruments and ECC meter 001-1, a secondary standard. During the past year, a Dasibi ultraviolet photometer was referenced to the NBS three meter pathlength photometer and established as a network standard. The standard maintained by NBS agrees closely with UV photometers built by several U.S. organizations (Wendt et al., 1979).

All measurements made by the ECC meter or Dasibi ozone meter since 1973 have been adjusted to the scale represented by the NBS photometer. All surface ozone data gathered by GMCC since 1973 and published in previous Summary Reports are superceded by the data published here.

In some cases we had difficulty tracing the calibration from the NBS photometer back to a field instrument. The NBS standard is accurate to approximately ± 3 nanobars (1 nanobar = 1 ppb at 1000 mb) over the range of interest. Other instruments used to transfer calibrations and for field operations have comparable accuracy. When dealing with ozone levels of the order of 5 to 40

nanobars, an uncertainty in the calibration of 3 nanobars in each of at least two transfers of calibration (from NBS standard to secondary standard to field instrument) becomes important when looking at long-term changes in ozone.

Surface ozone variations apparent in data presented here are on three time scales: a diurnal cycle, day-to-day changes, and a seasonal cycle.

The diurnal cycle at Mauna Loa in fig. 8 has been mentioned in previous reports and is closely associated with the mountain wind circulation. The larger data base now available has substantiated previously observed ozone variations.

At Samoa a diurnal variation (fig. 8) is detectable with a maximum around 0700 in the morning and a minimum in the afternoon. The cause of this variation has not been determined. A study of the local wind behavior does not reveal any important variation in wind speed or direction as a function of time of day. The monthly mean values of wind speed and direction for each hour of the day were investigated and no diurnal cycle was revealed. In addition, a large number of individual days on which a diurnal ozone variation appeared were checked with the wind observations to see if changing winds might leave the ozone sampling location in stagnant air or air that had a fetch from over vegetated land areas.

Although several curves in fig. 8 for Barrow appear to indicate a possible diurnal variation, this is not the case. These variations result from a few large day-to-day changes which bias the averages presented in this data representation.

At the South Pole (fig. 8) where the Sun is above the horizon for 6 months and below for 6 months, one would not expect any diurnal effects due to solar input. The constancy of the results in fig. 8 suggests that the data are not influenced by local pollution, instrument temperature variations, and other adverse effects that might be related to 24-h work schedules.

In contrast to the diurnal variation at the GMCC stations are measurements made at Fritz Peak (fig. 8). Although this site is not within an urban area, it is strongly influenced by pollution from Denver to the southeast. During the late spring and summer months in particular, the diurnal variation shows a minimum in the morning and an afternoon maximum typical of polluted environments. During winter months there is less sunshine available, and westerly air flow usually prevails, minimizing local ozone production.

Day-to-Day Variations

At all GMCC stations the day-to-day variations in surface ozone are pronounced. At the South Pole these variations are confined primarily to November, December, and January. The variations at the South Pole have been attributed to weakening of the near-surface temperature inversion during summer months, allowing the downward mixing of air from above and advection of air from lower polar latitudes (Oltmans and Komhyr, 1976). Although these summertime fluctuations are very large compared with the nearly constant readings obtained during the remaining months, they are relatively small compared with the variations seen at the other locations (fig. 9). Figure 10 shows an example of these variations where the daily values for a month are plotted for each GMCC stations and Fritz Peak.

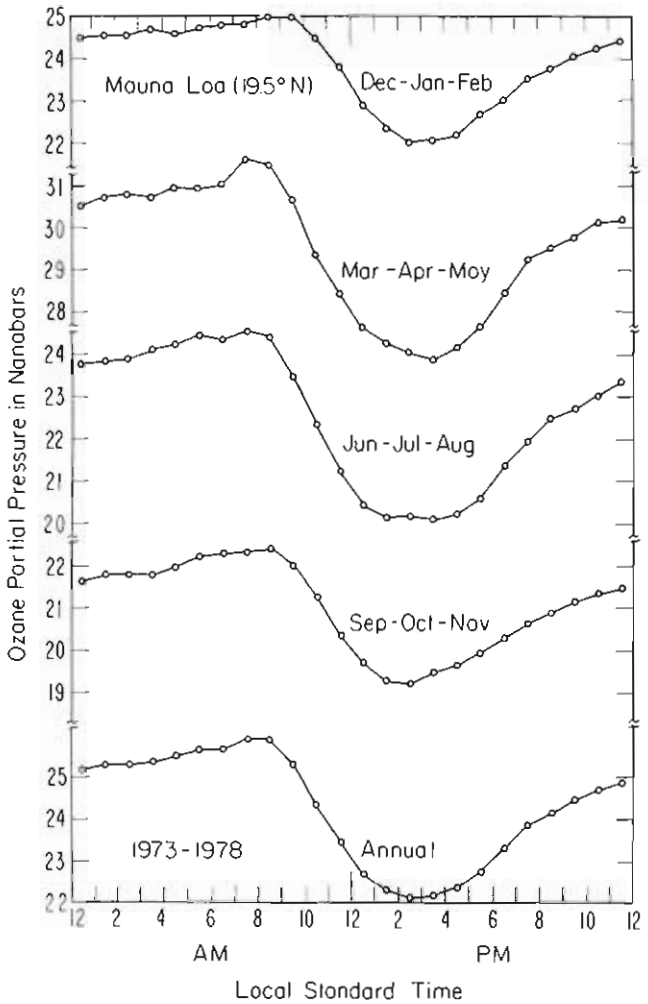
Mauna Loa (19.5° N)
Dec - Jan - Feb
Mar - Apr - May
Jun - Jul - Aug
Sep - Oct - Nov
Annual
1973 - 1978
Ozone Partial Pressure in Nanobars
AM
PM
Local Standard Time

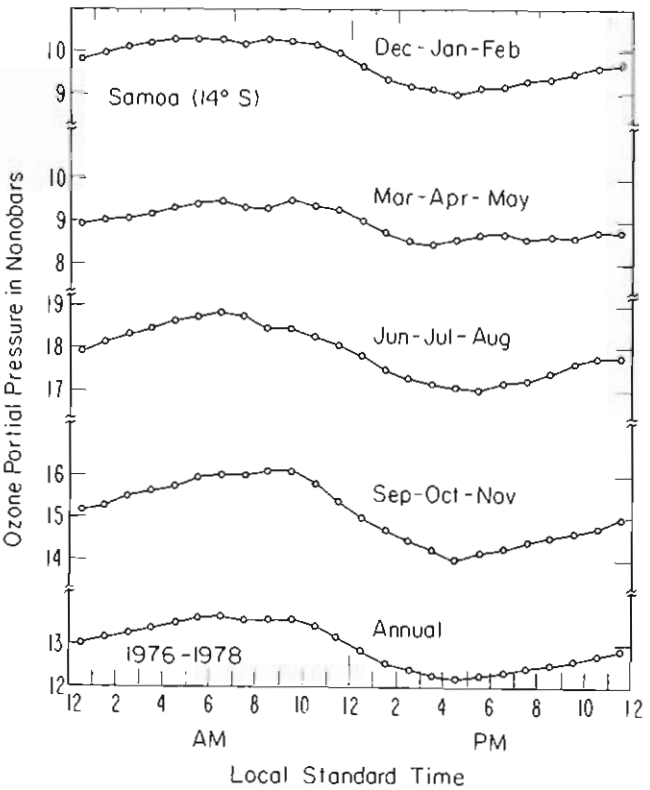
Samoa (14° S)
Dec - Jan - Feb
Mar - Apr - May
Jun - Jul - Aug
Sep - Oct - Nov
Annual
1976 - 1978
Ozone Partial Pressure in Nanobars
AM
PM
Local Standard Time

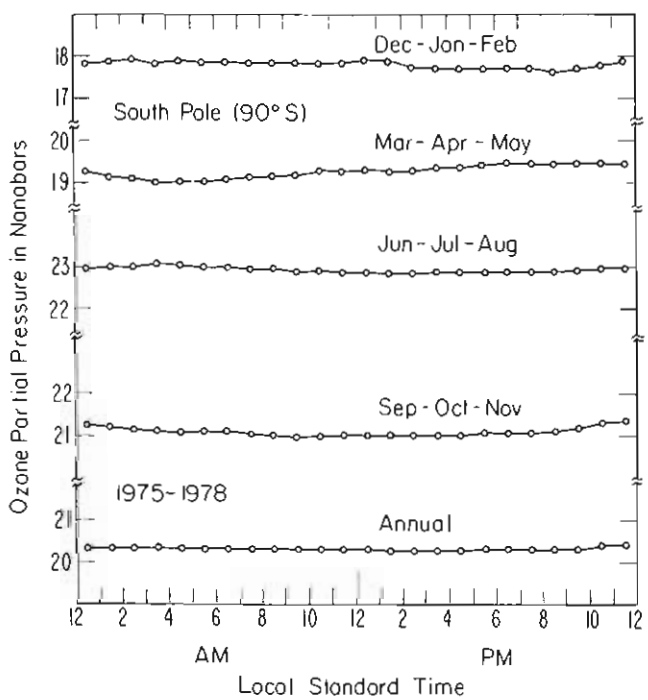
South Pole (90° S)
Dec - Jan - Feb
Mar - Apr - May
Jun - Jul - Aug
Sep - Oct - Nov
Annual
1975 - 1978
Ozone Partial Pressure in Nanobars
AM
PM
Local Standard Time

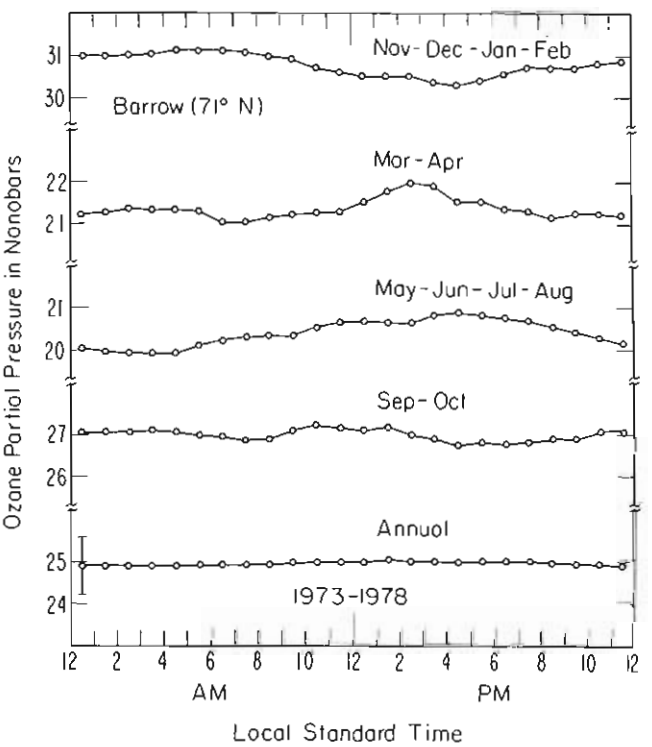
Barrow (71° N)
Nov - Dec - Jan - Feb
Mar - Apr
May - Jun - Jul - Aug
Sep - Oct
Annual
1973 - 1978
Ozone Partial Pressure in Nanobars
AM
PM
Local Standard Time

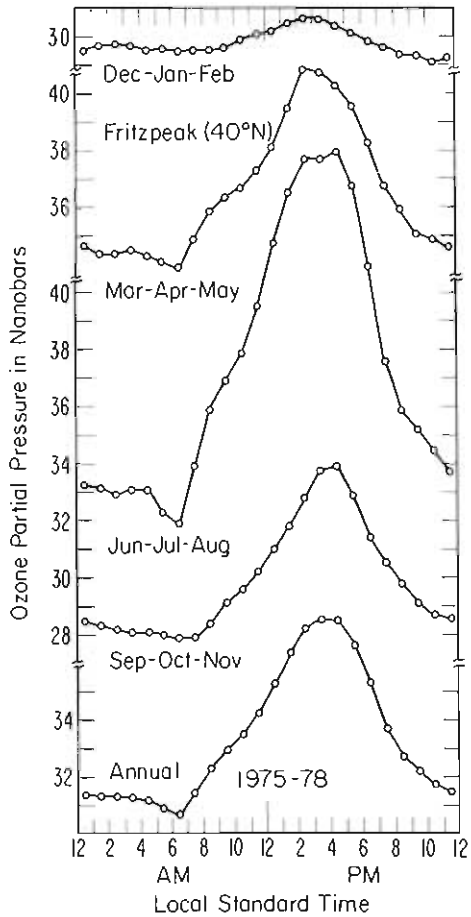

Figure 8.--Diurnal variation of surface ozone by season and for the year at Mauna Loa, Samoa, South Pole, and Barrow (p. 30), and at Fritz Peak, Colo. (p. 31).

These variations appear to take place on a scale of one to several days. This time frame is suggestive of synoptic scale weather events during which air masses of differing ozone content move over a station or meteorological conditions allow enhanced ozone mixing from ozone rich layers above.

The most pronounced day-to-day changes in surface ozone occur at Barrow during the spring when it is not unusual for daily ozone values to fluctuate from near zero to 30 to 40 nanobars. The near zero values may persist for a couple of days. It is not clear where air so depleted of ozone originates.

Seasonal Variation

Seasonal variation is a marked feature of the surface ozone behavior at the GMCC stations (fig. 11). At the South Pole where day-to-day changes are relatively small the most striking feature of the surface ozone record is the annual cycle with a range equal to about 50% of the average annual concentration. A rather sharp minimum occurs in February or March and a broad maximum from July through November (see fig. 9).

Unlike the behavior of surface ozone, the total ozone data at high latitudes in the Southern Hemisphere show a broad minimum centered around March and April and a sharp maximum in November following that in surface ozone by about

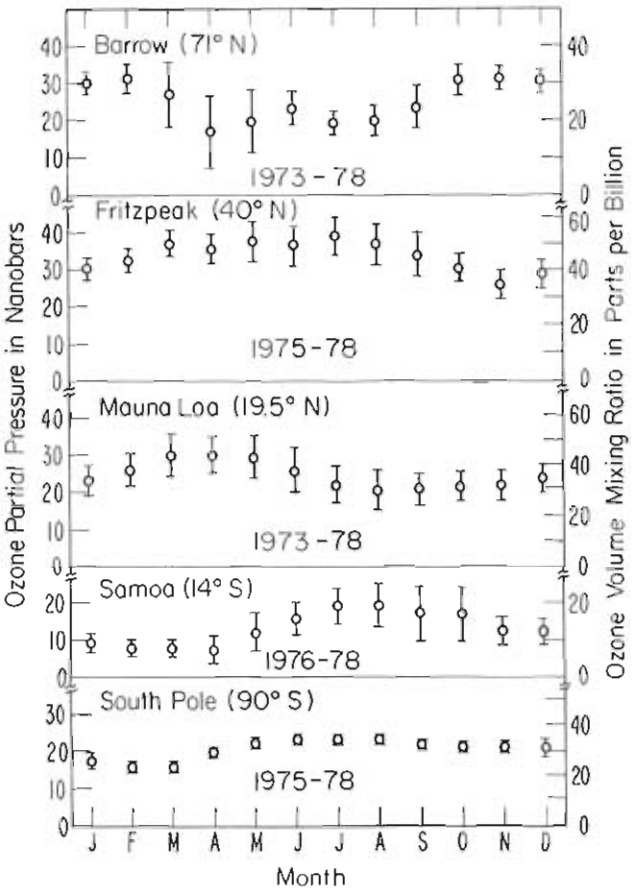

Figure 9.--Averaged monthly surface ozone amounts. Bars are plus and minus one standard deviation and represent variability within the month.

2 months. This difference in the annual cycle suggests loose coupling between the tropospheric and stratospheric ozone distributions at these latitudes.

At Samoa the maximum in surface ozone in July or August is sharp with the minimum extending over several months from January to April. Here again the surface ozone has a phasing relationship with total ozone in which the surface ozone maximum occurs earlier by about 2 months. This again could indicate that the coupling between ozone in the tropical troposphere and stratosphere of the Southern Hemisphere is relatively weak.

In high latitudes of the Northern Hemisphere at Barrow the surface ozone annual cycle is out of phase with that in total ozone. In surface ozone the maximum occurs early in the winter, several months before the maximum in total ozone. The minimum in surface ozone comes at about the time of maximum in total ozone. The month-to-month changes at Barrow are unique. Three relative maxima seem to occur in February, June, and November. These maxima do not appear to be an artifact of the averaging process brought about by the maximum shifting from month-to-month from one year to the next. They show up regularly each year (see fig. 11).

The minimum between November and February is a relatively small dip in generally high ozone values and occurs during the dark period at Barrow. The maximum in June is a small peak during generally lower values and occurs in the period when the Sun does not set at Barrow.

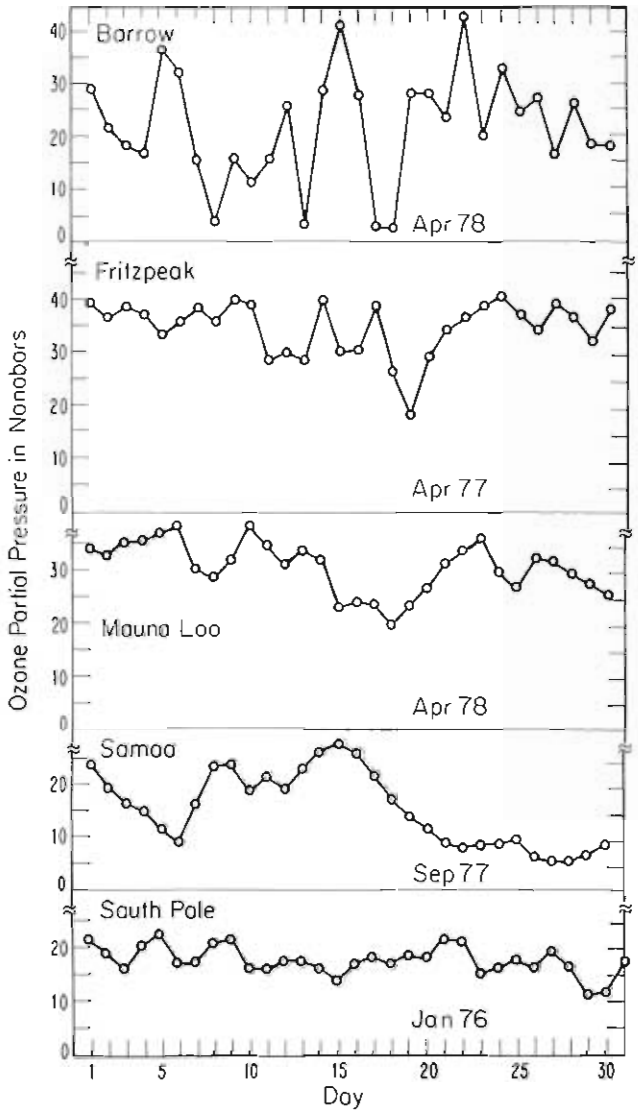

Figure 10.--Example of day-to-day variations of surface ozone.

At Mauna Loa the maximum comes in the spring, and the rather broad minimum extends from late summer through the fall. Both the maximum and minimum in surface ozone precede those in total ozone. At Mauna Loa this seems to indicate that a more direct relationship exists between stratospheric ozone and surface ozone since the maxima and minima of each fall during the same season but that other important factors must contribute to the timing of the annual cycle in surface ozone.

3.4 Stratospheric Water Vapor

In mid-1978 GMCC began to develop a program to measure regularly the water vapor content of the stratosphere. The program was managed by S. Oltmans within the Monitoring Trace Gases Group of GMCC, and F. Polacek was hired to prepare the instrumentation and make the balloon flights. This program will continue

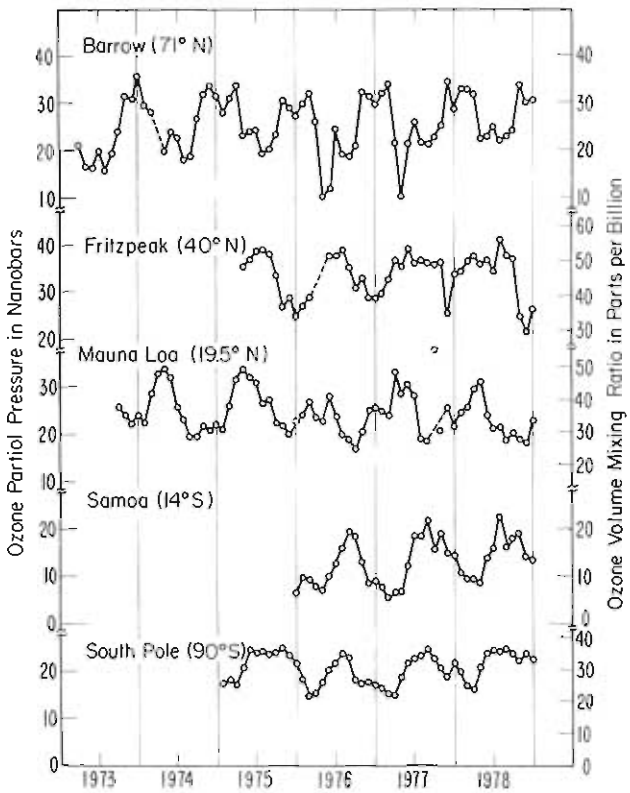

Figure 11.--Mean monthly surface ozone concentrations.

the long series of stratospheric water vapor measurements made by J. Mastenbrook of the Naval Research Laboratory since 1964 (Mastenbrook, 1971, 1973).

The latter half of the 1978 was spent training, procuring equipment, and securing an adequate facility for making the balloon flights. The balloon-borne package consists of the frost point instrument and a valving mechanism that allows the balloon to turn around at a predetermined altitude and descend at a controlled rate. Since measurements are made during descent, a major source of contamination is eliminated because the instrument is ahead of the balloon's wake.

In operation the frost point instrument (see fig. 12) maintains a condensate (ice or water) on a polished mirror interposed between an induction heater and a heat sink of freely boiling coolant. An optical detection system senses the scattering of light directed on the mirror and controls the input to the heater to keep the size of the condensate essentially constant and thus maintain the mirror temperature at the frost point temperature. A thermistor embedded in the surface of the mirror senses this temperature which is telemetered as a modulation of the standard radiosonde transmission. Periodically the mirror is cleared to reform a finer grain condensate at the edge of the condensate spot.

Previous versions of the instrument (Mastenbrook, 1968) were produced by Mastenbrook; the GMCC instrument will be produced commercially and will contain updated electronics, light sources, and sensors.

Initial plans call for monthly flights from Boulder to be made simultaneously with flights near Washington, D.C., by Mastenbrook. Future plans may include two flights a month from Boulder and the eventual establishment of a network of several stations.

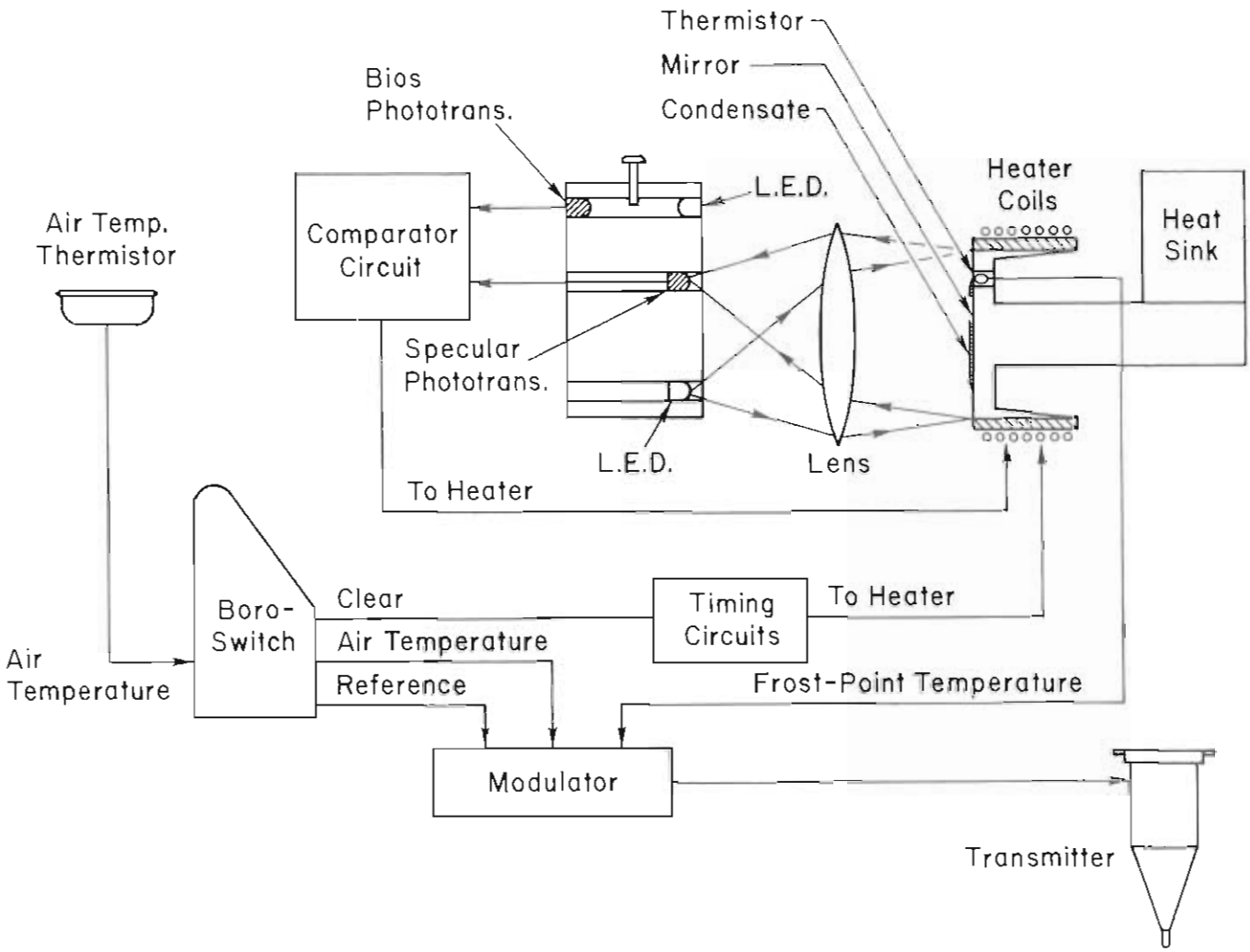

Figure 12.--Schematic diagram of the frost point hygrometer.

3.5 Halocarbons and N_2O

3.5.1 Operations

Few changes were made in the halocarbon and nitrous oxide monitoring programs during 1978. Data quality for all constituents measured (CCl_3F, CCl_2F_2, and N_2O) remained high, as it has since 1977 after sampling and analysis techniques were changed to use of pressurized dual sample flasks and calibration of the chromatograph with reference gases.

To upgrade the program further, research is continuing into a number of potential problems. Ambient air rather than dry air samples are currently collected, and analysis results are presented in terms of dry air using theoretically derived corrections based on measurements of pressure, temperature, and

relative humidity. Work is continuing to verify experimentally that the theoretically deduced corrections are highly reliable. Uncertainties of up to ± 10% may be associated with absolute calibrations of the CCl_3F, CCl_2F_2, and N_2O reference gases currently in use. Refinements in calibration gas preparation are needed to reduce this error to ± 1% or less. Tests are being made to assess the stability of the reference gases during prolonged storage. CCl_2F_2 contamination, caused by temporary use of pure CCl_2F_2 to calibrate a nephelometer at Barrow, is being investigated. Other potential problem areas under investigation relate to contamination of sample flasks, flask trace gas-wall effects, and chromatographic analysis apparatus nonlinearity characteristics.

3.5.2 Data Analysis

During the latter part of 1978 past and current data were processed to improve their reliability. Statistical and meteorological data selection criteria were applied to raw data to eliminate data degraded by sampling and analysis problems. The work included recalibration of reference gas standards, as well as interlaboratory calibration gas intercomparisons.

Raw and selected data obtained from 1973 through 1978 are being prepared for archiving at the National Climate Center, Computer Products Branch, Federal Building, Asheville, NC 28801. The data will also be available in a NOAA Technical Report that will describe the sampling and data selection procedures.

Linear regression lines fitted to the selected data are shown in figs. 13 and 14. Preliminary data analysis results, yielding CCl_3F, CCl_2F_2, and N_2O mixing ratios and mixing ratio growth rates, are given in table 10. Data for 1977 and

Table 10.--Summary of CCl_3F, CCl_2F_2, and N_2 measurement results

Trace gas	Date	Station	Mixing ratio growth rate	(95%) S.E. growth rate	Res. standard deviation	Corr. coeff. squared	Mixing ratio	(95%) S.E. mixing ratio
CCl_3F	Jan 1, 1978	BRW	13.1 pptv yr^{-1}	±1.8	3.8	0.756	165.3 pptv	±0.9
		NWR	13.1 "	±1.6	3.8	0.785	162.1 "	±0.9
		MLO	13.4 "	±1.6	3.9	0.774	155.0 "	±0.9
		SMO	13.2 "	±1.4	3.4	0.826	146.5 "	±0.8
		SPO	15.4 "	±7.4	12.8	0.408	146.5* "	±5.1
CCl_3F	Jan 1, 1975	BRW	20.3 "	±5.4	25.7	0.399	116.2 "	±6.5
		MLO	17.6 "	±3.7	21.9	0.469	107.4 "	±4.6
		SMO	17.7 "	±4.7	23.2	0.432	98.6	±6.7
CCl_2F_2	Jan 1, 1978	BRW	10.1 "	±8.1	5.2	0.161	296.9** "	±5.5
		NWR	19.1 "	±3.7	6.6	0.707	285.8 "	±2.3
		MLO	18.8 "	±3.7	5.8	0.656	279.9 "	±2.2
		SMO	18.4 "	±3.3	6.6	0.655	262.5 "	±1.5
		SPO	20.8 "	±6.1	10.2	0.652	258.6 "	±4.0
N_2O	Jan 1, 1978	BRW	-1.9 ppbv yr^{-1}	±1.5	2.0	0.097	336.0 ppbv	±0.8
		NWR	0.6	±1.7	2.6	0.009	335.8 "	±0.9
		MLO	-1.9 "	±1.4	2.1	0.109	334.4 "	±0.8
		SMO	1.3 "	±1.7	2.3	0.049	334.1 "	±0.9
		SPO	-4.3 "	±1.9	3.3	0.414	335.0 "	±1.2

*Value used in analysis was 143.8 pptv derived from observations made in Jan 1979 and extrapolated to Jan 1, 1978.
**Value used was Dec 31, 1978, result of 288.3 pptv derived from linear regression line, extrapolated to Jan 1, 1978.

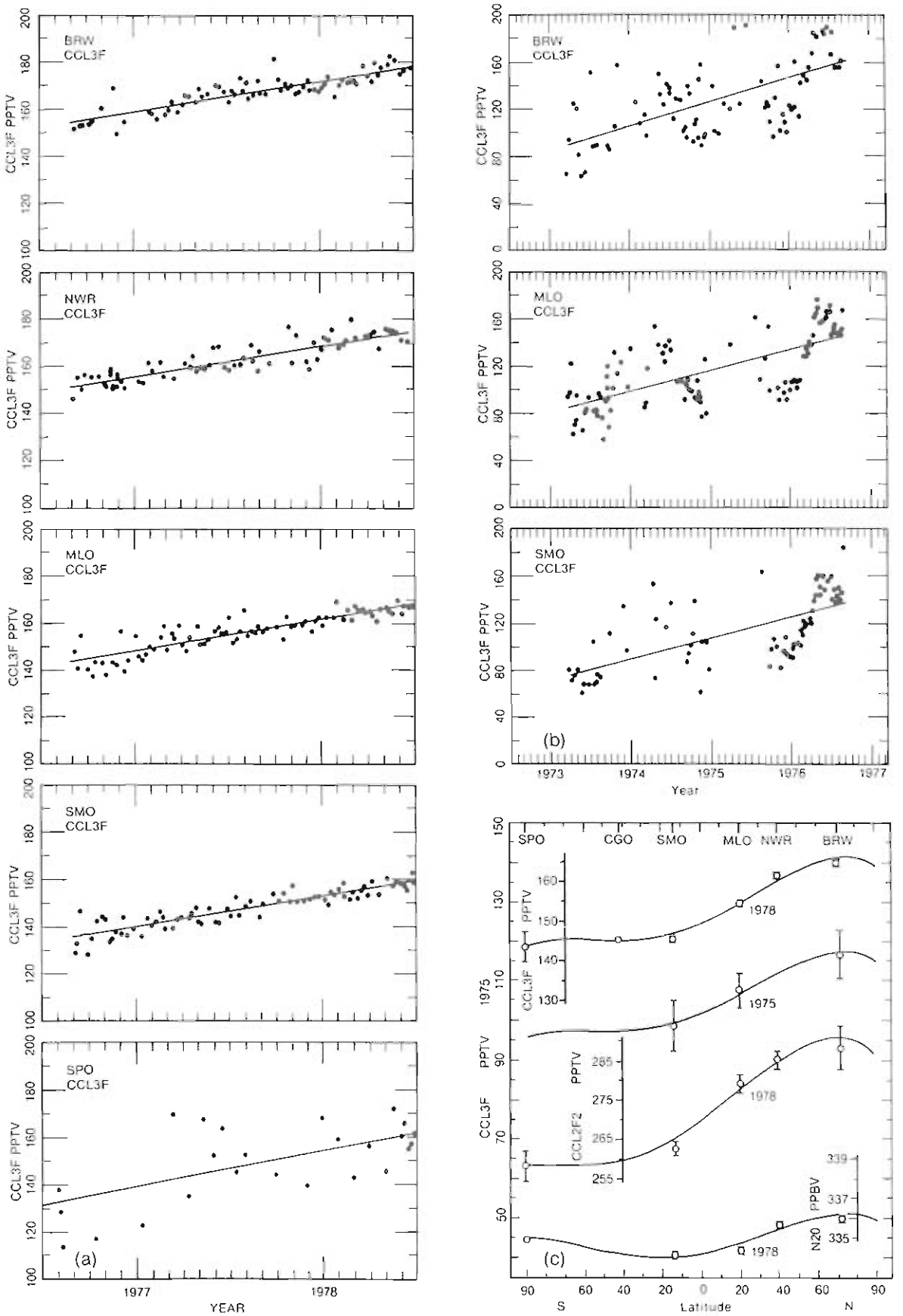

Figure 13.--Linear regression lines fitted to (a) selected 1977 and 1978 CCl_3F data and (b) selected 1973 to 1977 CCl_3F data; and (c) plots of latitudinal distributions of near ground-level CCl_3F, CCl_2F_2, and N_2O.

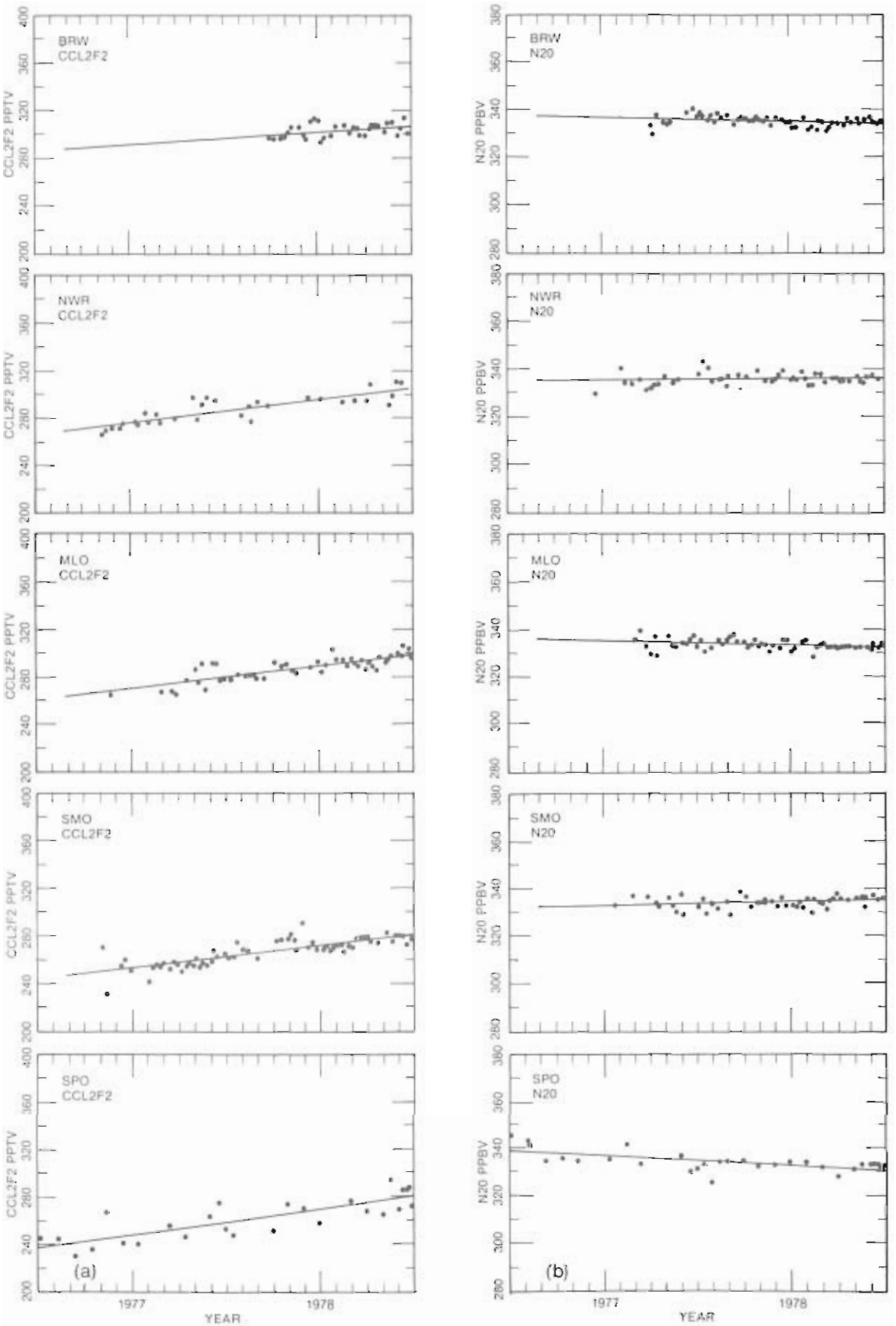

Figure 14.--Linear regression lines fitted to (a) selected 1977 and 1978 CCl_2F_2 data and (b) selected 1977 and 1978 N_2O data.

1978 are considered to be of high quality since air samples during this time interval were analyzed by using reference calibration gases traceable to R. A. Rasmussen standards maintained at the Oregon Graduate Center. Data obtained before 1977 are considerably less reliable since calibration gases were not used when analyzing samples; rather, reliance was placed on the coulometric performance of the chromatographic analysis apparatus.

Results of a preliminary analysis of the CCl_3F and CCl_2F_2 data are shown in tahle 11. The analysis has yielded best estimate tropospheric residence times of 86 yr for CCl_3F and 113 yr for CCl_2F_2. Taking into account measurement random standard errors, as well as estimated systematic errors associated with the calibration gas mixing ratios, minimum tropospheric residence times for CCl_3F and CCl_2F_2 of 30 and 33 yr, respectively, have been determined. Included in table 11 is information on global abundances, global mixing ratios, gradients, and interhemispheric exchange parameters derived from the CCl_3F and CCl_2F_2 measurement data.

3.6 Stratospheric Aerosols

3.6.1 Mauna Loa Lidar

Although the lidar performed exceptionally well during the first half of 1978, problems developed afterward. During spring 1978, the output etalon on the laser was replaced with a 35% dielectric reflector, which boosted power output and made adjustment much more stable. We were able to achieve output energies 50% greater than the manufacturer's specifications. The laser head was thoroughly rejuvenated at this time, and we also began using neutral density filters to attenuate the signal so that more accurate tropospheric profiles could be obtained.

Although the laser was operated at very high power levels during summer 1978, the laser output decreased slowly during the fall, probably because of damage to the new output reflector. The field staff did not find damage to the mirror during a system inspection, bnt subtle damage was apparent on closer inspection during the following spring, at which time the reflector was repaired.

From November to January minor problems in the data acquisition system prevented computer analysis, and Polaroid photos were taken.

3.6.2 Barrow Lidar

The Barrow lidar system is nearly completed. Development of the signal processing system was a major task this year. In spring 1978, a new dynode chain was designed and fabricated. After testing, it was fonnd that the signals were still being distorted by the strong return from the near atmosphere, so we tested the NCAR dynode design. The circuit was fabricated during winter 1978 and seemed satisfactory. It was also discovered that the Biomation transient digitizer on the Barrow lidar was more sensitive to overload than the Mauna Loa digitizer. This meant that we had to either develop a clipper unit and implement a switching amplifier as NCAR had done, or find another solution. During summer 1978 we tested the NCAR switching amplifier, and began fabricating our updated version of the NCAR unit. If the unit works well in Alaska, we will want to build one for the Mauna Loa lidar system.

Table 11.--Summary of CCl_3F and CCl_2F_2 data analysis results

Parameter	CCl_3F Jan 1, 1978	CCl_3F Jan 1, 1975	CCl_2F_2 Jan 1, 1978
Global mixing ratio, χ (pptv)	153.4 ± 0.9*	102.9 ± 3.9	272.5 ± 2.3
N.H. mixing ratio, χ (pptv)	159.8	109.9	283.8
S.H. mixing ratio, χ (pptv)	147.0	95.9	261.2
N.H.-S.H. mix. ratio diff. (%)	8.4	13.6	8.3
Global abundance, A ($\times 10^6$ kg)	3069.3 ± 18.4	2058.4 ± 78.2	4799.5 ± 40.5
N.H. abundance, A ($\times 10^6$ kg)	1599.0	1099.3	2499.4
S.H. abundance, A ($\times 10^6$ kg)	1470.3	959.1	2300.1
N.H.-S.H. abund.diff. ($\times 10^6$ kg)	128.7	140.2	199.3
Release, I(±10%) ($\times 10^6$ kg yr^{-1})	299.7	316.1	371.9
Measured atm. growth rate (pptv yr^{-1})	13.2 ± 0.8	17.7 ± 2.9	18.7 ± 2.2
Gradient 20° N-15° S (pptv per deg. lat.)	0.25	0.26	0.51
Interhemispheric diffusion coeff. K ($\times 10^6$ m^2 s^{-1})	0.5	0.7	0.4
Interhemispheric exchange rate, τ_e (yr)	1.2	0.9	1.5
Residence times; τ(± 0%) Cunnold et al. (1978) (yr)	-	-	101
$\tau(I_R + 3\%)$ Cunnold et al. (1978) (yr)	39	-	21
$\tau(I_R + 5\%)$ Cunnold et al. (1978) (yr)	30	-	18
τ(± 0%) new method (yr)	86	-	113
τ(M - 5%) new method (yr)	37	27	39
τ(M - 10%) new method (yr)	30	20	33

*Indicated errors in concentrations, abundances, and growth rates are 95% confidence interval random standard errors.

Two new dyes, Rhodamine B and Red 6, were tested with wavelengths of 0.62 μm and 0.695 μm, respectively, because the signal-to-noise ratio of the lidar is improved at longer wavelengths. Neither dye had a longer lifetime than the dye in use, Rhodamine 6G, and Red 6 contaminated the system and degraded performance for some time. We changed the dye solvent from methanol to ethanol to extend dye lifetime.

The optical assembly of the lidar was refined this year. We added provisions for using narrow-band interference filters to reduce skylight background noise during daytime operation. A collimating lens was added, and filter holders were redesigned so that the filters can be changed quickly. Filter holders for neutral density filters were added to optimize daylight operation. Experiments were performed to find the ideal view field to reduce the daylight background noise to the lowest possible value. During these tests the provision for easy laser alignment designed into this system was very easy to operate with narrow fields of view.

During the development of the lidar system, we took stratospheric data at Boulder. Although the data accuracy was not high because of system problems, we observed that there were no sharp layers of aerosol caused by the two volcanic events during this time.

This year we purchased additional computer memory to make a total of 16K words. This allowed us to write the lidar control program in FORTRAN at great savings of time. If the program needs to be modified after field testing, the use of FORTRAN makes this very easy. A wavelength tuning prism assembly was added to the laser so that narrow-band interference filters can be used. A Polaroid camera and monitor oscilloscope were purchased that will be used to set up and monitor the lidar's operation and provide backup data collection capabilities during partial system failure.

In January 1979 the real-time, multitask FORTRAN program to control the lidar and process the data was completed. The overall program is described in the 1977 Summary Report. The old program was written in assembly language and was therefore difficult to modify. A closed-loop water chiller was installed to cool the laser lamp and dye. We will use a 50% antifreeze solution in Barrow to avoid freezing.

3.6.3 Data Analysis

Some data analysis was performed during 1978. A modification in the analysis program allows the incorporation of rawinsonde temperature and height data so that the Rayleigh backscatter can be calculated more accurately. Although not very important at Mauna Loa, it will be important at higher latitudes where the temperature profiles depart markedly from a standard atmosphere. Final analysis of some older data was begun. The Polaroid photos from 1973 were reanalyzed by C. Shilvock. The paper tapes containing data from 1974 to the present were loaded onto the disc by M. Crabtree so that final analysis can proceed. J. Harris modified the lidar computer program so that the disc can be used as a source. A FORTRAN version of the analysis program was written during 1979 to try to streamline the data analysis procedures.

3.7 Surface Aerosols

The GMCC surface aerosol monitoring program for 1978 included the measurement of condensation nuclei at all sites and integrated aerosol light scattering at Barrow, Mauna Loa, and Samoa.

Condensation nuclei were measured continuously by using G.E. nuclei counters, which had been modified to improve sensitivity and reliability. A Pollak photoelectric nuclei counter, located at each site, served as a secondary standard and provided routine calibration for the other nuclei counters on site.

Four-wavelength nephelometers measured integrated aerosol light scattering continuously at the observatories. These instruments were calibrated every 2 months by filling them with CO_2 gas and adjusting the instrument output to the known scattering coefficients of CO_2. An internal calibration check was performed weekly.

3.7.1 Barrow

Pollak counter SN16 was operated routinely at Barrow without problems throughout 1978. Daily observations provided routine calibration checks for the G.E. counter. Five consecutive Pollak observations were made weekly to provide for a calibration adjustment of the G.E. counter.

During DOY 108-160, the Barrow G.E. counter was sent to Boulder for cleaning of the casting and rewiring of the chassis. Otherwise, the instrument was down only occasionally for maintenance and was operational for 67% of 1978. Calibrations were performed weekly (only during background conditions) and a routine daily check provided quality control. All data were recorded on magnetic tape and a backup chart recorder.

Four-wavelength nephelometer SN105 operated properly throughout most of 1978. The instrument was sent to Boulder for repair on DOY 171 and returned to Barrow on DOY 216. The interior of the instrument was cleaned and painted, and both white objects were painted with Eastman white reflectance coating. The Barrow nephelometer was operational for 71% of 1978, and all data were recorded on magnetic tape and a backup chart recorder.

3.7.2 Mauna Loa

Pollak counter SN13 was operated hourly during the normal working day throughout 1978 with no problems. In addition, five consecutive Pollak observations were made weekly to provide calibration for the G.E. counter.

From DOY 236-270, the Mauna Loa G.E. counter was sent to Boulder for repairs and the casting was cleaned and the optical chamber repainted. The Mauna Loa G.E. counter was operational for 82% of 1978.

The Mauna Loa four-wavelength nephelometer was on line from DOY 31-364 except for minor downtime for maintenance and calibration. The instrument was operational for 85% of 1978, and all data were recorded on magnetic tape and a backup chart recorder.

3.7.3 Samoa

Pollak counter SN20 operated routinely at Samoa during 1978 with no problems. Daily observations were performed for quality control on the G.E. counter and a weekly set of five Pollak observations was made for the calibration of the G.E. counter.

The Samoa G.E. counter operated properly throughout the year, but because of numerous station power outages, the data set it produced was equivalent to 85% of the hours in the year.

The Samoa four-wavelength nephelometer was inoperative from DOY 301-365 and was sent to Boulder for repair. Its problems were a clogged inlet port on the blower box, causing the blower to overheat and shut down, and loss of sensitivity in the infrared in the photomultiplier, which required replacement. The instrument's interior was cleaned and painted with optical black paint, and the two white objects were painted with Eastman white reflectance coating. The instrument was returned to Samoa on March 16, 1979. It was operational for 70% of 1978, and all data were recorded on magnetic tape and a backup chart recorder.

3.7.4 South Pole

Pollak counter SN15 was operated twice daily during clean conditions with no problems during 1978. The G.E. counter operated properly throughout the entire year and produced good data for 96% of the year. South Pole G.E. counter data have all been scaled by using a linear regression technique to bring them into agreement with the Pollak counter data. All data were recorded on magnetic tape and a backup chart recorder.

3.7.5 Data Analysis

Aerosol data are routinely analyzed by using the procedure and flow diagram presented in last year's annual report. Briefly, all observer notes and chart records are examined immediately when they are received (approximately every 2 weeks) to verify instrument performance and data quality. Ouce a monthly tape is available from the Data Acquisition and Management Group, hourly aerosol data are loaded into a disc file in the NOAA CDC 6600 computer for calibration and editing. At this time, missing data are filled in from the chart records, data quality is evaluated, and a final disc file is constructed of all acceptable data. All data through 1978 are available from GMCC in Boulder, Colo.

3.7.6 Discussion of Selected Data

Condensation nuclei and light scattering data from all GMCC stations are presented in fig. 15. Monthly geometric means of all data are plotted for Barrow, Samoa, and South Pole. Monthly means of 0100-0700 LST Mauna Loa data were used to avoid contamination from the well-known daytime upslope wind. The Barrow light scattering data suggest an annual cycle with winter values greater than 10^{-5} m^{-1} and summer values as low as 10^{-6} m^{-1}. However, Aitken nuclei data at Barrow show a biannual cycle with maxima in spring and late summer. To reveal more clearly the annual cycles, departures from the annual mean by month of light scattering (solid line) and condensation nuclei (dashed line) are given in fig. 16.

The Mauna Loa light scattering data in fig. 15 suggest an annual cycle with a maximum in late spring and minimum during the winter. However, no obvious

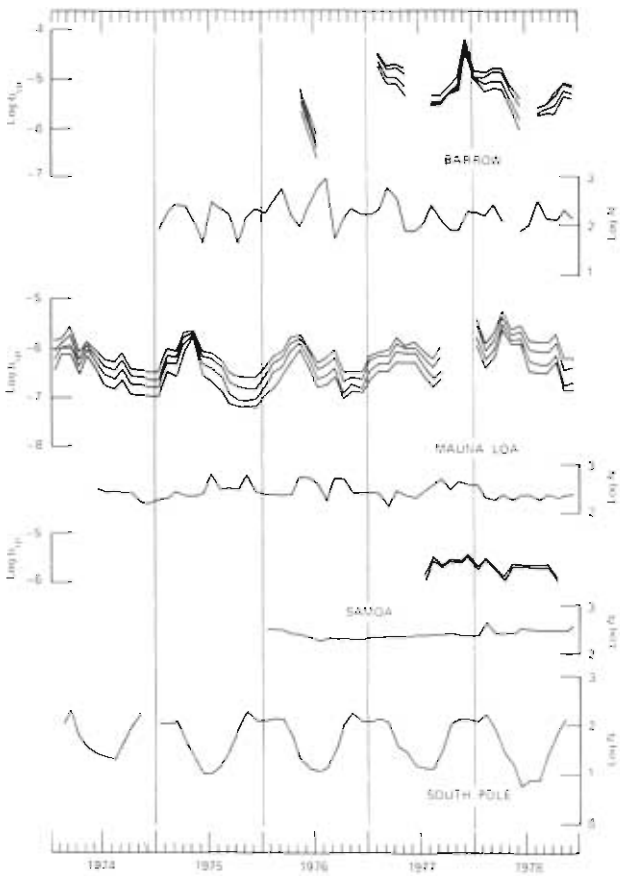

Figure 15.--Light scattering (b_{sp}) and Aitken nuclei (N) data for all GMCC stations. Barrow and Mauna Loa light scattering data show four wavelengths in order 450, 550, 700, and 850 nm whereas Samoa data are in order 450, 850, 700, and 550 nm.

cycle is present in the Mauna Loa Aitken nuclei data. Departures from the annual means by month for Mauna Loa light scattering and condensation nuclei data are shown in fig. 17 to reveal annual cycles. The annual cycle in light scattering data with a maximum in April-May and a small secondary peak in September shows up strongly although there is no apparent annual trend in the Aitken nuclei data. Because there are 5 full years of data from Mauna Loa, we can take departures from the mean for each year and then calculate a mean and standard deviation for each month of the year.

Samoa light scattering and condensation nuclei data shown in fig. 15 clearly represent a marine aerosol and exhibit no obvious annual cycles. The departures

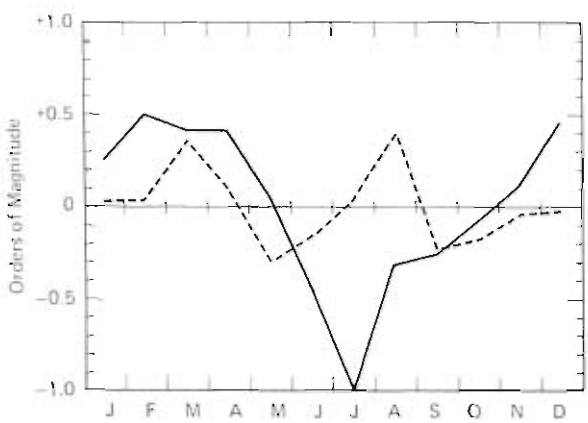

Figure 16.--Departures from the mean by month of light scattering (solid line) and Aitken nuclei (dashed line) data for Barrow. Geometric means are used so that the ordinate is expressed in orders of magnitude.

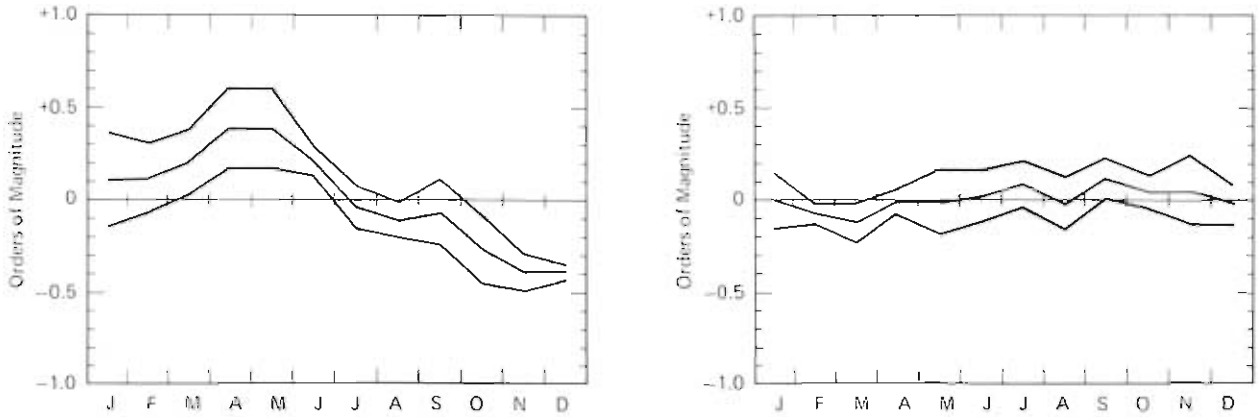

Figure 17.--Departures from the annual mean by month of 550-nm wavelength light scattering (left) and Aitken nuclei (right) data for Mauna Loa. Departures from the mean were determined for each year, and then a mean (middle line) and standard deviation (upper and lower lines) were calculated for each month.

from the annual mean by month of light scattering and Aitken nuclei shown in fig. 18 further confirm the absence of any annual cycles.

The well-known annual cycle in Aitken nuclei at South Pole shows up strongly in fig. 15, and its repeatability is apparent from fig. 19, which gives departures from the annual mean by month along with the standard deviations by month for the 5 years of data. The annual cycles (or lack of them) at the four stations are discussed in more detail by Bodhaine (1979).

Figure 20 shows monthly geometric means of light scattering at Barrow for each hour of the day. Time of day is given in GMT. The magnitude of the light scattering is highest during early spring and lowest during summer. For all

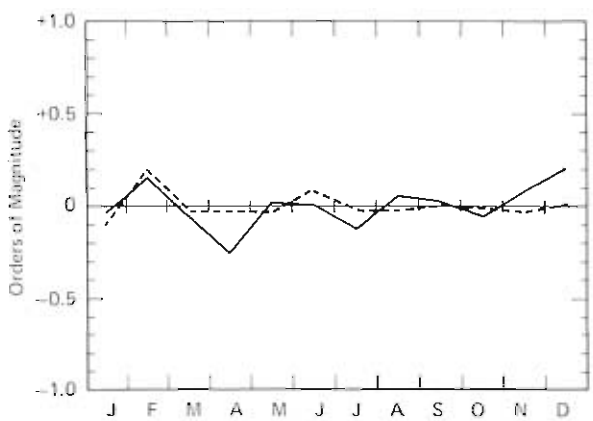

Figure 18.--Departures from the mean by month of light scattering (solid line) and Aitken nuclei (dashed line) data for Samoa.

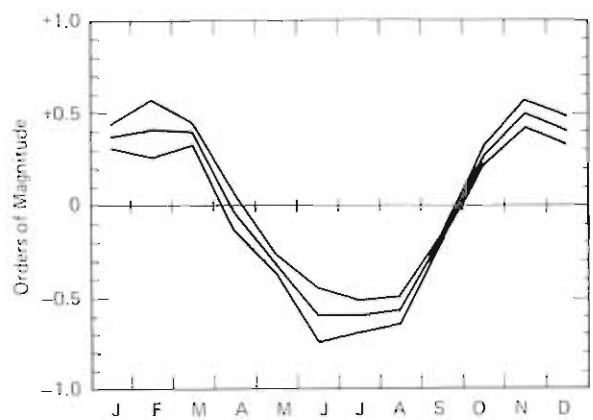

Figure 19.--Departures from the annual mean by month of Aitken nuclei at South Pole. Departures from the mean were determined for each year and then mean (middle line) and standard deviations (upper and lower lines) were calculated for each month.

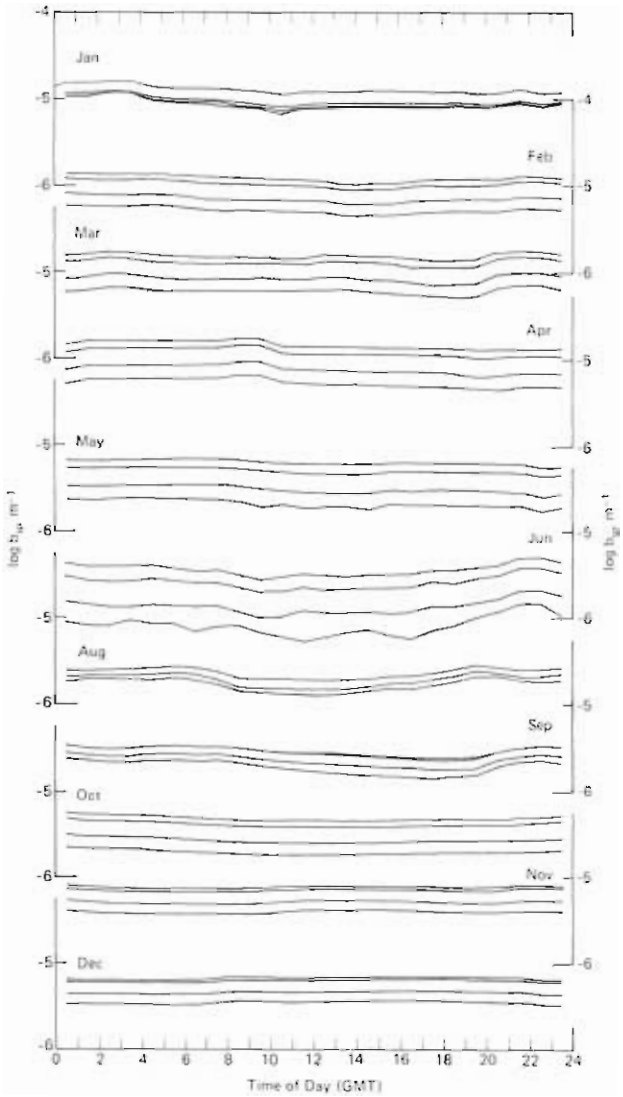

Figure 20.--Monthly geometric means for each hour of the day for the Barrow nephelometer in 1978. The four channels of light scattering data are in order 450, 550, 700, and 850 nm.

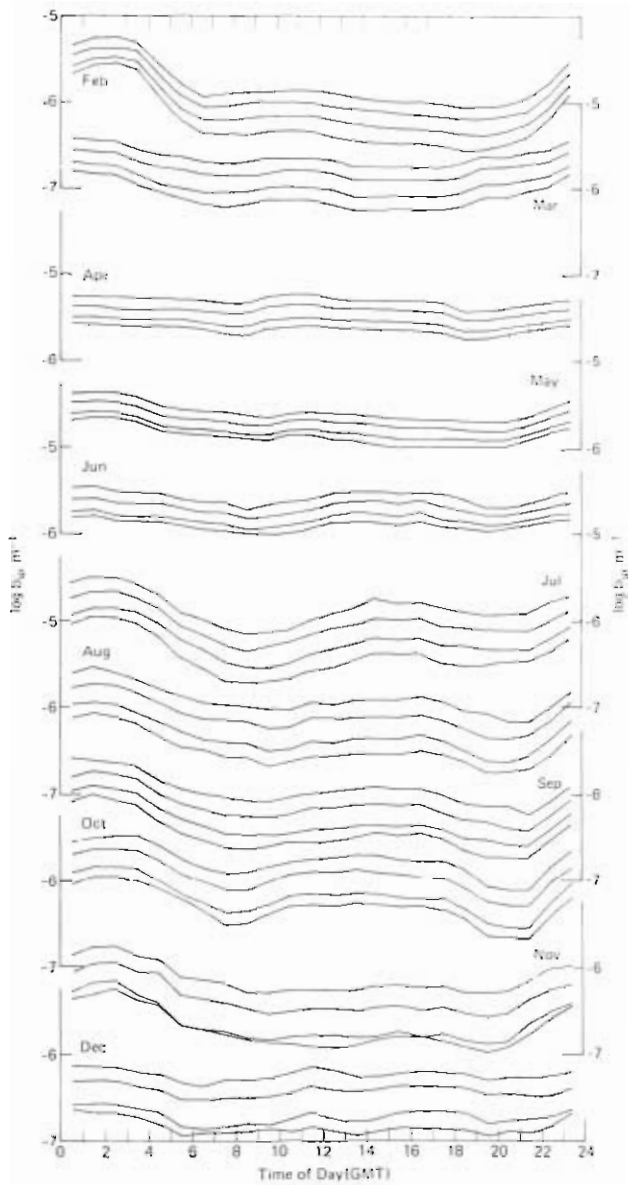

Figure 21.--Monthly geometric means for each hour of the day for the Mauna Loa nephelometer in 1978. The four channels of light scattering data are in order 450, 550, 700, and 850 nm.

months, light scattering data are greatest at 450 nm and decrease in the order 550, 700, and 850 nm. However, spacing of the four channels indicates a tendency towards larger aerosols in January, August, and September, and small aerosols in June. Furthermore, a small diurnal cycle is present, apparently related to the length of daylight at the Barrow stations. This effect is seen most clearly in the data for March, August, and September, and suggests slightly higher light scattering values during daylight hours.

Figure 21 shows monthly geometric means of light scattering at MLO for each hour of the day. Note that time-of-day is given as GMT rather than LST as in

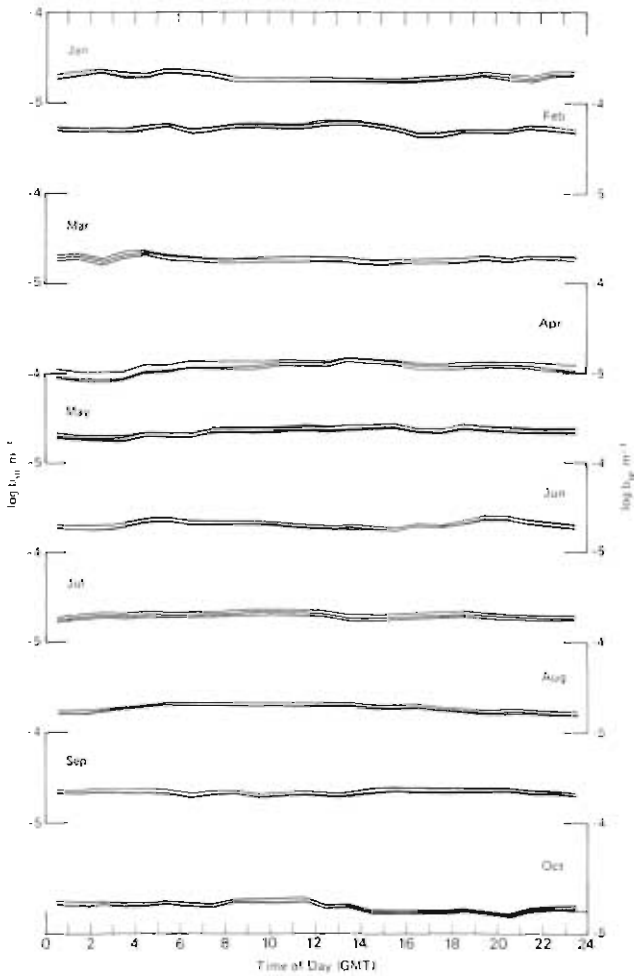

Figure 22.--Monthly geometric means for each hour of the day for the Samoa nephelometer in 1978. The four channels of light scattering data are in order 450, 850, 700, and 550 nm.

the previous summary reports. For Mauna Loa, LST = GMT-10. The data show the same general features as similar data given in previous GMCC summary reports. For example, the daytime upslope wind effect shows up clearly during most months and the magnitude of the nighttime data is highest in early summer and lowest in winter. However, it should be noted that, in general, the light scattering values are higher in 1978 than in previous years and show a less-pronounced upslope wind effect. In particular, the December 1978 data, unlike previous years, show very little diurnal effect.

Samoa light scattering data continue to show no obvious long-term trends. To examine the data for diurnal trends, monthly geometric means of light scattering for each hour of the day were calculated similarly to those for Mauna Loa and are presented in fig. 22. Although the magnitude of light scattering varies somewhat from month to month, no trend and no apparent diurnal effect are obvious in any of the months. For most months light scattering is greatest for the 450-nm wavelength and decreases in the order 850, 700, and 500 nm. The light scattering values at 450 and 850 nm are usually nearly equal, and sometimes the 850-nm data are greater than the 450-nm data. As discussed in GMCC Summary Report 1977, $\alpha 12$ is always positive whereas $\alpha 23$ and $\alpha 34$ are always negative, suggesting a narrow aerosol size distribution for the Samoa marine aerosol.

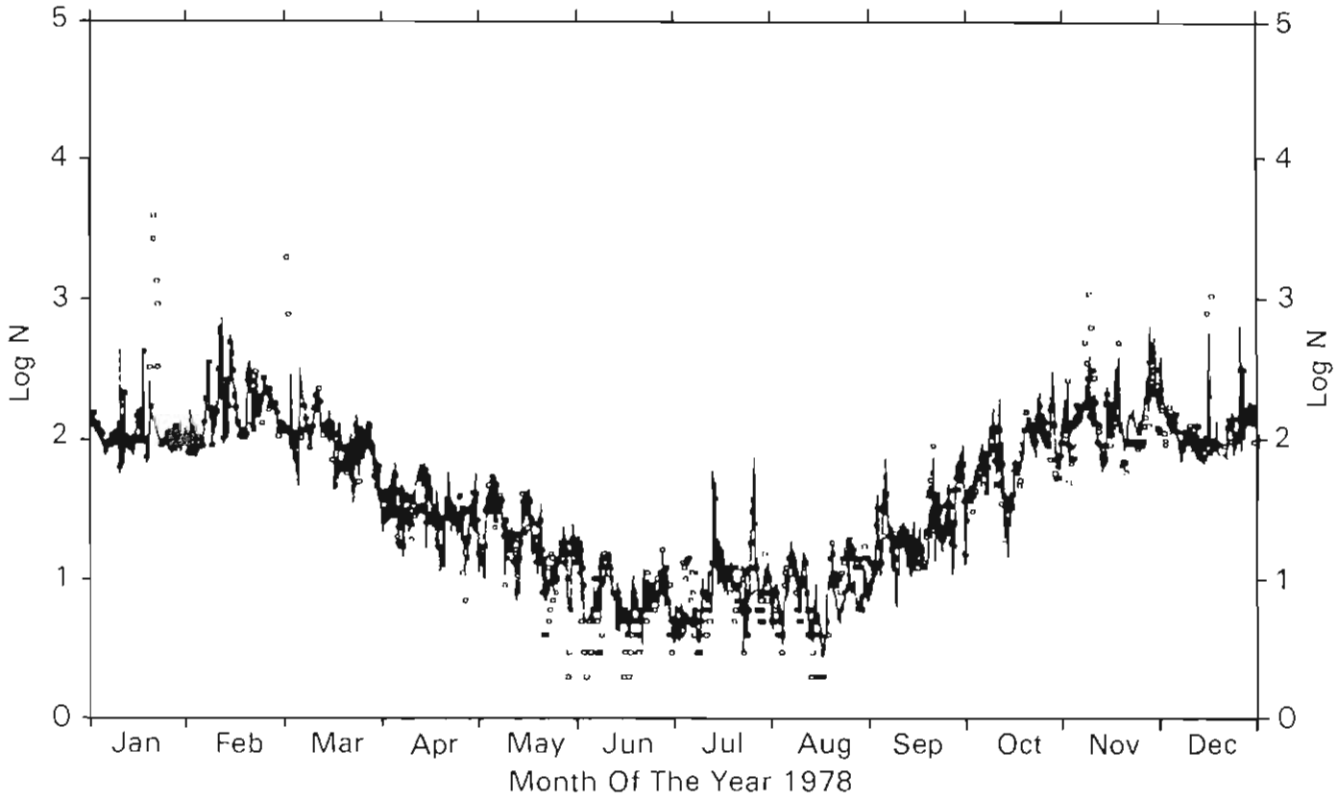

Figure 23.--Aitken nuclei data for South Pole in 1978. The solid line shows hourly means of scaled continuous condensation nuclei data whereas the squares show individual Pollak counter observations.

Condensation nuclei data for the South Pole have all been processed and are available in final edited form for 1974-1978. All automatic condensation nuclei data have been scaled according to a linear regression technique for best agreement with the daily Pollak counter calibration points. Figure 23 presents all automatic condensation nuclei data (solid) by hour and all Pollak counter data (squares) for the year 1978. Monthly means of condensation nuclei concentrations for both the G.E. counter and the Pollak counter are given in table 12.

Table 12.--Monthly means of condensation nuclei concentration (cm^{-3}) at South Pole in 1978

Counter	J	F	M	A	M	J	J	A	S	O	N	D
Pollak	111	166	84	29	17	6	8	8	24	70	131	120
G.E.	103	168	92	31	18	7	8	7	21	77	151	113

3.8 Solar Radiation Measurements

The four GMCC baseline stations continued to record solar irradiance data with the basic instrument set established in 1975-76. The instrument set includes four Eppley global pyranometers with quartz, GG22, OG1, and RG8 filter domes, Eppley UV pyranometers (excluding Samoa), and Eppley normal incidence pyrheliometers (NIP) for measurement of direct solar irradiance (excluding Barrow). Measurements are made continuously with these instruments. Data are archived as 2-min integrals in kJ m^{-2} on the absolute radiation scale.

The four GMCC observatories are also collecting discrete measurements of direct solar irradiance with Eppley NIP's. Measurements are made through a quartz window as well as OG1, RG2, and RG8 Schott glass filters.

3.8.1 Instrument Calibrations

Field instruments are calibrated at least once a year by comparison with working standard instruments at the GMCC offices in Boulder. Table 13 shows the results of intercomparisons completed in 1977 and 1978. The measurements of the filtered instruments are also compared to the quartz standard measurements. The ratio of the measurements from the filtered pyranometers to those from the standard quartz instrument is determined and compared with theoretical calculations. Year-to-year changes in the ratios indicate possible dome degradation. Additional tests are performed on the NIP Schott glass filters by comparing them with a standard filter set. Filter factors are determined after each intercomparison period and checked with the results of previous tests. The results in table 13 imply that the filters have remained stable since their initial installation. The exception is SMO where the pyranometer filter domes have degraded, probably because of the tropical environment.

Table 13.--1977-1978 field instrument calibration tests

Station	Date	Std. inst. serial no.	Cal. const. mV mW^{-1} cm^{-2}	Test inst. serial no.	Cal. const. mV mW^{-1} cm^{-2}	Response std./test	Difference (%)	Filter Factors OG1	RG2	RG8
Pyranometer comparisons										
MLO	1/26-1/31/77	10155	0.0725	12616	0.0794	1.0035	-0.35			
MLO	6/19-7/11/78	12617	0.0810	12616	0.0794	1.0041	-0.41			
BRW	5/2-5/6/77	10155	0.0725	12263	0.0919	0.9919	0.81			
SMO	7/19-8/6/78	12617	0.0810	12273	0.0927	1.0100	-1.00			
SPO	1/7-1/9/77	12617	0.0810	12271	0.1072	0.9951	0.49			
SPO	1/1-1/10/78	12617	0.0810	12271	0.1072	0.9961	0.39			
MLO	6/19-7/11/78	12617	0.0810	12560	0.0970	0.9864	1.36			
Pyrheliometer comparisons										
MLO	11/22-11/28/77	13909	0.0774	13910	0.0825	1.0071	-0.71	1.095	1.093	1.103
MLO	6/30-7/11/78	13909	0.0774	13910	0.0825	1.0097	-0.97	1.108	1.096	1.107
BRW	2/2-2/4/77	13911	0.0856	13913	0.0826	0.9845	1.55	1.105	1.110	1.111
BRW	5/2-5/5/77	13909	0.0774	13913	0.0826	1.0039	-0.39			
BLD	10/1-10/2/77	13909	0.0774	13911	0.0826	1.0092	0.92			
BLD	2/2/78	13911	0.0856	13913	0.0826	0.9848	1.52	1.106	1.111	1.111
SMO	1/6-1/8/77	13909	0.0774	13914	0.0829	1.0110	-1.10	1.095	1.105	1.100
SMO	7/5-7/6/78	13909	0.0774	13914	0.0829	1.0123	-1.23	1.098	1.103	1.100
SMO	7/19-8/9/78	13909	0.0774	13914	0.0829	1.0075	-0.75	1.095	1.100	1.104
SPO	12/19-12/30/78	13911	0.0856	13912	0.0815	0.9978	0.22	1.094	1.098	1.122
MLO	11/22-11/28/77	13909	0.0774	2119	0.0295	0.9998	0.02			
MLO	7/5-7/11/78	13909	0.0774	2119	0.0295	1.0079	-0.21			
SPO	12/19-12/30/78	13911	0.0856	2968	0.0295	1.0706	-7.06			

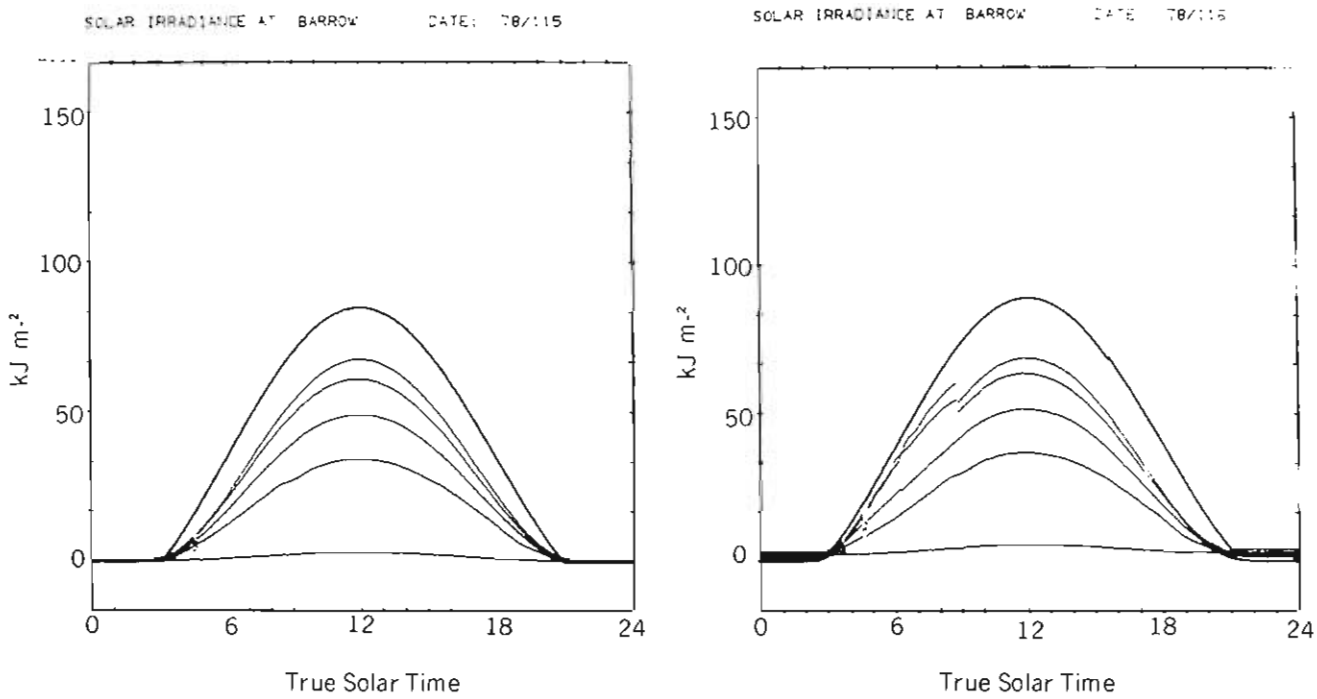

Figure 24.--(left) Clear day at BRW when pyranometer domes remained unobstructed by ice. Curves from top to bottom: calculated extraterrestrial radiation, quartz, GG22, OG1, RG8, and UV pyranometers. (right) Clear day at BRW when ice buildup occurred on quartz and GG22 pyranometer domes. Domes were freed of ice at about 0830 TST, causing a sharp decrease in the energy seen by the sensors.

3.8.2 Field Site Activities

South Pole and Barrow

The major problem at the South Pole and Barrow is ice crystal buildup on the pyranometer domes. Figure 24 (left) shows a clear day at Barrow (April 25, 1978) when the domes remained ice free. On the following day (April 26, 1978, fig. 24, right) a thin coating of ice was observed on the quartz and GG22 pyranometer domes. In this case the ice magnified the energy viewed by the sensor. The irradiance as seen by the sensor may be intensified or decreased, depending on the thickness or distribution of the ice buildup on the dome. Incidences of ice were identified and removed from the archived data set.

On November 17, 1977, new ring blowers were installed on the quartz and GG22 pyranometers at the Pole to prevent ice buildup on the domes. The ring blowers clamp to the outer perimeter of the pyranometer radiation shield. Warmed air is pumped to the ring blower through insulated plastic tubing and forced out small holes in the ring. This system replaced an old blower system which forced warm air up next to the dome through a metal ring attached underneath the pyranometer radiation shield. No improvement was observed with the new ring air blowers although the new blower system was installed primarily to improve the efficiency of keeping the domes ice free and to eliminate the possibility of data contamination caused by artificial heating of the instrument body by the old blower system. Since the new blower system proved to be less effective and preliminary tests of the old system did not indicate data contamination, the old system was reinstalled on December 21, 1977.

Tests of the blower systems at the South Pole and Barrow were conducted throughout 1978, and the systems were modified to improve their efficiency. Similar tests were made at the Boulder facility during the winter months. Although final results of the tests have not been completed, preliminary results indicate that the old blower system does not significantly affect the pyranometer output. None of the systems tested has been 100% effective.

Solar radiation data at the South Pole were contaminated for short periods of time on a daily basis by shading from GMCC and University of Maryland air sampling stacks. Shading occurred between 0800-1000 CUT for the pyranometers and 1000-1100 CUT for the NIP. Actual shading time for an individual day lasted only a few minutes within these time intervals. The shaded periods were identified and removed from the archived data set.

Mauna Loa

The solar radiation program ran smoothly during the year. A new chart recorder replaced an old Honeywell recorder used for NIP observations since 1958.

Several shading devices for continuous measurement of diffuse radiation were tested at MLO during the year. All the devices proved to be unsatisfactory because of their design. In November an Eppley shading disc was installed and operated well for the remainder of the year.

The MLO Eppley UV pyranometer (10232) was returned to Eppley on October 25 for repair and recalibration. It was placed back in service on November 27. Tests at Eppley showed that the narrow bandpass filter had deteriorated and sensitivity had decreased by nearly 74%. A new filter was installed in the instrument and a new calibration factor established.

The 13-channel radiometer was brought back on line in December 1978. The instrument's output will be analyzed to determine its relative accuracy, and some modification may be undertaken in 1979. An evaluation of the instrument as a monitoring tool is continuing.

Samoa

In 1977, deterioration of the RG8 and OG1 pyranometer domes caused glass discoloration and a degradation of 5% or more in the observed irradiance. The exact cause of the dome deterioration is unknown. The OG1 and RG8 domes were replaced in May 1977, but by May 1978 they had to be replaced again. Attempts to solve this problem are continuing.

Data

In fig. 25 3 years of normal incidence irradiance data for the South Pole are plotted for "clear" days. The solid line envelops the upper range of the measurements. The wide scatter of points (lower values) is the result of measurements taken through ice crystal precipitation periods or very thin cirrus clouds. Note the values obtained in summer reach ≈78% of the extraterrestrial value.

Plots of the daily integrals of horizontal incidence irradiance from quartz filter pyranometer for Barrow and Samoa (fig. 26) show the annual variation in

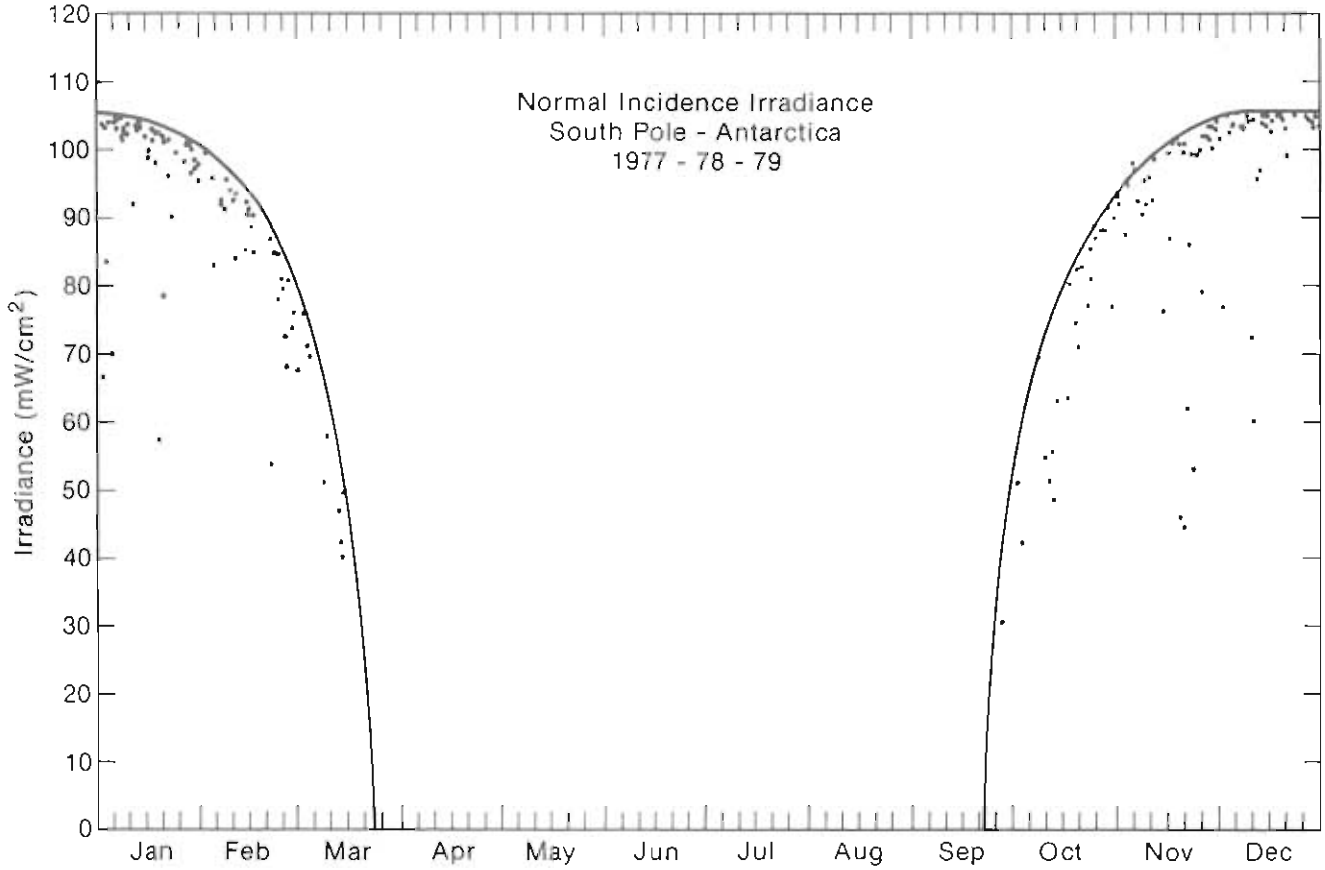

Figure 25.--1977-78-79 normal incidence solar irradiance measurements taken at SPO during clear sky, transparent cirrus and ice crystal precipitation periods. The solid line envelops upper limits of measured irradiances over the 3-yr period.

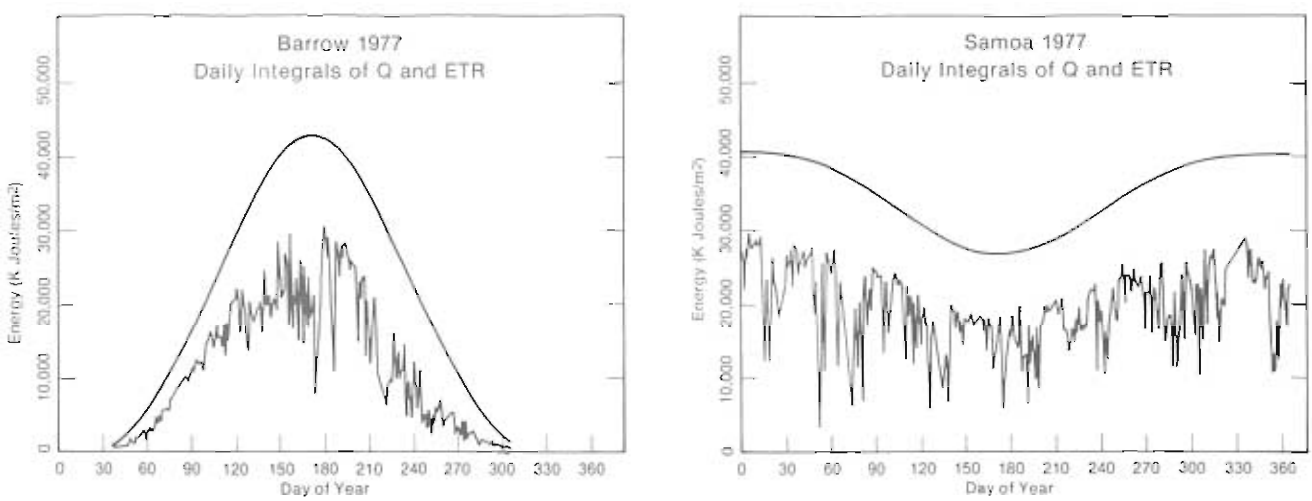

Figure 26.--Daily integrals of solar irradiances show the annual variation at Barrow (left) and Samoa (right). All days (clouds and clear) are included in the data. The extra-terrestrial solar irradiance on a horizontal surface at the top of the atmosphere for each station is shown by the upper curve.

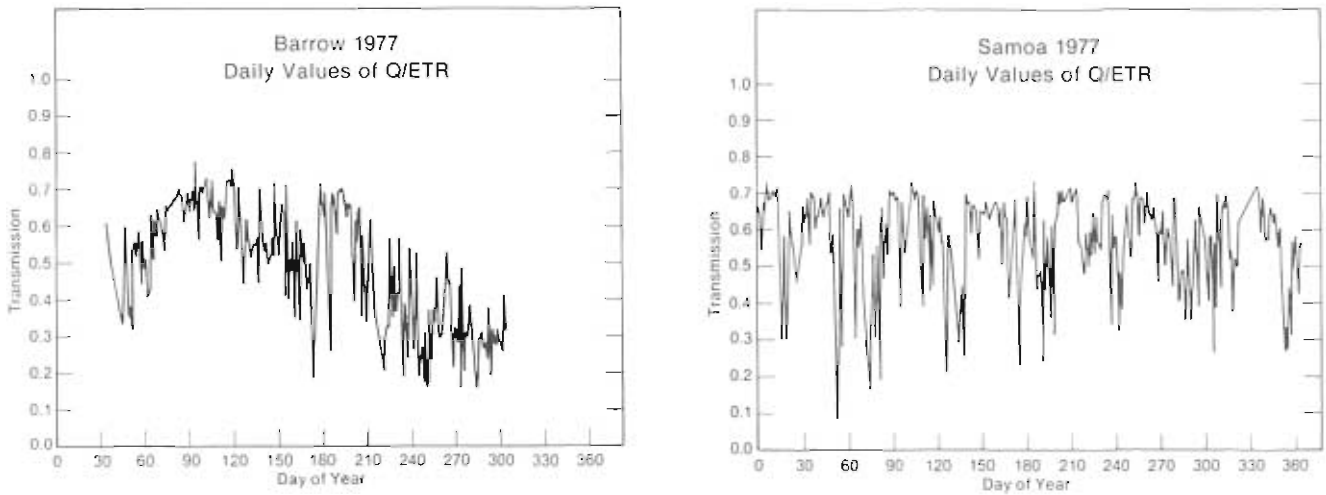

Figure 27.--Atmospheric transmission ($\frac{\text{quartz pyranometer irradiance}}{\text{ETR}}$) for Barrow (left) and Samoa (right) are plotted for day of year. Samoa shows no obvious annual cycle whereas Barrow has a springtime maximum.

solar irradiance. The solid line plotted shows the extraterrestrial value of horizontal global irradiance available at the two sites.

A simple measure of atmospheric transmission is plotted throughout the year for Barrow (fig. 27, left) and Samoa (fig. 27, right). Note that for Samoa the transmission shows no change throughout the year. Other than dips during cloudy periods the upper values remain constant at ≈70% for the year. A definite annual trend in transmission is observed for Barrow with a maximum in spring when cloudiness is at a minimum and the ice off the coast has not yet broken up. Once the ice breaks in May and June and moisture is available, cloudiness increases and transmission decreases. This decrease in transmission caused by cloudiness is prevalent for the rest of the daylight period in Barrow. It is interesting to note that the clearest sky conditions occur in Barrow when the Arctic haze phenomenon is at its peak. Consequently, the Arctic haze impact on atmospheric transmission in early spring may be significant under the clear-sky conditions that prevail during this period in Barrow.

3.9 Meteorological Measurements

3.9.1 Barrow Climatology

The GMCC Barrow Observatory, located on tundra between two saltwater marshes, is about 7 km from Point Barrow. The wind is mainly determined by large-scale weather systems, since no significant topographic barriers are found within a 300-km radius of the observatory. Between stormy periods, when the winds are westerly, the local winds result from the outflow from the polar anticyclone, which produces a persistant, easterly wind at the surface. Barrow's radiation climate is strongly influenced by the low-stratus cloud layer that forms in May and persists throughout most of the summer. The coastal cloud

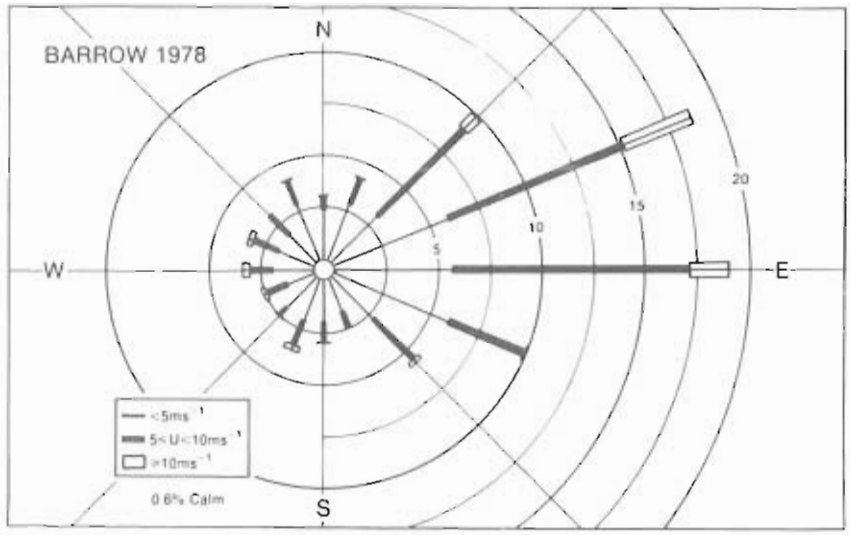

Figure 28.--Distribution of wind direction and speed for Barrow. Units are percent occurrence for the year (1978). Wind speed is presented as a function of direction in three classes: less than 5 m s^{-1}, 5 to less than 10 m s^{-1}, and equal to or greater than 10 m s^{-1}.

layer forms when incoming solar radiation in spring and summer is increasing at the same time that extensive leads in the ice pack open along the coast. On an average, only 7 days a month during the summer have clear or partly cloudy conditions. However, during the winter and early spring, clear and partly cloudy skies dominate.

The distributions of the wind direction and speed are shown in fig. 28. For almost 60% of the hours in 1978 the wind was from an easterly direction, within the sector bounded by 30 degrees to 120 degrees. The highest percentage of stronger winds also occurred in this sector. Calm conditions, when average wind speeds were less than 0.5 m s^{-1}, were observed only 0.6% of the time. As in previous years east-northeasterly winds predominated through most of the year (table 14). The maximum hourly average wind speed observed during the year was 18 m s^{-1} from an east-northeasterly direction.

Examination of the successive differences in the monthly average values of wind speed and temperature clearly indicates that two distinct seasons occurred with brief transition periods in April-May and October-November. The surface winds were lighter during the summer months. The average winter temperature was about -22°C, whereas in the short summer season the average temperature was only a few degrees above zero. The minimum hourly-average temperature observed in 1978 was -44°C in December. On the average, the wind speed observed at the GMCC Observatory was about 0.5 m s^{-1} higher, and the temperatures about 0.5°C cooler than those observed in Barrow village (NWS, 1978).

3.9.2 Mauna Loa Climatology

In the absence of a strong pressure gradient, the meteorological conditions at MLO are controlled by the diurnal heating and cooling of the surface of the

Table 14.--1978 Barrow Observatory monthly climate summary

	Jan	Feb	Mar	Apr	May	Jun	Jul	Aug	Sep	Oct	Nov	Dec
Prevailing wind directions	ENE	ENE	NE	ENE	E	E	E	E	E	NE	E	E
Average wind speed ($m\ s^{-1}$)	6.9	5.7	5.1	6.1	5.7	5.1	5.0	5.0	5.4	5.7	6.6	6.3
Maximum wind speed* ($m\ s^{-1}$)	16	12	14	13	11	13	13	12	14	18	17	15
Direction of max. wind* (deg.)	90	102	57	106	126	80	266	117	53	69	87	98
Average station pressure (mb)	1016.4	1011.1	1019.8	1017.2	1019.4	1011.2	1011.8	1010.7	1006.9	1013.7	1009.0	1008.5
Maximum pressure* (mb)	1042	1032	1037	1032	1027	1019	1019	1022	1025	1013	1041	1032
Minimum pressure* (mb)	996	988	1004	1003	1006	1000	1000	992	988	993	979	985
Average air temperature (°C)	-21.6	-26.4	-24.1	-17.1	- 9.6	- 0.8	2.8	1.8	.7	-14.1	-15.3	-25.7
Maximum temperature* (°C)	-9	-12	0	1	0	7	17	16	13	-3	0	-8
Minimum temperature* (°C)	-34	-42	-37	-32	-17	-6	-2	-3	-10	-24	-28	-44

*Maximum and minimum values are hourly averages.

mountain. At the altitude of the observatory, 3.4 km, the day is relatively evenly divided between two flow regimes, nocturnal downslope wind from the south and an upslope flow during daytime hours from the north. The wind rose in fig. 29 shows the predominance of winds from the south-southeasterly and southwesterly directions. The relatively large proportion of stronger winds, $\geq$ 10 $m\ s^{-1}$, from these directions is the result of gradient wind flow from synoptic conditions that supplement the downslope winds. Winds from the northerly direction are generally light and variable. Calm conditions occur on about 1.8% of the hours during the year. Since a northerly wind is an upslope, daytime condition, the plot of wind speed as a function of time-of-day shows slightly lower wind speeds in day light hours (Peterson, 1978, fig. 28). Wind speed minimums occur when the shift from one regime to the other occurs at 0800-0900 and at 1800 LST. Average daytime temperatures at MLO are about 11°C, and average nighttime temperatures are about 4°C.

Monthly variations in the meteorological parameters are small compared to the diurnal variations. Westerly winds are generally more common in the winter months than at other times when southerly wind prevails (table 15). The average wind speed for the year is 5.4 $m\ s^{-1}$, with the maximum speed of 19 $m\ s^{-1}$ from a direction of 256 degrees. The average station pressure is 680.9 mb, with an average range of 8 mb between maximum and minimum values. Both the average and the separation between maximum and minimum vary little through the year. The air temperature shows a small annual cycle with an amplitude of about 3°C. Maximum and minimum values show this cycle as well.

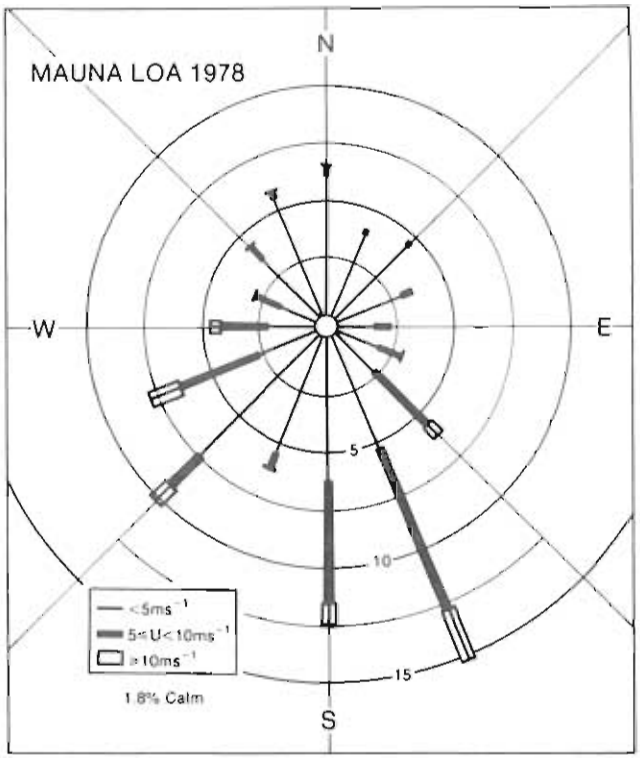

Figure 29.--As in fig. 28, except for Mauna Loa Observatory.

Table 15.--1978 Mauna Loa Observatory monthly climate summary

	Jan	Feb	Mar	Apr	May	Jun	Jul	Aug	Sep	Oct	Nov	Dec
Prevailing wind directions	SW	WSW	SSE	SSE	SSE	SSE	S	SSE	S	S	SW	S
Average wind speed (m s^{-1})	4.7	8.0	8.8	4.8	4.9	4.6	5.1	3.9	4.2	3.6	5.2	6.4
Maximum wind speed* (m s^{-1})	13	13	19	12	15	13	17	13	12	9	18	17
Direction of max. wind* (deg.)	255	273	256	138	150	163	161	185	170	162	230	164
Average station pressure (mb)	681.7	680.7	680.1	680.3	681.2	681.3	681.3	681.7	681.5	681.0	679.7	680.1
Maximum pressure* (mb)	685	685	684	685	685	684	685	684	684	684	683	684
Minimum pressure* (mb)	676	673	674	677	677	678	677	676	679	677	675	674
Average air temperature (°C)	5.2	4.7	5.1	4.8	6.4	7.2	7.3	7.6	7.4	6.8	4.3	4.1
Maximum temperature* (°C)	14	14	14	14	16	16	15	16	17	16	11	13
Minimum temperature* (°C)	-2	-3	-4	-2	0	-1	1	1	0	1	-2	-4

*Maximum and minimum values are hourly averages.

3.9.3 South Pole Climatology

The surface winds from a grid-northeasterly direction are the most persistent feature of the climate at the South Pole. These inversion winds are relatively steady compared to the more intermittent katabatic winds common to drainage situations. The prevailing wind is from the north-northeast, a direction approximately 50 degrees right of the direction of the Antarctic dome. The station is located on the Amundsen-Scott plateau (elevation 2.85 km) which has little topographic change within a 100-km radius of the station. The plateau is a depression near the western edge of the main high ridge of East Antarctica. The highest point on the plateau is about 900 km east-northeast of the Pole at an elevation of about 4 km.

Figure 30 shows the distribution of the wind direction and speed for 1978 in polar coordinates. As in previous years the most persistent direction is from the north-northeast occurring more than 20% of the time. On 85% of the hours during year the wind blows from the northeastern quadrant. The stronger winds are from the north and tend to occur more frequently during the Austral winter months (see table 16). The average wind speed for the year was 5.2 m s^{-1}. The maximum wind speed observed during the year was only 13 m s^{-1}. Calm conditions occurred for only 0.1% of the hours in 1978.

The change in the monthly average temperature shows a rapid transition from summer to winter, which is typical of the Arctic region. The average temperature remains below -50°C for 8 months of the year. The average temperature for 1978 was -48.4°C. The maximum hourly average temperature was -13°C; the minimum was -77°C.

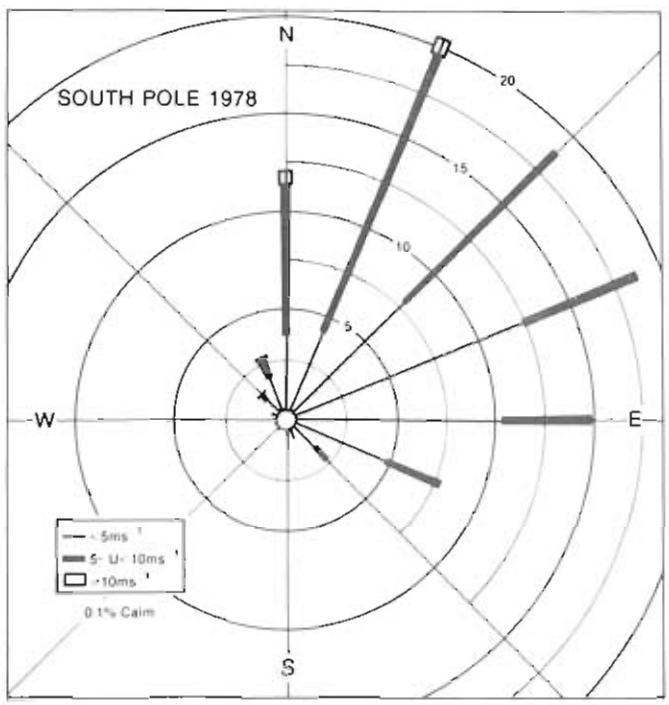

Figure 30.--As in fig. 28, except for South Pole Observatory.

Table 16.--1978 South Pole Observatory monthly climate summary

	Jan	Feb	Mar	Apr	May	Jun	Jul	Aug	Sep	Oct	Nov	Dec
Prevailing wind directions	ENE	NNE	NE	N	N	NNE	ENE	NNE	ENE	N	NNE	N
Average wind speed ($m\ s^{-1}$)	3.1	5.1	5.7	5.8	6.0	5.1	5.7	5.7	5.3	5.5	5.0	4.8
Maximum wind speed* ($m\ s^{-1}$)	8	9	11	11	11	10	10	11	13	12	10	12
Direction of max. wind (deg.)	013	032	014	018	359	030	031	012	017	339	320	013
Average station pressure (mb)	682.7	682.7	681.1	682.3	679.8	676.2	679.0	663.3	672.2	676.1	681.2	685.8
Maximum pressure* (mb)	691	694	692	700	697	690	691	680	685	699	690	703
Minimum pressure* (mb)	674	670	671	670	665	662	661	649	656	659	673	673
Average air temperature (°C)	-28.0	-39.2	-53.6	-50.6	-56.4	-60.2	-60.1	-62.1	-59.9	-48.5	-36.2	-25.8
Maximum temperature* (°C)	-21	-29	-44	-37	-39	-39	-45	-41	-38	-30	-29	-13
Minimum temperature* (°C)	-37	-56	-65	-64	-71	-75	-68	-77	-77	-66	-47	-36

*Maximum and minimum values are hourly averages.

3.9.4 Samoa Climatology

Since the relocation of the meteorological sensors atop Lauagae Ridge at Cape Matatula in February 1977, wind, temperature, and humidity have been measured from this position. At this location the anemometer is placed about 85 m above sea level, and the temperature measurements are made at 75 m above sea level. The records indicate the persistant nature of the trade winds from a southeasterly direction (fig. 31). On more than half the hours in the year the wind is from this direction. Also the stronger winds are from the southeasterly direction. The average wind speed for the year 1978 was 4.7 $m\ s^{-1}$. Calm winds, an average wind speed of less than 0.5 $m\ s^{-1}$, were observed 1.6% of the hours.

The constant nature of the climate at Cape Matatula is clearly illustrated in table 17. There is only a small indication of stronger winds and cooler temperatures in winter than in summer. The average temperature for 1978 was 27.6°C, with the maximum and minimum hourly values at 33°C and 22°C, respectively. Diurnal variations of wind and temperature are also small. Due to the diurnal pressure wave in the tropics the diurnal variation in station pressure is greater than the annual variation (Miller, 1975). The average station pressure for 1978 was 1000.5 mb.

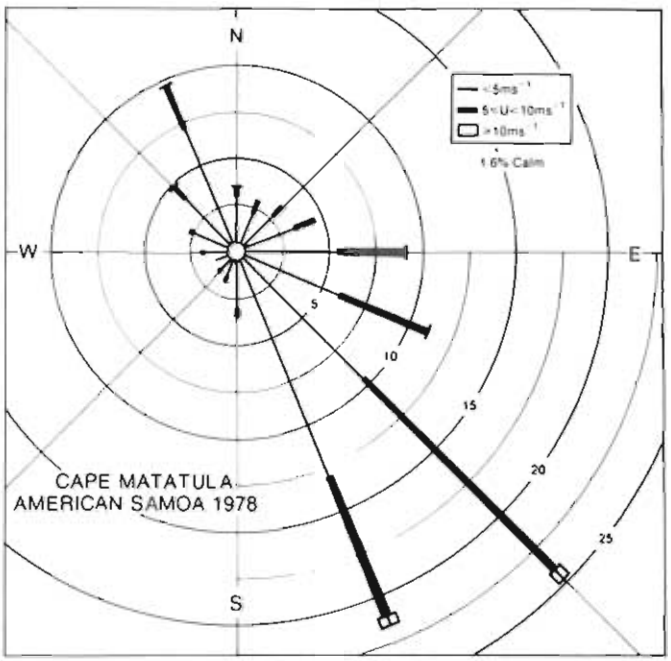

Figure 31.--As in fig. 28, except for Samoa Observatory.

Table 17.--1978 Samoa Observatory monthly climate summary

	Jan	Feb	Mar	Apr	May	Jun	Jul	Aug	Sep	Oct	Nov	Dec
Prevailing wind directions	NNW	SE	NNW	SE	SE	SE	SSE	SE	SSE	SE	SSE	SE
Average wind speed ($m\ s^{-1}$)	4.8	2.7	4.6	3.2	4.6	6.5	5.6	4.8	4.4	5.0	4.7	5.2
Maximum wind speed* ($m\ s^{-1}$)	12	8	12	9	11	10	12	10	10	14	12	11
Direction of max. wind* (deg.)	326	325	320	150	147	122	144	138	116	143	124	324
Average station pressure (mb)	999.1	997.1	1000.3	1001.2	1001.8	1001.8	1001.9	1001.1	1001.7	1001.3	999.9	999.2
Maximum pressure* (mb)	1005	1005	1007	1006	1007	1005	1007	1007	1006	1008	1005	1004
Minimum pressure* (mb)	990	989	996	996	996	998	999	988	998	996	996	993
Average air temperature (°C)	27.6	28.6	27.4	27.9	27.8	27.5	27.1	27.0	27.0	27.6	27.3	28.2
Maximum temperature* (°C)	31	33	33	32	31	31	31	33	30	32	34	34
Minimum temperature* (°C)	25	25	22	24	24	23	24	22	23	24	23	23

*Maximum and minimum values are hourly averages.

3.10 Precipitation Chemistry

Measurements of precipitation chemistry were continued at the 4 baseline observatories, 10 regional stations, and 6 Washington, D.C., area sites. Monthly samples were returned from the baseline and regional sites to EPA and DOE laboratories for analysis. Throughout the year, event, biweekly, and weekly samples from Hawaii, Samoa, and Alaska were analyzed at the MLO Laboratory in Hilo for pH, conductivity, and selected anions. A special project to study the direct effects of the Kilauea Volcano on the local precipitation chemistry (see table 18 for outline) was conducted by D. Harding. Earlier issues of the GMCC Summary Report give details on collection sites, collection techniques, etc.

3.10.1 Baseline Measurements

The pH measurements from the monthly collection program are shown in fig. 32. Misco indicates that samples were collected in a Misco collector and shipped to EPA for analysis. The EML data are monthly samples, collected in an Aerochem

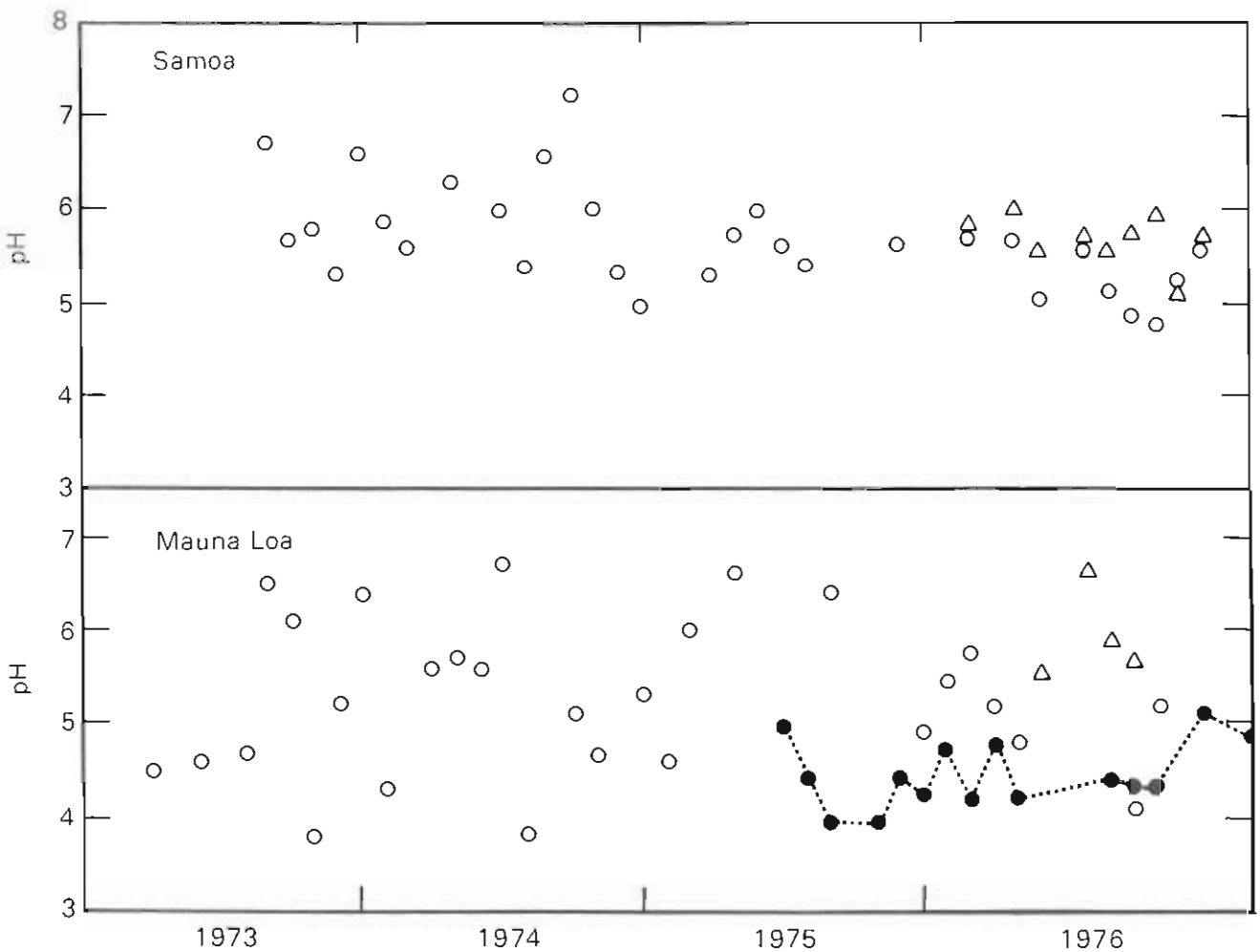

Figure 32.--pH values measured at SMO and MLO in monthly rain samples sent to EPA (Misco - o) and EML (Δ) for analysis. Bulk ph values measured on site are plotted for MLO (•).

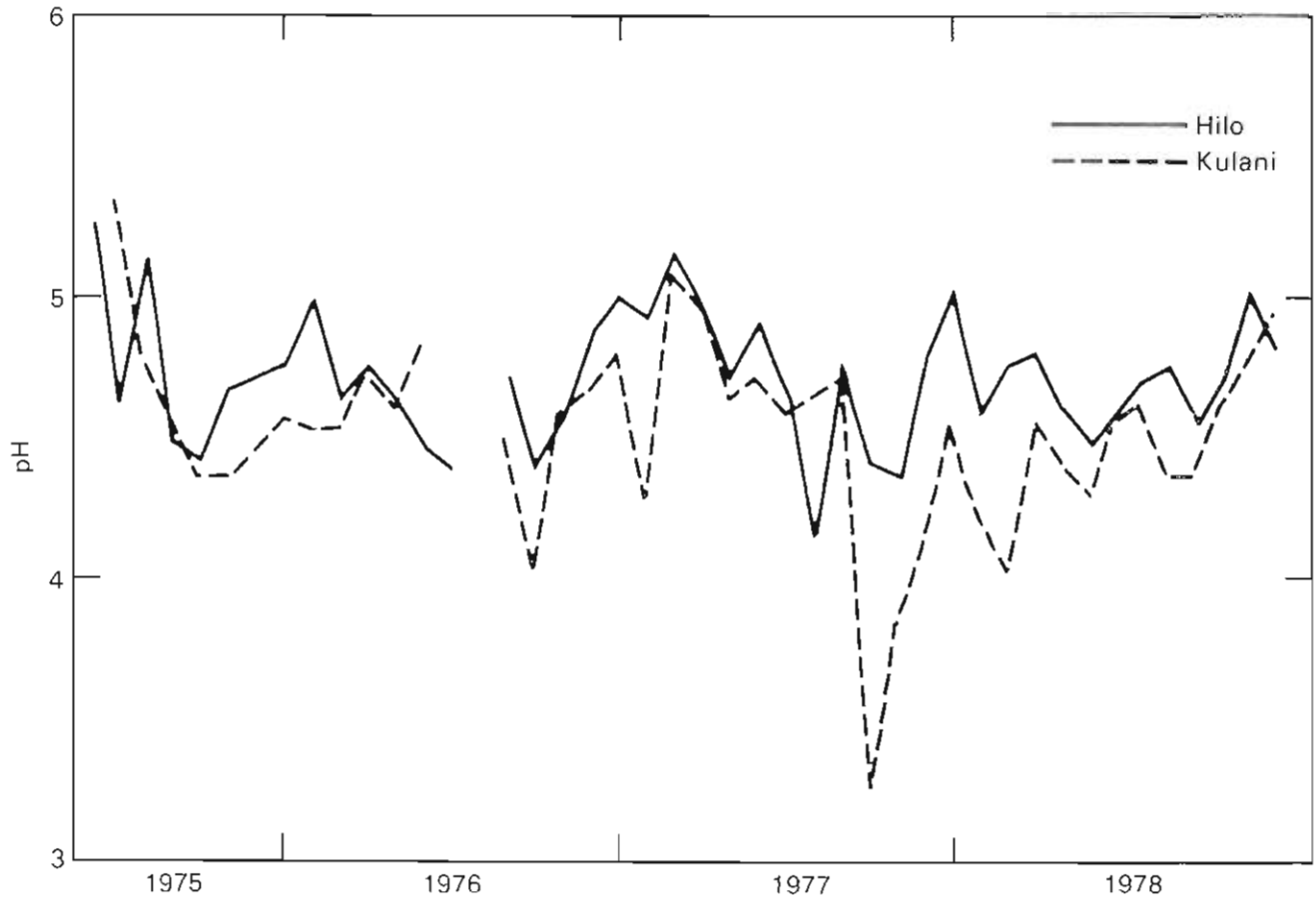

Figure 33.--Average monthly pH valnes at Hilo (120 m) and Kulani (2500 m) collected in bulk collectors on a daily or biweekly collection schednle and analyzed on site.

Metrics collector, that are shipped to the Environmental Measurements Laboratory, DOE, for analysis. The Samoa samples are fairly consistent during the 4-yr period. The Mauna Loa pH values, however, show large scatter because of such factors as wide variability of precipitation amount, sample evaporation, or failure of the collector to open. In contrast, the pH values of samples from a bulk or open collector (biweekly) show consistently lower values when averaged over the month. MLO staff, with EPA and DOE, are investigating this problem.

Examples of monthly weighted averages from two other sites in Hawaii are shown in fig. 33. The Hilo site (120 m) and Kulani site (2500 m) represent a low-level marine and a high-altitude environment, respectively, well above the trade inversion. Values are generally well below pH 5.0. Figure 34 shows a summary of all sites on Hawaii. The increase in acidity with elevation reported in earlier Summary Reports can still be seen.

Because of possible local contamination by volcanoes on the Island of Hawaii, a site was established on the Island of Kauai about 500 km north. The first 4 months of data are almost identical to those from a similar site on the Island of Hawaii (fig. 35). The pH values represent monthly weighted averages of event samples measured on site at both locations. This similarity is one indication that samples collected on Hawaii are representative of regional precipitation.

Table 18.--Precipitation chemistry programs in GMCC 1978

Type of program	Location	No. sites	Sponsor
Baseline	Mauna Loa	5	DOE, EPA
	Samoa	2	DOE, EPA
	Barrow	1	URI
	South Pole	grab samples	
Regional		10	EPA
Local	Washington, D.C., area	6	
Special research (Harding)	Kilauea Volcano		

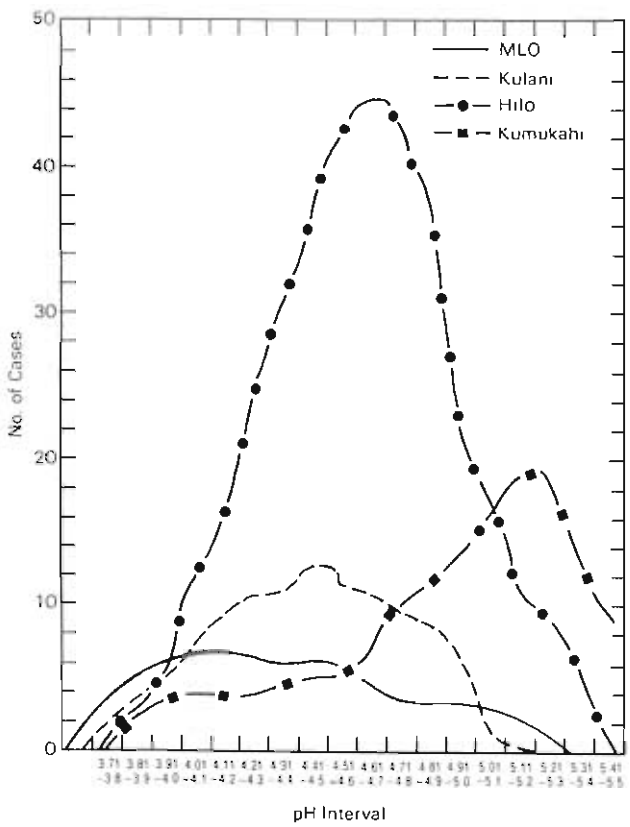

Figure 34.--Histogram of all pH values measured on the Island of Hawaii during a 3-yr period at the main four collection sites.

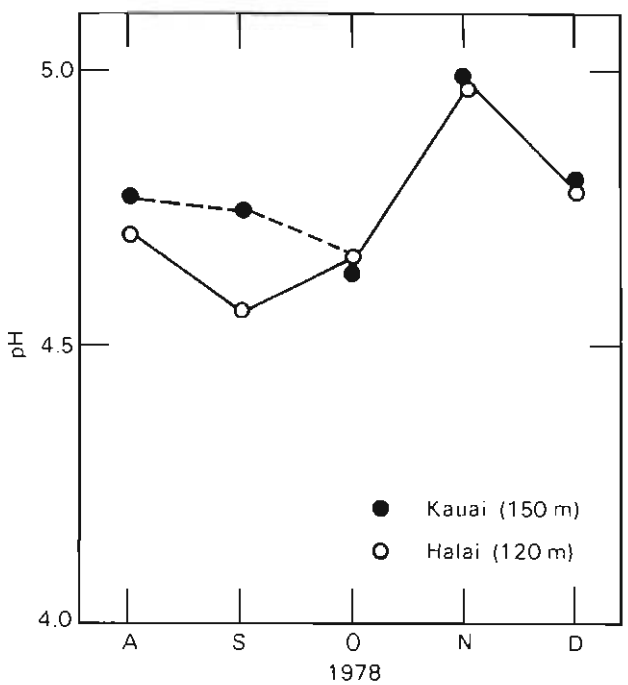

Figure 35.--Average monthly pH values measured on the Islands of Kauai and Hawaii.

3.10.2. Regional Site Evaluation

Reevaluation of the regional sites began in 1978 with visits to Pendleton, Ore., Bishop, Calif., and Alamosa, Colo. New Aerochem Metrics collectors have been received and will be shipped to the sites in 1979. Figure 36 shows a summary of the pH data from five eastern stations. Although pH values were low (4.0) during the 5-yr period, no discernible trend can be detected.

3.10.3 Local Washington, D.C., Network

In contrast to the regional sites, with monthly collections, the six-station network in the Washington, D.C., area shows a definite seasonal cycle but no yearly trend. Samples are collected on an event basis. Figure 37 shows the areal weighted pH values plotted for the 4-yr period. A peak in acidity (low pH values) can be seen during each summer season.

3.11 Rain Chemistry at Kilauea Summit

Hawaiian rainwater has been collected and analyzed for pH by Mauna Loa Observatory for 6 years. However, since the summit of Kilauea Volcano has not been studied, a 1-yr research project was started in March 1978.

Six rain collection sites were established from 3.5 km northeast to 12 km southwest of the Kilauea Caldera (see fig. 38). Each site had a plastic funnel-and-bottle collector for 3- to 4-day integrated samples. In addition, there were six 32-qt buckets; each could be lined with a polyethylene bag for event samples. Rainfall was measured with a 4-in plastic rain gauge.

Samples were collected twice a week from May 1978 through February 1979. All samples were analyzed in 3 days or less for pH and conductivity. The samples were later analyzed with the ion chromatograph for the anions F^-, Cl^-, NO_2^-, PO_4^{-3}, Br^-, NO_3^-, and SO_4^{-2}.

The major anions in the rainwater were found to be Fl^-, Cl^-, and especially $SO_4^=$. The pH of a rain sample depends on the following factors: location of the pollutant sources and their source strengths, location of the sample collector, wind direction, wind speed, and rainfall intensity.

Kilauea Caldera, particularly Halemaumau pit, is the major source of rainwater contaminants in the summit area. R. Stoiber and L. Malinconico of Dartmouth College were invited by Mauna Loa Observatory and Hawaiian Volcano Observatory to measure the output of SO_2 gas from Kilauea Caldera. By using a correlation spectrometer, they measured an emission rate of 200 Mg day^{-1}. In contrast, they found that the SO_2 flux from Mauna Loa Volcano was below the detection limit of the spectrometer; the output was estimated at 0.5 to 5.0 Mg day^{-1}. The spectrometer was also used to measure the SO_2 outgassing at the Sulfur Banks area of the national park. The test showed little, if any, SO_2 outgassing at the time. More measurements will be needed to determine how the emission rates of gasses and particles vary with time at the sites tested.

Six recording wind vanes were set up to test whether the Kilauea summit area is dominated by trade winds. Although four vanes were originally connected to Esterline-Angus chart recorders, the recorders started to corrode within

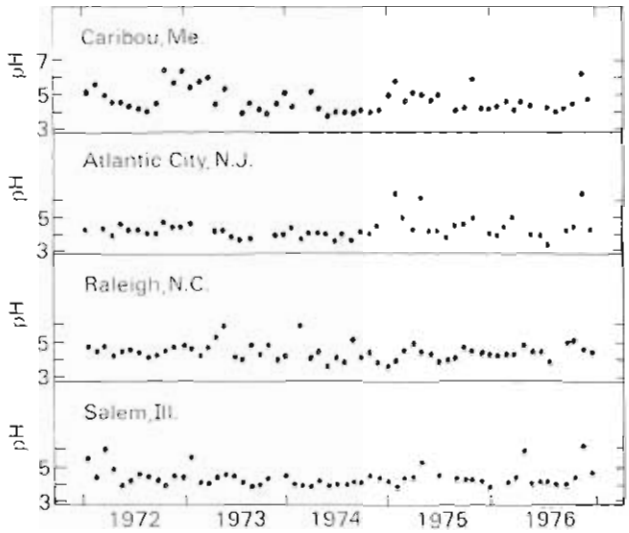

Figure 36.--pH values measured at four WMO regional sites.

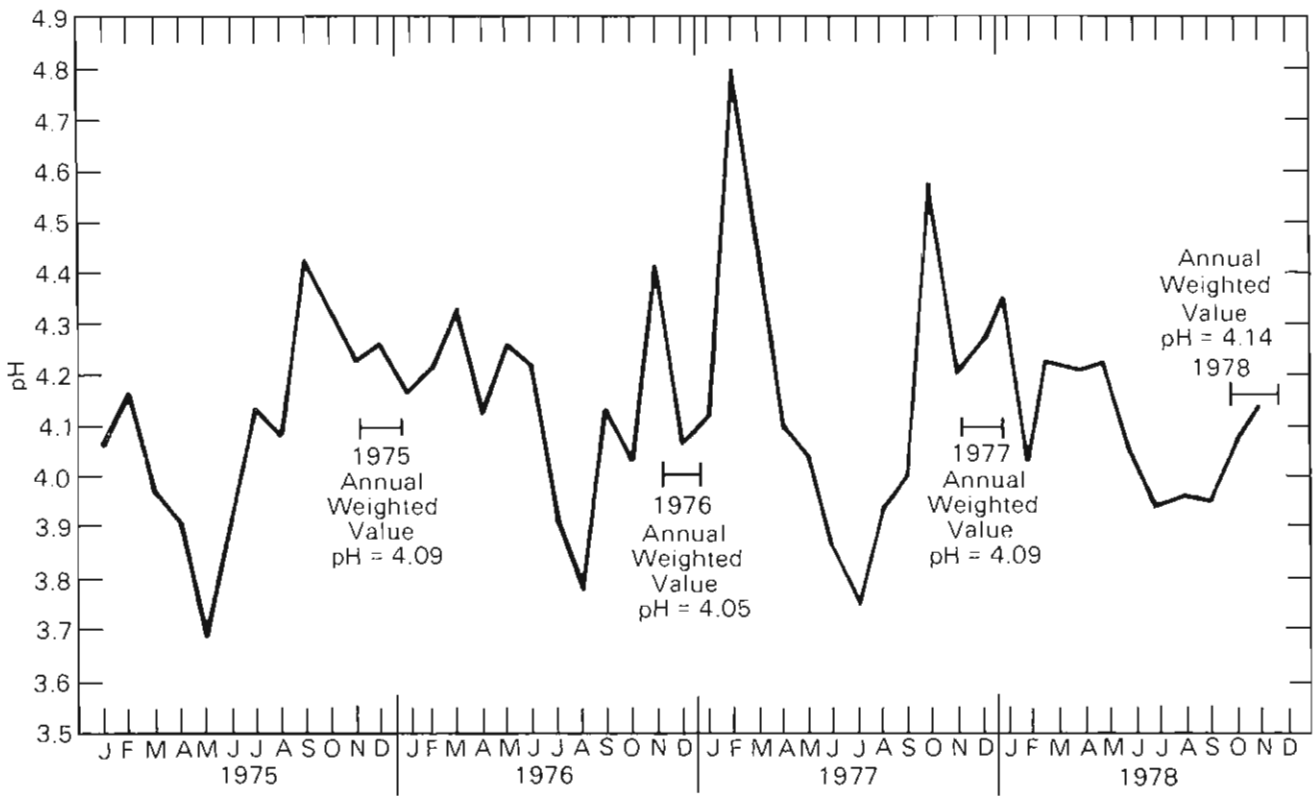

Figure 37.--Average areal weighted pH values for Washington, D.C., area.

weeks and were removed. Only a portable weather station at the far southwest end of the network recorded continuously throughout the year. Charts from the one recorder plus visual observation showed that trade winds commonly occur only in the immediate vicinity of the summit and north and south of it. Several kilometers southwest of the summit the winds are often anabatic (local upslope) from the southwest. This discovery was tempered by the discovery that the convergence area is known as Namakani Paio--dueling winds.

Nearly all daytime rain periods can be described by the diagrams in fig. 39. In type 1, the trade winds are strong. Southwest of the caldera the clouds quickly evaporate in the downdraft. Often heavy rain changes abruptly to blue sky. In type 2 rain period, the trade winds are lighter. On the sunny southwest side, the upslope winds lift the trades, which carry scattered showers toward the southwest. Type 1 weather appears to prevail whenever the wind speed northeast of the caldera is greater than about 15 mph. Type 3 represents the rain caused by the anabatic winds. On most mornings upslope winds create one or two

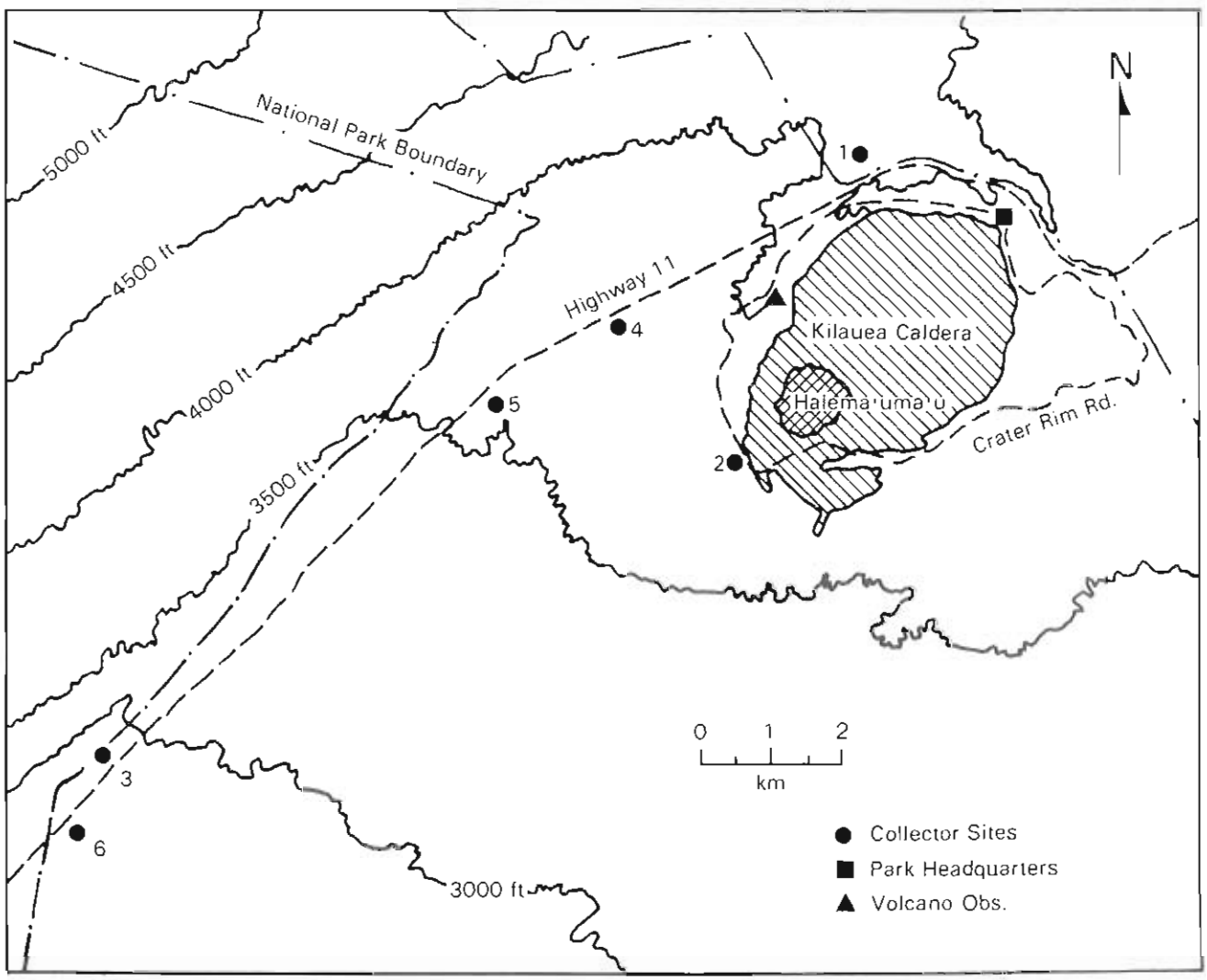

Figure 38.--Rain collection sites near summit of Kilauea Volcano.

bands of stratocumulus on the southern flank of Mauna Loa and above the valley northeast of Kilauea. Sometimes, strong convective activity develops and massive cumulus congestus form in about an hour. Once the cloud top reaches a critical height, the cloud mass quickly spreads laterally and encroaches on the edge of the collection network at Firing Range. This type has been observed mostly in the summer.

Because of the reliability of the winds, the measured pH values at any station (fig. 40) were grouped into general regimes: pH 4.0 to pH 5.2 at Golf Course; pH 3.2 to pH 4.0 at SW Rift; and pH 3.8 to pH 4.6 at Firing Range. The lowest measured value was pH 2.99 at SW Rift.

For fig. 40, the 4-wk running average was computed to smooth out the data. For most of the year, the pH was lowest at SW Rift and highest at Golf Course. However, during winter months southwest winds are more common, and the average pH increased at both SW Rift and Firing Range and decreased at Golf Course.

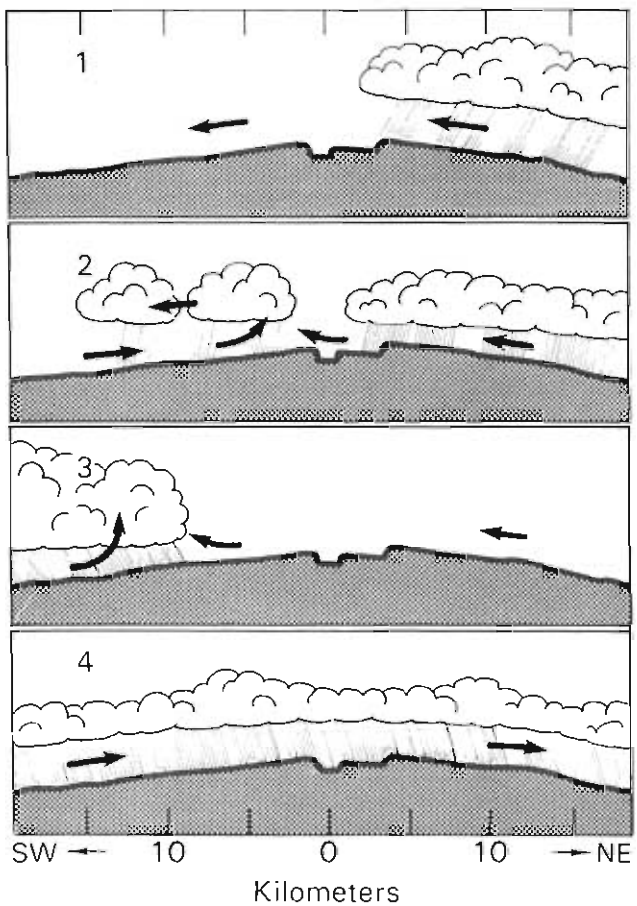

Figure 39.--Four types of rain occurrences at Kilauea Caldera.

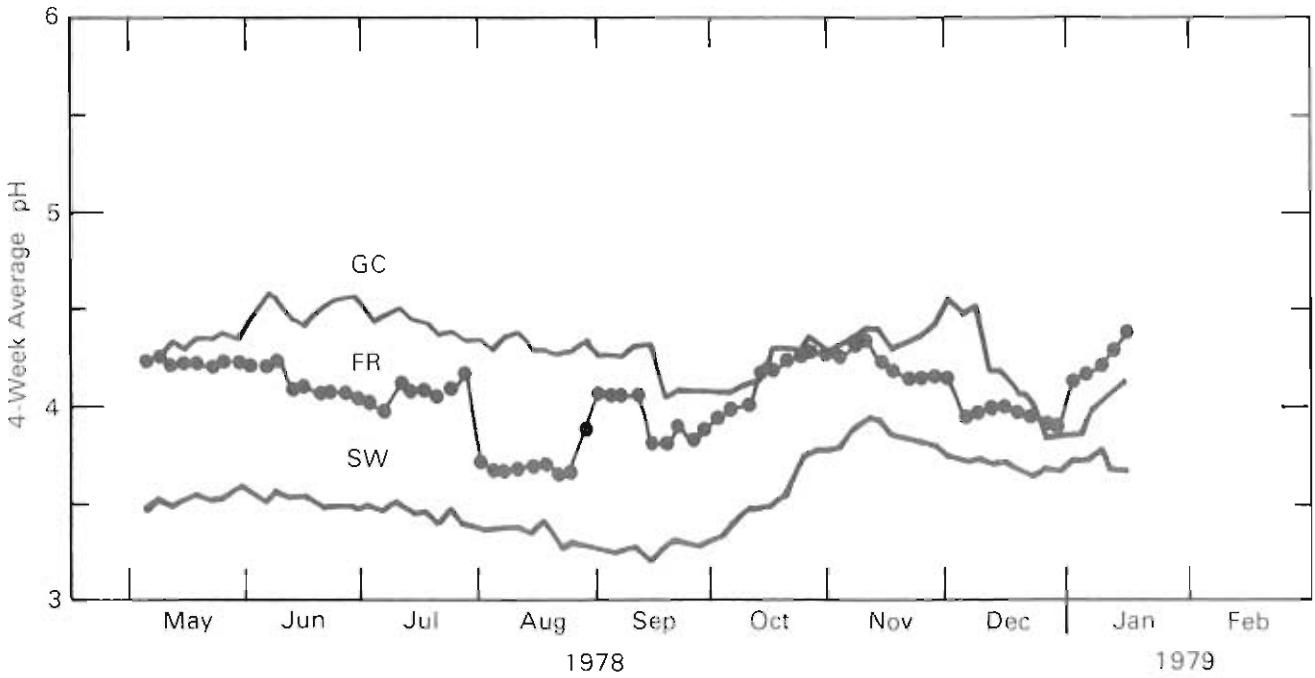

Figure 40.--Four-week running averages of pH for three sites: Golf Course (GC), Firing Range (FR), and SW Rift (SW).

3.12 Data Management

3.12.1 Data Acquisition

Hardware

In 1978 the reliability of the Instrumentation Control and Data Acquisition Systems (ICDAS) at the observatories improved greatly. For all stations combined the system was off line an average of 23 days in 1977, an improvement of 52 days over 1977. The ICDAS at MLO was down during much of 1978 causing the relatively large value in fig. 41. The renovation of MLO and the installation of central air-conditioning created a better operating environment for electronic components. The performance at the other stations improved in part because of startup software changes; specifically, the restart procedure was made easier for the operators and more reliable because it ensured the correct positioning of the tape. The new program also recaptures calibration constants automatically from the last hourly record on the data tape. The most reliable system was at the South Pole where the total down time was only 8.6 days.

The noise in the field data acquisition systems at both audio and radio frequencies was dealt with this year. The primary source of the noise was the power supply of the minicomputer. Linear power supplies of sufficiently small size were found to replace the noisy switching supplies furnished by the manufacturer. After extensive testing, the linear power supplies were installed in the

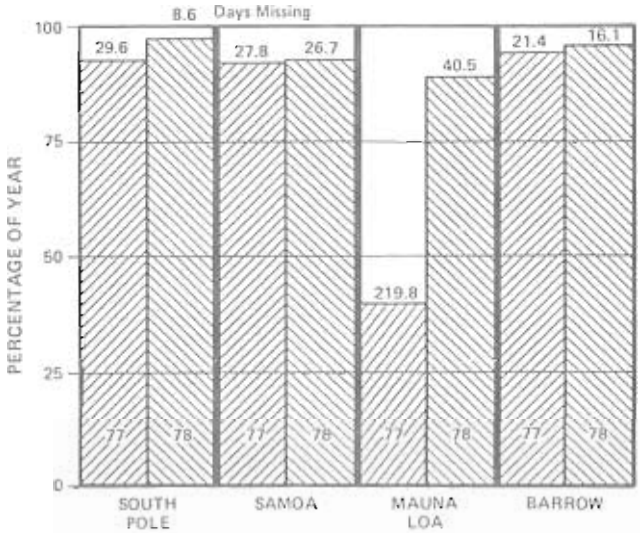

Figure 41.--ICDAS operations for 1977/1978.

minicomputer in the training facility and in the reduction facility. Noise levels were reduced by as much as a factor of 5 at the input to the system. Linear power supplies are to be installed in the minicomputers at the stations in 1979. With the elimination of the noise from the switching power supply, the staff can begin a systematic evaluation of other noise sources.

Another major hardware project involved the adaptation of the ICDAS to accomodate data in digital form. The standarized CAMAC system had been purchased earlier and evaluated for this purpose. Unfortunately, the interface electronics were unreliable and the cost and software overhead excessive. A simpler solution that used a DGC NOVA communication port with an RS-232 compatible port and standard communication protocol will be explored. The prototype of the CO_2 reference tank controller (see fig. 42) was designed and built. Final testing was completed early in 1979. A microprocessor was used to control the order in which CO_2 reference tanks were sampled and to digitize the resulting signals.

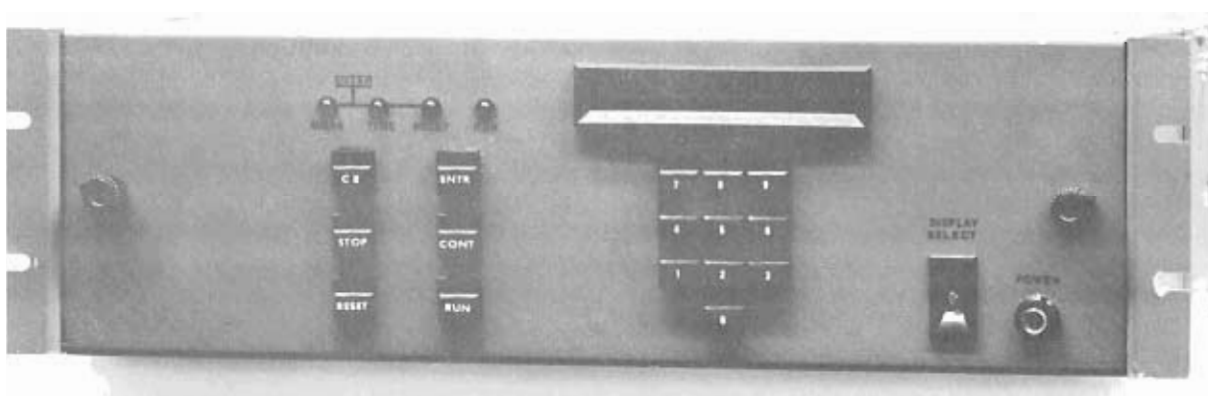

Figure 42.--Prototype CO_2 reference tank controller.

Table 19.--Inventory of GMCC data tapes sent to WDC-A

No.	Tape name	Date of issue	Parameter	Stations	Period of data
1	GPOP01	1/16/78	Aerosol count	BRW MLO SPO	1975, 1976 1975, 1976 1975, 1976
2	A78076	3/17/78	Solar irradiance	MLO	1977
3	A78083	3/24/78	Solar irradiance	SMO	1977
4	A78100	4/10/78	Solar irradiance	BRW	1977
5	A78104	4/14/78	Solar irradiance	MLO	1976
6	A78132	5/12/78	NIP radiation	BRW, MLO SMO, APO	1977
7	A78139	5/19/78	Wind, pressure, temp., humidity	BRW, MLO SMO, SPO	1977
8	A78146	5/26/78	Solar irradiance	SMO	1976
9	A78160	6/9/78	Solar irradiance	SPO	1976, 1977
10	A78230	8/18/78	Solar irradiance	BRW	1976
11	A78272	9/29/78	Solar irradiance	BRW, MLO	First half 1978
12	A78279	10/6/78	Solar irradiance	SMO	First half 1978

Software

Minor problems with the operating software were identified and corrected. An MLO problem with the control of the CO_2 reference gases after a power outage and a tape positioning problem were corrected, and the start-up procedure was further streamlined. The time between changes of the data tape was increased from 10 to 14 days. The revised operating software was issued as Basic Operating Software System (BOSS) 79001, replacing BOSS 77280 at all stations except the South Pole, which will be upgraded next year.

3.12.2 Processing

Reduction of Station Tapes

During 1978 two major hardware problems in the reduction laboratory slowed processing of ICDAS data tapes. During the first half of the year, the phase-encoded monthly tapes produced in the reduction lab could not be read on the

tape drives in the NBS computer facility. After much testing we determined that the read-write head of the drive in the reduction lab was recording at very low levels. Replacing it with a new head from the factory solved the problem. Second, the heads crashed on the disc drives, which are used for program storage in the reduction lab. While the drives were being repaired, many programs which process the field data tapes could not be run; most of these programs have been put on backup image tapes so that they can be run without the disc drives.

Beginning with January 1978, we decided to rerecord each monthly tape on the CDC 6600 in internal format. This procedure has two purposes: to provide a tape created in the most reliable format for use on the CDC 6600, and to produce a tape in CDC 6600 floating point format so that the conversion from NOVA BASIC is made once and not every time the tape is accessed on the CDC 6600.

New Software

Design and programming of the CO_2 continuous data base were completed in mid-year. The software reformats ICDAS and old card data and allows missing data to be inserted from strip charts. The data may be edited and output as daily tables of hourly values. Likewise, software to process meteorology data was developed throughout 1978. These programs edit the data statistically and climatologically and allow missing data to be inserted from strip charts via cards before final checking, a climatology run, and archiving.

3.12.3 Archiving

Table 19 lists the names of magnetic tapes sent to the National Archive in 1978. Data on the tapes are blocked into files, each file being preceded by a section containing a description of the data in alphanumeric form. Copies of the GMCC tapes can be obtained from the Computer Production Branch, National Climatic Center, Asheville, NC 28801, FTS 672-0203 or (704) 258-2850, ex. 203.

4. SPECIAL PROJECTS

4.1 The Short Umkehr Method

A theoretical study was performed to explore the possibility of shortening the 2-3 hours required for a Dobson Umkehr observation by incorporating more wavelength pairs in the measurement procedure. In essence, the Umkehr measurement uses wavelength in place of solar zenith angle as the independent variable. Practical and physical limitations restrict the variable wavelength method to solar zenith angles $75^\circ < \theta_o < 90^\circ$. We used solution residual variance and correlation criteria to jndge the statistical information of each method to establish a degree of equivalence between the two. To check the validity of the theoretical approach, a limited eigenvalue analysis was performed on the synthesized Umkehr observations, and this was compared with eigenanalyses on real Umkehr data reported by other investigators.

4.1.1 Residual Variance

This section is an extension of the preliminary work reported in GMCC Summary Report 1977, section 4.1. Of particular interest is the behavior of the diagonal elements of covariance, $S_{\hat{\underset{\sim}{f}}-\underset{\sim}{f}}$ and $S_{\underset{\sim}{f}}$ ($\hat{\underset{\sim}{f}}$ is a solution vector and $\underset{\sim}{f}$ is an observation of ozone profile), the difference of which may be interpreted as information added by the radiation measurements. We used a variation of the Westwater-Strand (1968) method of evaluation. Figure 43 shows $\sigma_{\hat{\underset{\sim}{f}}-\underset{\sim}{f}}$, which is the square root of the diagonal elements (root-mean-square deviation or RMSD) of $S_{\hat{\underset{\sim}{f}}-\underset{\sim}{f}}$, and for measurement errors of 1% and 10%. From fig. 43 we see that $\sigma_{\hat{\underset{\sim}{f}}-\underset{\sim}{f}}$, for a 1% measurement error, is at least one half or smaller than the magnitude of $\sigma_{\underset{\sim}{f}}$ for the observed ozone profiles. For a 10% measurement error the RMSD becomes larger, but significant information is still gained in certain levels, e.g., layer 6-8. The solid line for $\sigma_{\underset{\sim}{f}}$ is the limit beyond which no new information would be available. Little difference is seen between the results of the mw (short method) and Umkehr method, which indicates that they do not differ greatly.

4.1.2 Correlation Between $\hat{\underset{\sim}{f}}$ and $\underset{\sim}{f}$

Next we examine the correlation between $\hat{\underset{\sim}{f}}$ and $\underset{\sim}{f}$, which can be interpreted as the degree to which the solution ozone profiles follow the actual ozone profiles. This correlation provides a measure of the nonrandom statistical information reproduced in $S_{\hat{\underset{\sim}{f}}}$. Figure 44 shows $C_{\hat{\underset{\sim}{f}},\underset{\sim}{f}}$ which was derived under the same conditions, i.e., using the maximum likelihood method and for measurement errors of 1% and 10%. The Umkehr and mw methods have almost the same correlations at every level, except for layer 1 for the 1% error case where a substantially lower correlation is seen for the Umkehr. The peculiar dip seen in the correlation for layer 5 is a region of transition, where the seasonal cycles of ozone above and below are out of phase by 4-6 mo. Note that the residual variance does not reveal a corresponding variation in the transition region, although a variance anomaly is seen in the a priori statistics $\sigma_{\underset{\sim}{f}}^2$.

4.1.3 Eigenanalysis of the Umkehr and mw Methods

The first four normalized eigenvalues and eigenvectors (lower table) of $S_{\underset{\sim}{g}}$ ($\underset{\sim}{g}$ is a measurement vector) for the Umkehr and mw methods in the present

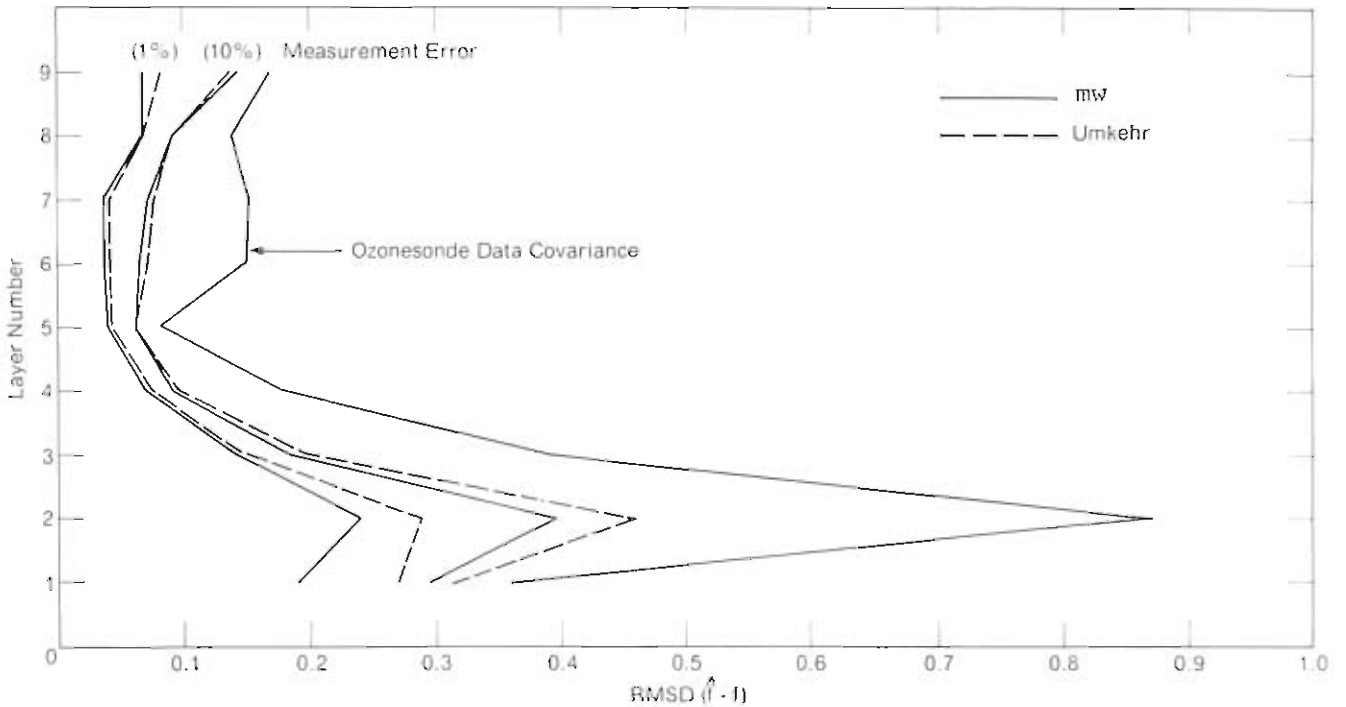

Figure 43.--Residual root mean square deviations connected by straight lines, showing results of Umkehr and multiple-wavelength (mw) solutions. Ozonesonde data plot is limit at which no new information is available from measurements. $\hat{f}$ is solution ozone; f is hypothetical true ozone.

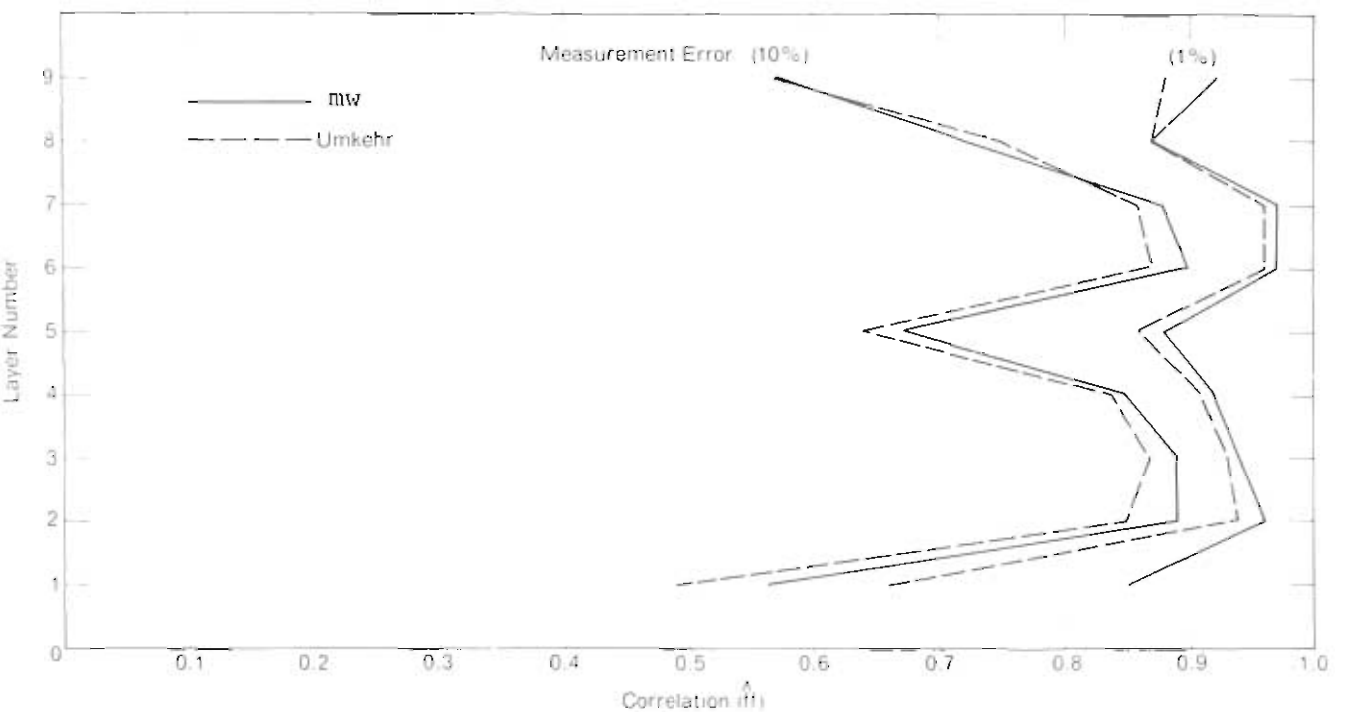

Figure 44.--Correlations between $\hat{f}$ (solution ozone) and f (hypothetical true ozone) connected by straight lines.

Table 20.--Comparison of first four eigenvalues E_i of S_g

	E_1	E_2	E_3	E_4
Umkehr (present study)	0.741	0.239	0.019	0.001
mw method (present study)	0.826	0.167	0.005	0.001
Umkehr (Mateer, 1965)	0.656	0.293	0.030	0.009
Umkehr (Craig, 1976)	0.709	0.238	0.034	0.006

study are given in table 20. Also included are eigenvalues from the results of Mateer (1965) and Craig (1976). Inspection of the Umkehr eigenvalues from all 3 sources does not reveal unusual differences. Some difference should be expected in the results of this study because it deals with synthesized Umkehr data whereas the analyses by Mateer (1965) and Craig (1976) were done with real data. Other factors that may contribute to the differences are the omission of total ozone used in the other analyses, unaccounted nonlinearities in the method used to calculate S_g, different kinds of errors in S_g between actual and synthesized data and differences in locations for Umkehr and ozonesonde data. Mateer's (1965) data were for North America and Craig's (1976) data were for Tallahassee, Fla.

4.2 Evaluation of the Robinson-Berger Meter Response

The Robinson-Berger (RB) meter measures UV flux in a moderately wide wavelength band that simulates the human skin action spectrum. However, the band pass of the RB meter is not exactly like that of the human skin action spectrum, and it thus allows more UV radiation to bias the instrument's readings. The extent to which this bias may be serious is not well known. In the present investigation we will evaluate the performance of the RB meter by making simultaneous, clear-sky solar radiation measurements with an RB meter and with a higher quality spectroradiometer, calibrated in absolute radiometric units. The spectroradiometer measurements are convoluted with the human skin action spectrum.

The units of the RB-meter measurements are minimum erythemal doses (MED's), where one MED is the amount of UV radiation just sufficient to produce a reddening of untanned human skin. The method used to calibrate the RB meter is not a part of the present evaluation. The spectroradiometer measurements are given in terms of absolute units $\mu W\ cm^{-2}$, and since a conversion factor does not exist for the RB meter, the two measurements cannot be related directly. Thus we chose to compare the two measurements on a relative basis with respect to a change in solar zenith angle. During the course of a change in solar zenith angle, say over the period of a few hours, if the two instruments disagree, a divergence or convergence in the measurements will occur.

Figure 45 shows the results of some preliminary analyses for solar zenith angles 51°, 59°, and 67°. Straight lines join the points for the various measurements shown on the graph. The curve labeled MED represents the RB measurements and has a scale on the right-hand side. The calculated RB curve is found by the convolution of a published RB spectral band pass with the spectroradiometer measurements. The calculated erythermal curve is found by convoluting the human skin action spectrum with the spectroradiometric measurements. The curve labeled Dave (307.5) is taken from published theoretical calculations of monochromatic

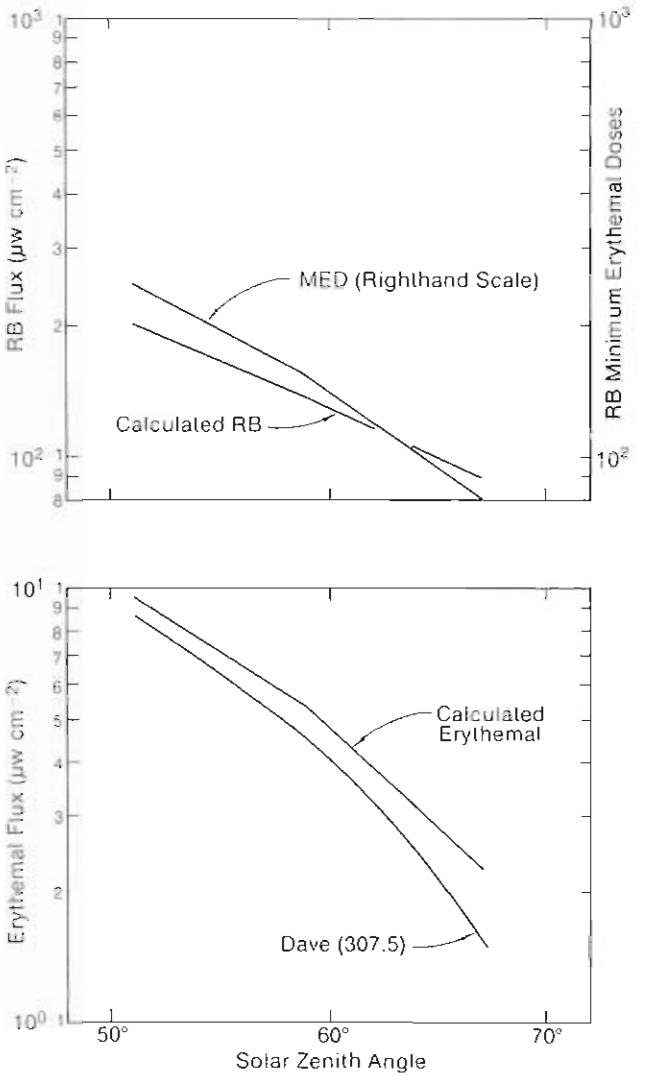

Figure 45.--Plots of UV radiation vs. solar zenith angle.

hemispheric radiation at a wavelength of 307.5 μm and total columnar ozone of .341 cm STP (Dave and Furukawa, 1966). This wavelength happens to be quite close to, if not directly at, the peak of the convoluted human skin action spectrum and the incident hemispheric UV flux.

In fig. 45, the slope of the calculated erythermal response is steeper than the RB-meter response, implying that they diverge with increasing solar zenith angle. This is consistent with the RB-meter spectral band pass, which permits UV radiation at longer wavelengths to pass onward to the sensor. The calculated RB response is seen to be quite bad. We found later that more RB spectral response curves were published and the one used was the worst available.

The Dave curve in fig. 45 falls off more steeply than all other curves. This occurs because the ozone, .34 cm STP, for Dave's calculations is considerably higher than the .27 cm STP. Calculations with correct ozone amounts will be used in the future comparisons.

In summary, the RB-meter measurements depart significantly from the spectroradiometric measurements. A more in-depth analysis will be performed on the remaining data to quantify the magnitude of the departure.

4.3 Umkehr Vertical Ozone Profile Errors Caused by the Presence of Stratospheric Aerosols

The present investigation is concerned with errors to the Umkehr ozone profiles following the violent eruption of Mount Agung in 1963. Large quantities of aerosols from the eruption were injected into the troposphere and stratosphere over the Southern Hemisphere. A short time later, increases in stratospheric aerosol concentrations were observed in the Northern Hemisphere. Following Agung a dramatic change occurred in Umkehr ozone profiles observed at Aspendale, Australia. Smaller, but nevertheless significant, changes to Umkehr ozone profiles also occurred in the Northern Hemisphere record, which consisted of data from several stations.

The changes to the ozone profiles at Aspendale are so large that it is possible to deduce empirically the haze error effects to the Umkehr ozone profile by comparing averages of ozone profiles observed almost immediately after Agung with ozone profiles observed for several years when the stratosphere was without serious aerosol contamination.

The present investigation also involves a theoretical approach in which aerosol errors to the Umkehr measurement are calculated and, accordingly, corrections are made to deduced ozone profiles. Model vertical profiles of aerosols and observed changes to stratospheric aerosol optical depths are used for the calculations. Insight into the physical processes that are responsible for the causes of the ozone profile errors is gained from the theoretical approach.

Figure 46 shows two plots of haze errors to the Umkehr ozone profiles as determined from the Aspendale data. Two-month averages are used, June-July and

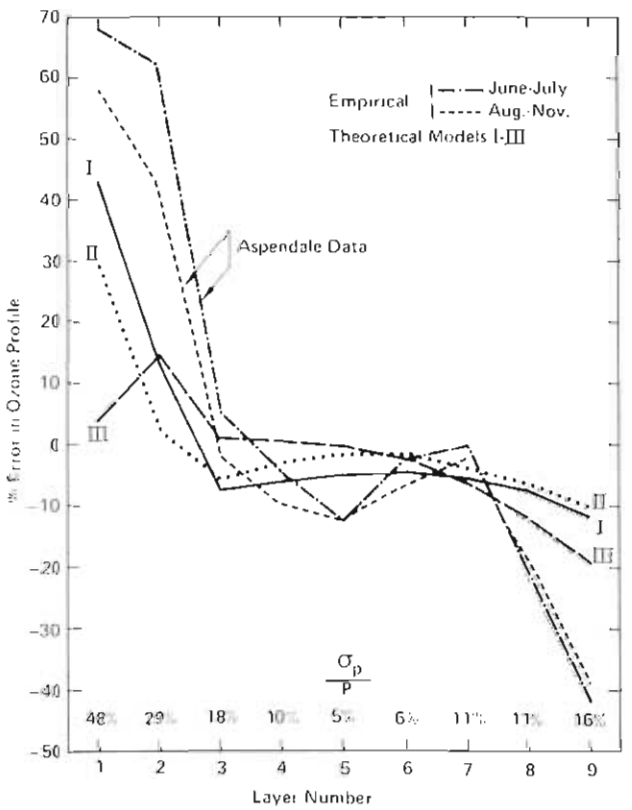

Figure 46.--Umkehr ozone profile haze errors. Plots for Aspendale data were empirically determined; plots I, II, and III were theoretically calculated by using model vertical aerosol concentration profiles.

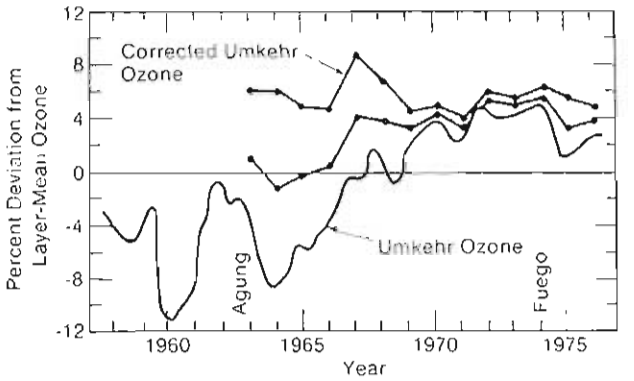

Figure 47.--(top) Stratospheric aerosol corrections to annual means of the lower plot. (bottom) Observed deviations of Umkehr ozone concentrations from the long-term mean in a layer from 32 to 46 km.

August-November, to increase the number of data points for a smoother plot. Also plotted on the figure are theoretically calculated haze errors. Below the plots the observed standard deviation divided by the average partial pressure for the summer season at Aspendale is given for each layer. These values, derived from a set of about 100 observations during about 10 years, show the normally expected spread in observed ozone profiles plus errors intrinsic to the Umkehr method.

4.3.1 Haze Error Correction

The correction procedure is specifically intended for an increase in stratospheric aerosol content in the Northeru Hemisphere following the eruption of Agung. Atmospheric transmission data from Mendonca et al. (1978) indicate than an average increase of stratospheric aerosol optical depth of 0.014 occurred in the Northern Hemisphere temperate latitudes during 1965. In the years subsequent to Agung the transmission varied considerably as it slowly tended toward the pre-Agung values.

Figure 47 shows a smooth plot of Umkehr ozone data (lower plot) representing the sum of the absolute abundances of ozone in layers 7-9 (or a layer approximately 32-46 km thick) versus time (Angell and Korshover, 1978) for 10 stations in the north temperate latitudes. The ordinate is the percent deviation in ozone from the long-term mean. Tick marks on the abscissa represent the middle of the year. Also shown in the figure is a hatched area plot of corrected midyear Umkehr ozone concentrations (upper plot) for the same 32- to 46-km layer. This area plot depicts the range within which the actual ozone abundances are more likely to exist. Corrections to the lower plot are based on the estimated upper and lower limits of the change in the observed optical depth for each year from 1963 to 1976.

4.4 Confidence Interval for CO_2 Flask Sampling

A primary task of the GMCC measurement program is to determine the true mean value of a particular pollutant in the atmosphere. A model suggested by Hunt (1972) defines the precision with which discrete samples of an atmospheric constituent or pollutant represent the true mean value, when the constituent is assumed to be log-normally distributed. In this study, the 1977 CO_2 data (both continuous and flask sampling) from the South Pole and Samoa stations will be used to determine the confidence limits that must be assigned to flask sample

concentrations based on the geometric standard deviation and the sampling and averaging period.

4.4.1 Nature of Variability

The statistics used to test Hunt's model were drawn from continuous 1977 (hourly-averaged) measurements of the concentration of atmospheric carbon dioxide at the Amundsen-Scott station at the South Pole, Antarctica, and the GMCC station at Cape Matatula, Samoa. For both stations long-term trends and the annual cycle were removed by evaluating the distribution and statistics from the residual values formed by subtracting the monthly mean values from the data. The resulting distribution (fig. 48) shows good agreement with a log-normal distribution over the upper 90% of the data. The geometric standard deviation of 0.2 ppm was computed from the South Pole data; the Samoa data gave a larger value of 0.7 ppm.

4.4.2 Results

In fig. 49, the results of model calculations with standard deviations of 0.2 and 0.7 are plotted. Confidence intervals of 80% and 90% are graphed, assuming a mean value of 330 ppm; the uncertainty in the monthly mean values ranges from 0.1 to 3.0 ppm. Flask sample data currently used by GMCC are collected on 2, 4, and 8 days mo^{-1}. These data were compared to the 30 daily values per month obtained from continuous sampling. The expected difference between the sample geometric monthly mean CO_2 concentration and the true geometric monthly mean concentration was therefore determined at two confidence levels and two levels of variability, and over a wide range of sampling intervals. For weekly sampling the uncertainty at the 90% level for tropical measurement is on the order of ± 0.7 ppm and for Antarctica about ± 0.2 ppm. Doubling the sampling rate reduces the uncertainty by a factor of 2. If the basic uncertainty of the measurement is on the order of ± 0.2 to ± 0.3 ppm, little will be learned by sampling more frequently than 4 to 8 times mo^{-1}. A standard

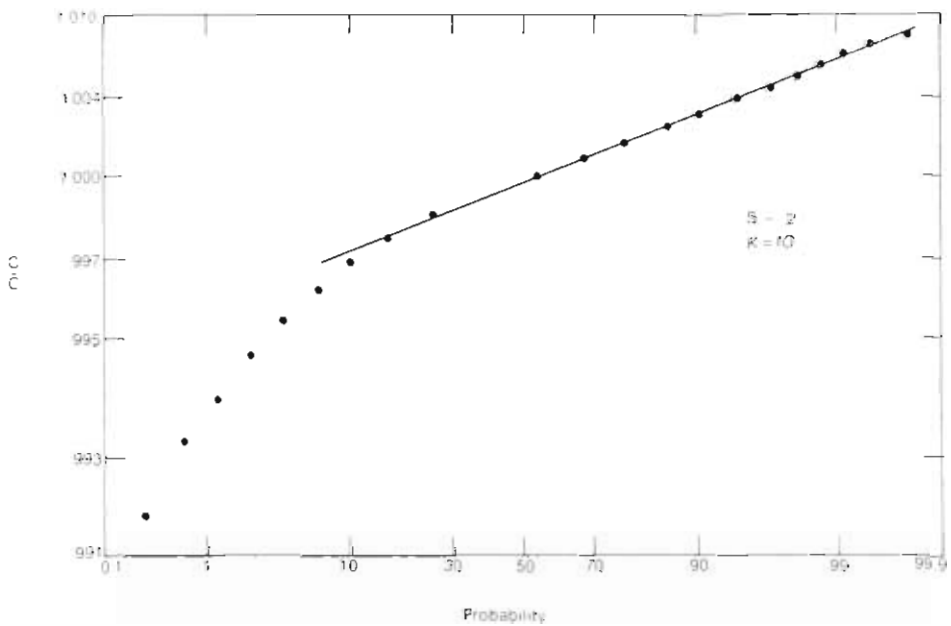

Figure 48.--Cumulative probability of equaling a particular CO_2 concentration ratio ($C/\bar{C}$). Data from South Pole.

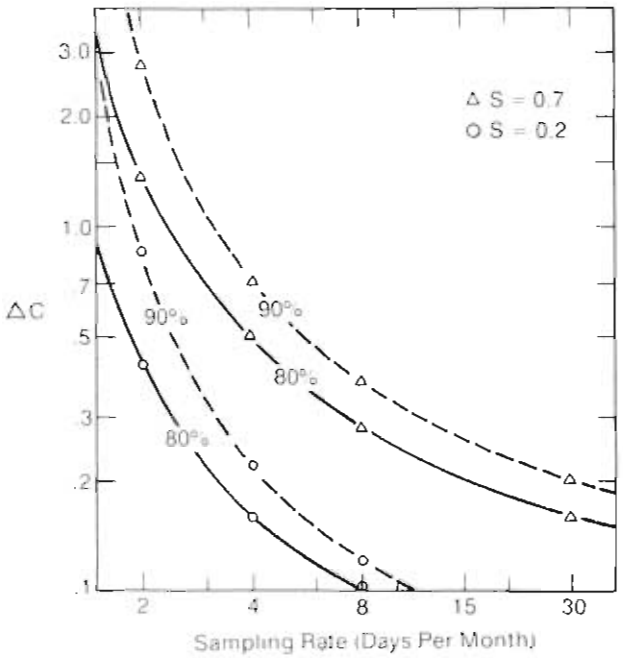

Figure 49.--Comparison of confidence intervals for sampling plans by using geometric standard deviations of 0.2 (SPO) and 0.7 (SMO).

deviation of 0.2 ppm is probably a minimum value applicable only at the South Pole. Further study of the detrended variability at all stations making continuous measurements is needed.

4.5 Isotopes of Carbon: Effect of Adding Limestone Derived CO_2 to the Atmosphere

Records of carbon isotopes provide considerable information on the carbon cycle. Ratios of carbon isotopes vary because of temperature, biological growth cycles, and changes in carbon pool content. Carbon 13 to carbon 12 ratios are valuable in determining the history of fossil fuel combustion since fossil fuel contains practically no C^{14} and a C^{13}/C^{12} value lower than that found in atmospheric CO_2. This investigation attempted to foresee the consequence of converting carbonate and dolomite to atmospheric CO_2 on C^{13}/C^{12} observations. This fossil material also contains practically no C^{14} but is enriched in C^{13} compared with atmospheric CO_2.

Table 21 summarizes the sources of CO_2 derived from limestone. Industrial emissions have been previously considered, but the contributions from gas wells (due to metamorphism of carbonates) have not been widely discussed. The figure 8.3×10^{15}g of CO_2 is estimated from Rocky Mountain reserves in the United States Volcanic emissions of CO_2 were obtained by assuming a ratio of unity for CO_2 to

Table 21.--Estimated CO_2 atmospheric contributions from limestone

Igneous intrusion into carbonates		Industrial emissions	
Gas wells	Volcanic emissions	Portland cement	Steel
8.3×10^{15}g	0.0004×10^{15}g yr^{-1} 0.000008×10^{15}g yr^{-1}	0.3×10^{15}g yr^{-1}	0.015×10^{15}g yr^{-1}

sulfur gases and using the sulfuric gas emission data of other scientists in the field.

When limestone-derived CO_2 is injected into the air, values of $\delta^{13}C$ are raised and ratios of C^{14} to total carbon are lowered. A simple model incorporating the atmosphere (uniformly mixed), the mixed layer of the ocean, and differing sources of CO_2 was used to calculate values of $\delta^{13}C$ for differing source strengths. The model assumed equilibrium for atmospheric-oceanic mixed-layer isotopic ratios and assumed the following for limestone:

$$\delta^{13}C = 0 \text{ and } C^{14}/C^{12} = 0.$$

A quantity of 8.3×10^{15}g of CO_2 was injected into the atmosphere, and C^{13} and C^{14} ratios were computed from the relationship

$$\frac{C^*_{atmos}}{C_{atmos}} = \frac{F/G}{(1+F/G)} \cdot \frac{C^*_{o,atmos}}{C_{o,atmos}} \frac{(1+G) + C^*_{injected}}{(1 + \sum_i \frac{(\delta PCO_2)_i}{PCO_2})}$$

where C^*_{atmos} is the concentration of the carbon isotope, C_{atmos} is the total concentration of CO_2, $C^*_{o,atmos}$ is the initial atmospheric concentration of the carbon isotope, $C_{o,atmos}$ is the initial CO_2 concentration in the atmosphere.

$$F = \frac{1 + \sum_i \frac{(\delta PCO_2)_i}{PCO_2}}{1 + B\sum_i \frac{(\delta PCO_2)_i}{PCO_2}}$$

where PCO_2 is the partial pressure of CO_2 in the atmosphere, $(\delta PCO_2)_i$ is the change of the partial pressure of CO_2 due to addition of contribution i, and B is the buffer factor (assumed equal to 0.1), G is the initial ratio of CO_2 in the mixed layer to that in the atmosphere, and $C^*_{injected}$ is the total quantity of carbon isotope injected into the atmosphere from all sources.

Injection of 8.3×10^{15}g of limestone-derived CO_2 into the atmosphere increases the $\delta^{13}C$ value for atmospheric CO_2 by 0.042. The effect of raising the $\delta^{13}C$ value was moderated (reduced) by the ocean. Although the effect of metamorphic CO_2 is not large, it is sufficient to show that all CO_2 sources should be inventoried if detailed work on carbon isotopes is planned. The importance of this source of CO_2 may be shown from the ratio of increase of $\delta^{13}C$ values corresponding to a decrease of C^{14} ratios

$$\Delta\delta^{13}C = -0.084S$$

where S is the decrease of C^{14} in percentage whereas for fossil fuel burning the relation

$$\Delta\delta^{13}C = +0.18S$$

was given by Stuiver (1978). Thus, a mixture of the two sources acting in two directions to change $\delta^{13}C$ could lead to faulty interpretations if one source were neglected.

4.6 Special Nephelometer Calibration Studies

A 4-wavelength nephelometer was first installed at MLO in January 1974. Since then similar instruments have been installed at Barrow, Samoa, and South Pole so that a continuous record of data is being obtained at all GMCC sites.

Calibration, the most important factor in any long-term measurement program, requires that field measurements be related to a fundamental, reproducible standard. In the past, nephelometers were calibrated by filling them with Freon-12 and adjusting the output voltage to agree with the known scattering coefficient of Freon-12. However, concern over the release of chlorofluorocarbons into the atmosphere and the fact that trace concentrations of F11 and F12 are measured at the GMCC observatories preclude the use of F12 at these sites. Consequently, carbon dioxide has been adopted as the calibration standard because its properties are well-known.

To establish calibration standards for the GMCC program, experiments were undertaken at the Boulder laboratories (Bodhaine, 1979) to test the scattering properties of argon, air, carbon dioxide, and Freon-12. The scattering coefficients of these gases, which have been accepted for the calibration of nephelometers in the GMCC program, are presented in table 22.

These scattering coefficients are given for standard temperature and pressure (STP). Therefore, they must be scaled by density to the operating temperature and pressure at each measurement site.

Table 22.--Rayleigh scattering coefficients for air, CO_2, argon, and F12 at T = 0°C and P = 1013.25 mb

Wavelength (nm)	Air ($\times 10^{-5}$ m^{-1})	CO_2 ($\times 10^{-5}$ m^{-1})	Argon ($\times 10^{-5}$ m^{-1})	F12 ($\times 10^{-5}$ m^{-1})
455	2.665	6.956	2.34	40.8
500	1.810	4.724	1.59	27.7
550	1.226	3.200	1.08	18.8
700	0.4605	1.202	.405	7.05
835	0.2259	0.5896	.199	3.46

4.7 Urban-Rural Solar Radiation Measurements at St. Louis

Simultaneous measurements of incident solar radiation from six locations in metropolitan St. Louis, Mo., have been analyzed. The measurements, part of the EPA-sponsored Regional Air Pollution Study, were taken continuously from September 1975 through March 1977 with pyranometers having all-wave and 395-nm and 695-nm cutoff filters. The objective of the study was to document typical urban-rural variations of incident solar radiation. The work was sponsored by the U.S. Department of Energy through an interagency agreement with ARL/NOAA. A discussion of preliminary results and experimental design was given in last year's Summary Report (section 4.4). A report describing the complete analysis is also available (Peterson and Stoffel, 1979).

Atmospheric pollutants over the center of metropolitan St. Louis reduced incident all-wave solar irradiation by about 3%. Differences between urban and rural irradiation were about 1% greater than average during winter and 1% less than average in summer. At two suburban sites, the irradiation depletion averaged 1% and 2% for summer and winter seasons, respectively. Under all conditions the ratios between stations for the complete experiment were similar to those for cloudfree conditions. Thus, any variations in cloudiness over the network evidently were not sufficiently large to affect the grand average irradiation distribution over the network.

Although the comparisions were stratified according to wind direction and speed, visibility, time of day, and day of the week, only wind direction had a significant effect on the interstation ratios. For cloudless days two suburban sites and a rural site north of the city received about 3.5% more relative irradiation with north than south winds. The explanation for this wind direction effect is that pollutants were advected from major sources near the city center. The two urban sites exhibited only about 1% change due to north-south wind differences. The interstation comparisons for all days during the complete experiment were also partitioned by wind direction. With north winds, the suburban and northern rural sites showed about 2% to 3% more relative irradiation on all days than on cloudless days for both the summer period and the complete experiment.

4.8 Cooperative U.S.A.-U.S.S.R. Atmospheric Transparency Measurements

Under the U.S.A.-U.S.S.R. Agreement on Cooperation in the Field of Environmental Protection, Working Group VIII was established to develop cooperative projects that will increase understanding of the sensitivity of climate to natural and anthropogenic environmental changes. One project of Working Group VIII included a joint program to compare atmospheric transparency values derived from the use of U.S.S.R. and U.S. instruments. Some results of those comparisons and measurements of atmospheric turbidity are described here. Additional information is presented in Peterson and Kovalyev (1979).

Intensity of the direct solar beam was measured from August 14-23, 1978, at Voeikovo in the Soviet Union, an experimental site of the Main Geophysical Observatory, about 25 km east of Leningrad, in gently rolling, rural terrain. Atmospheric transparency (P) was determined from measurements of direct solar beam intensity (I_λ) at wavelength λ from the following expression:

$$P_\lambda = (I_\lambda / I_{\lambda_o})^{\frac{1}{m}}$$

where I_λ is the solar intensity above the atmosphere and m is optical air mass. The U.S. instrument, operated by J. Peterson of GMCC, was a portable Volz sunphotometer that uses narrowband filters with maximum transmissions at 380- and 500-nm wavelength (Flowers et al., 1969). Soviet measurements during the comparisons were taken with an M-83 instrument that is used routinely at some 30 locations in the U.S.S.R. to measure the direct solar beam in narrow wavelength intervals to obtain total atmospheric ozone values and atmospheric transparency at six wavelengths. The 369- and 530-nm wavelength measurements were used for these intercomparisons.

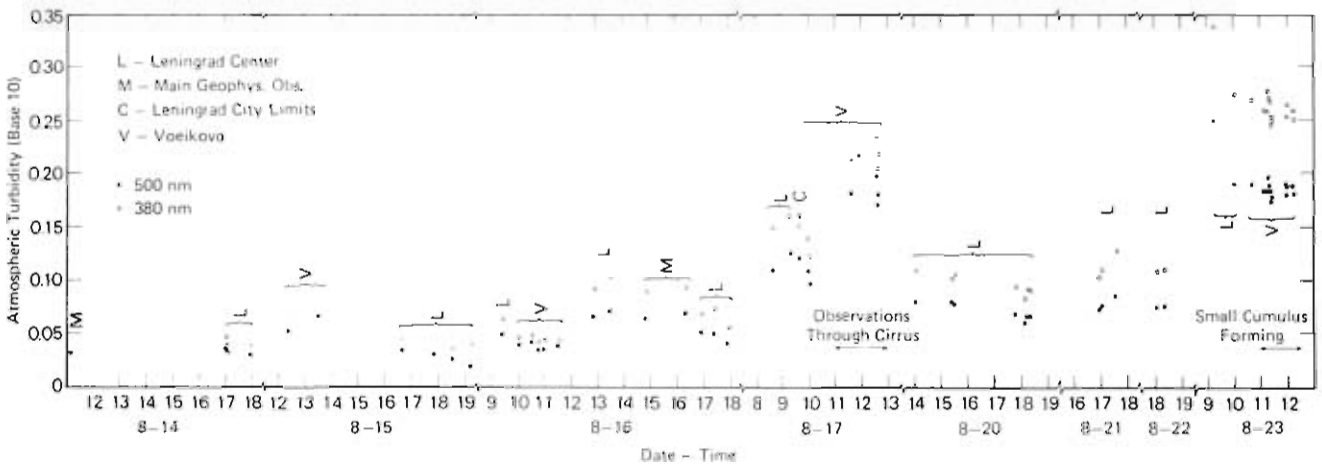

Figure 50.--Atmospheric turbidity measurements at 380- and 500-nm wavelengths in the vicinity of Leningrad, during August 1978.

Values of atmospheric transparency from the two instruments generally agreed well. After correction for wavelength differences, the two instruments measured atmospheric transparency within about 2% of each other; much of this discrepancy probably resulted from instrument aperture differences. The M-83 has an aperature of 6° whereas the sunphotometer has an aperture of 1° 51'. A complete report of these intercomparisons is planned in the Soviet literature.

Besides the measurements at Voeikovo, the Volz sunphotometer was used periodically to obtain atmospheric turbidity (aerosol optical thickness) from the center of Leningrad and at the Main Geophysical Observatory (MGO). MGO is located in a suburban area about 10 km northeast of the city center. For the turbidity measurements presented in fig. 50, values are expressed in the customary decadic base, and time is Leningrad local time (standard time advanced one hour), GMT + 3 h. On August 16, 17, and 23, urban turbidities were noticeably greater than the non-urban readings. On August 15 the non-urban values were greater. On this day westerly winds advected clean air from the Gulf of Finland over the city whereas Voeikovo was downwind of the urban industrial area. (The city center is only a few kilometers from the Gulf.) For 8 days with urban turbidity measurements, average daily 500-nm turbidity was 0.086. This value is similar to summertime averages at many western U.S. locations (Flowers et al., 1969). Turbidity varied over a fairly wide range, however. On August 14 and 15 the atmosphere was quite clean, following a strong cold frontal passage and rain on the 13th. Turbidity averaged about 0.03. In contrast, on the last day of measurements average urban turbidity exceeded 0.2.

4.9 Mt. Kenya Site Survey Evaluation

During 1976 and 1977 the United Nations Environmental Program (UNEP) and the World Meteorological Organization (WMO) sponsored a program to assess the feasibility of Mt. Kenya, Kenya, as a site for baseline measurements. Several expeditions were undertaken to measure CO_2, Aitken nuclei, and surface meteorological conditions at several locations on the mountain, all above 10,000-ft elevation and several as high as 14,000 ft. In February 1978, GMCC was requested by

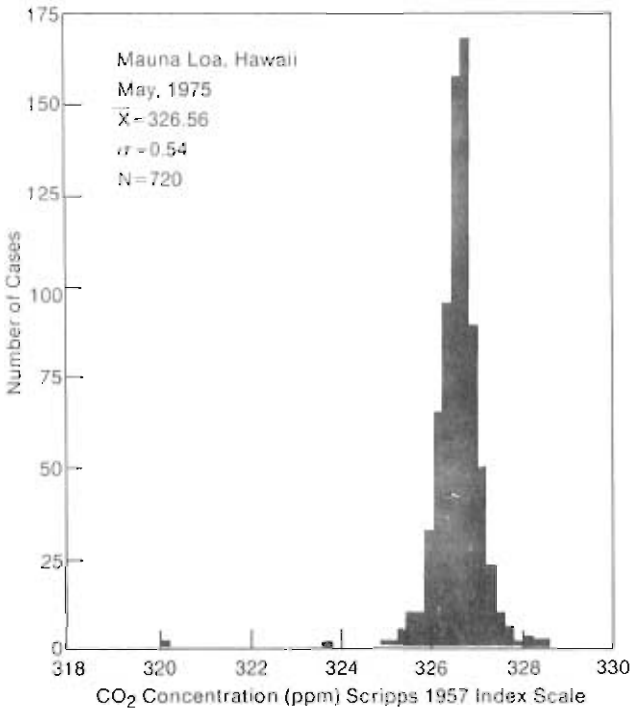

Figure 51.--Histogram of hourly CO_2 concentrations during May 1975, at Mauna Loa Observatory, Hawaii. Each bar represents the number of values within 0.2-ppm intervals. Data are given on the Scripps 1957 index scale.

WMO and UNEP to assess the Mt. Kenya measurements to evaluate the suitability of the area for a baseline monitoring station. Subsequently, a report (summarized here) was prepared (Peterson and Hanson, 1978) and transmitted to the Mt. Kenya Advisory Group for their consideration.

The assessment focused on analyses of CO_2 data and intercomparisons from three locations, Mt. Kenya, Mauna Loa, and Barrow. Almost all the Kenya CO_2 data showed a diurnal cycle. Vegetative photosynthesis takes up CO_2 during daytime whereas respiration during the evening gives off CO_2. Because of the usual tropical convective activity, ground-level vegetation affected CO_2 concentrations for a considerable height into the troposphere. A few MONEX aircraft measurements over the Indian Ocean indicated significant variability of mid-tropospheric CO_2 in the Mt. Kenya region. The 31 over-ocean measurements on June 28 and 29, for example, had a mean of 328.7 and standard deviation of 0.83 ppm. If this tropospheric variability is common over the tropical Indian Ocean upwind of Mt. Kenya, it would be unrealistic to expect extended periods of steady concentrations on the mountain like those found at Mauna Loa Observatory.

One of the Kenyan CO_2 measurement series with least variability was that at Timau Hill during August 1978. Eighty-six CO_2 measurements were made with an overall mean of 328.7 and standard deviation of 1.66 ppm. If the measurements are assumed to be from a normal distribution, the computed 95% confidence interval about the mean is $\pm$ 0.35 ppm. Thus, there is only a 5% chance that the true mean CO_2 concentration at Timau Hill during this period was outside the interval 328.7 $\pm$ 0.35 ppm.

Two examples of Mauna Loa CO_2 measurements were presented as a guide to variability of the record at that observatory. Figures 51 and 52 are histograms of hourly CO_2 measurements at Mauna Loa for May 1975 and May 1976, respectively. Each bar represents the number of values within a 0.2-ppm interval. The monthly

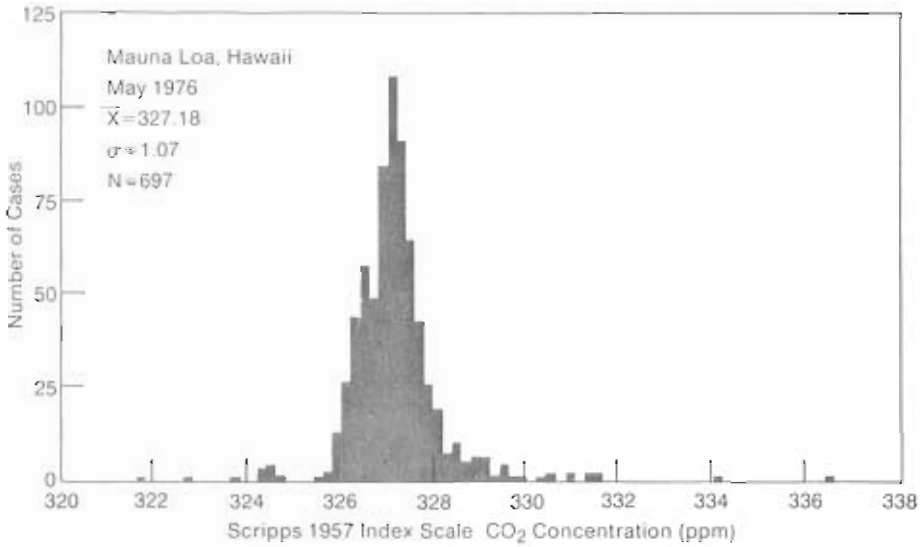

Figure 52.--Histogram of hourly CO_2 concentrations during May 1976, at Mauna Loa Observatory, Hawaii. Each bar represents the number of values within 0.2-ppm intervals. Data are given on the Scripps 1957 index scale.

mean ($\bar{x}$), standard deviation (σ), and number of hourly measurements (N) are given in the legend. During May 1975, relatively little variability can be seen, whereas during May 1976 the variability was quite large. The standard deviations vary by almost a factor of 2 between the months. Even though large variability occurred during May 1976, the majority of the measurements fell within a 2-ppm range. The lowest readings probably corresponded to afternoon upslope airflow depleted of CO_2 by vegetative photosynthesis. The highest values probably occurred when nighttime downslope flow brought volcanic gases from the summit of the mountain.

CO_2 data were also presented from the Pt. Barrow, Alaska, baseline station. The within-year variability of average daily CO_2 concentrations at Pt. Barrow is greater than that at any other U.S. baseline station and most resembled the Kenyan data. Average concentrations during late winter and spring are about 13 ppm greater than those during August. During late summer, daily average concentrations range over about 5 ppm with individual hourly values ranging over about 10 ppm.

Daily average CO_2 concentrations at Barrow from day-of-the-year (DOY) 129, 1976, through the end of 1977 are presented in fig. 53. Several typical features of the Barrow CO_2 record are evident. First, there is an annual cycle of about 12 ppm. Second, there is an annual cycle of the day-to-day variability. The record from about DOY 25-175 is quite smooth. There are several periods of some 10 consecutive days where the range of daily average concentrations is less than 1 ppm. In contrast, from about DOY 200-290 day-to-day variability of about 5 ppm is common. From DOY 290 through the end of the year there are both steady periods and times of daily variation of a few ppm. Third, the 1977 data are approximately 1 ppm greater than corresponding 1976 measurements. These changes are presumably part of the global anthropogenic CO_2 increase. Finally, during summer there is the suggestion that the lowest daily averages form an envelope

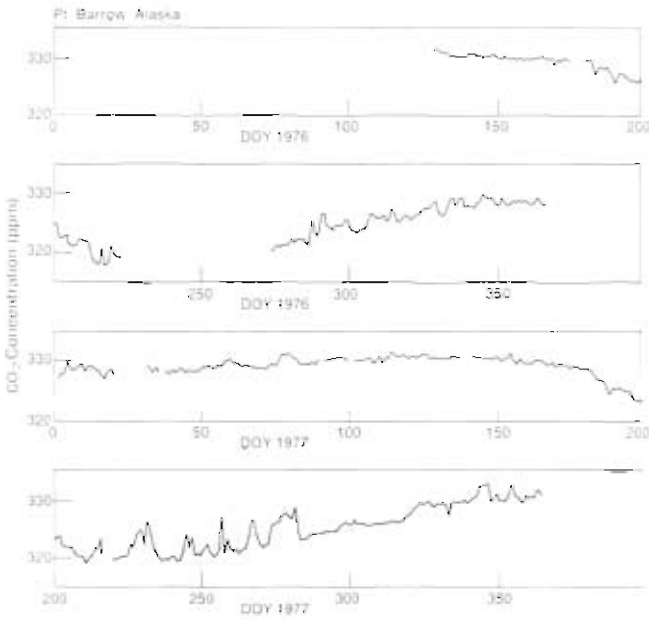

Figure 53.--Daily average CO_2 concentrations at Pt. Barrow, Alaska, for 1976 and 1977. Data are given on the Scripps 1957 index scale.

representing regional background conditions for that place and time, and that the higher daily values include some measurements of nonbackground air. Within the summer season at Barrow we have a poor understanding of the air-land-vegetation-water-ice CO_2 interactions in the Barrow and adjacent polar regions. There is also increased human activity during summer around the settlement southwest and west of the observatory. These complex local factors make it difficult to separate the hemispheric seasonal decrease from local effects. However, selection of those days with small within-day variability and those hours when wind direction was from the clean-air sector (0° to 120°) yielded a measure of background conditions largely following the envelope of lowest values discussed above.

The conclusion drawn from this exercise was that although the summertime Barrow CO_2 record does have extensive variability, measurements representing background conditions could be selected out of the full data set based on meteorological criteria and/or hour-to-hour variability. Similar meteorological and statistical concepts needed to be applied to the Kenyan data to show that periods of background conditions could be identified and that background CO_2 levels could be estimated with small uncertainty. In addition, typical meteorological regimes, both on a local scale (e.g., upslope-downslope) and regional scale should be identified and typed. As such, we recommended that a broad meteorological program including trajectory analyses be included in the Kenyan program.

4.10 Trends in Atmospheric Transmission at Mauna Loa

Ellis and Pueschel (1971) and Mendonca et al. (1978) have reported on the long-term variations in atmospheric transmissions determined from normal incidence irradiance measurements at Mauna Loa. Secular variations greater than a year have been observed and attributed to ejections of volcanic debris to stratospheric heights. Years are required for volcanic debris to be removed from the atmosphere depending on the quantity ejected, the location of the ejection, and the natural cleansing mechanisms.

Figure 54 shows the major departures from the 20-yr monthly averages in atmospheric transmission measured at Mauna Loa. The decreases in transmission in 1963, 1966, 1974, and 1979 follow the major eruptions of Mt. Agung, Awu, De Fuego, and Soufriere, respectively. The gradual decrease in transmission from 1969 to 1974 is unexplained; however, explosive volcanic activity during this period was primarily centered at latitudes greater than 50°. Whether an accumulative effect of the debris from these high latitude eruptions is associated with the gradual decrease in average transmission for this period must still be explored. The transmissions during winter 1977 and 1978 are some of the highest observed in the 20-yr record. The measured transmissions during 1977 and 1978 reached the levels of the pre-Agung period and recovered from the secular attenuations in transmissions which started with the Agung eruption in 1963. During 1977-78, Northern Hemispheric circulation patterns in winter over Mauna Loa altered, and storm tracks over the Eastern and Northwest United States changed to produce severe winters in the East and droughts in the Northwest.

Table 23 lists the monthly average atmospheric transmissions for Mauna Loa Observatory for the 20-yr period. The transmissions are obtained from daily measurements of normal incidence solar irradiances under clear-sky conditions at secant zenith angles of 5, 4, 3, 2.

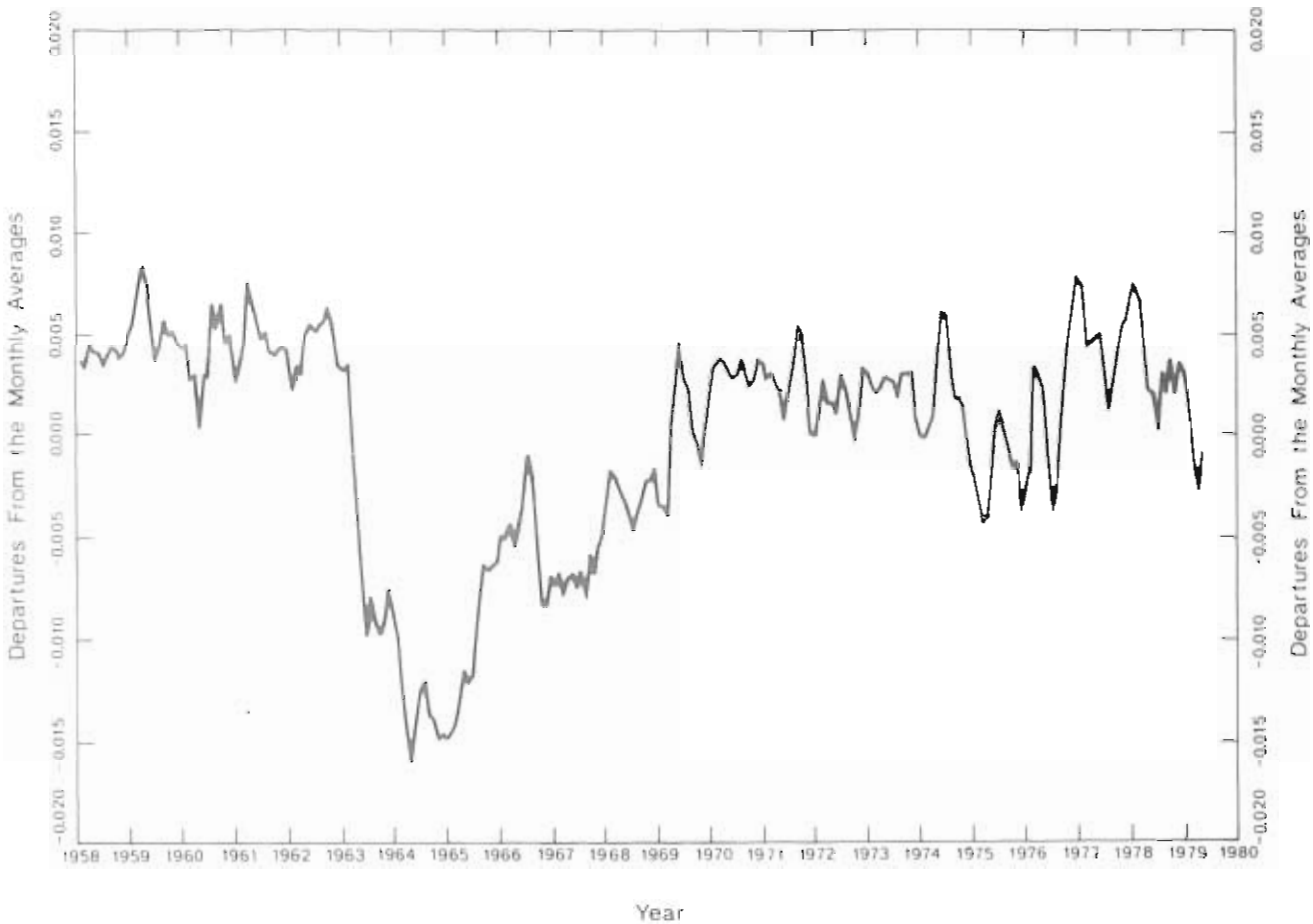

Figure 54.--Plot of the Mauna Loa transmission departures from the composite monthly averages for all years. Departures are the differences between transmissions for individual months and mean transmission of the same months, i.e., Jan 1958 transmission minus Jan mean, Feb 1958 transmission minus Feb mean, etc.

Table 23.--Average apparent solar irradiance transmission ($\bar{T}$)* at Mauna Loa Observatory

	Monthly averages (a.m. values)											
Year	Jan	Feb	Mar	Apr	May	Jun	Jul	Aug	Sep	Oct	Nov	Dec
1958	.936	.933	.933	.929	.930	.931	.933	.933	.934	.935	.933	.935
1959	.938	.936	.934	.934	.935	.930	.931	.936	.934	.936	.935	.937
1960	.936	.934	.935	.924	.928	.925	.936	.933	.938	.934	.937	.935
1961	.937	.931	.934	.933	.933	.930	.934	.936	.934	.932	.936	.937
1962	.934	.936	.929	.930	.928	.933	.936	.932	.936	.937	.935	.936
1963	.933	.935	.934	.926	.909	.920	.922	.920	.919	.921	.923	.925
1964	.921	.918	.913	.909	.908	.918	.917	.915	.915	.917	.913	.918
1965	.919	.914	.917	.915	.912	.914	.920	.925	.922	.923	.925	.925
1966	.926	.929	.922	.921	.919	.922	.929	.932	.923	.920	.923	.924
1967	.926	.922	.923	.916	.918	.922	.919	.926	.920	.926	.924	.926
1968	.929	.929	.928	----	.923	.922	.925	.925	.927	.927	.929	.929
1969	.931	.924	.926	.923	.931	.929	.934	.931	.930	.928	.930	.929
1970	.937	.935	.930	.931	.928	.927	.934	.934	.932	.932	.933	.935
1971	.937	.933	.930	.931	.924	.928	.931	.934	.934	.937	.934	.930
1972	.930	.934	.932	.927	.924	.930	.930	.935	.931	.927	.931	.936
1973	.937	.931	.931**	.929**	.925**	.931**	.933	.930	.931	.937	.931	.933
1974	.932	.929	.930	.927	.924	.938	.937	.929	.931	.934	.930	.932
1975	.928	.928	.926	.918	.922	.929	.931	.930	.928	.929	.928	.931
1976	.924	.932	.931	.932	.924	.927	.926	.922	.932	.935	.933	.939
1977	.941	.938	.935	.925	.932	.934	.930	.932	.930	.935	.937	.936
1978	.938	.941	.935	.929	.928	.926	.933	.928	.937	.930	.934	.934
1979	.937	.933	.927	.921	.922	.931	.932	.931				

* $\bar{T} = \frac{1}{3} \cdot \left(\frac{I_5}{I_4} + \frac{I_4}{I_3} + \frac{I_3}{I_2} \right)$ where $\bar{T}$ = average apparent solar irradiance transmission,

I_n = measure of normal incidence irradiance at MLO at sec Z = n, and n = integers 5 to 2.

**Average for 1970-1974 (data missing for these months).

4.11 Smithsonian Radiation Data Evaluation

The Astrophysical Observatory of the Smithsonian Institution (APO) measured the solar constant on the Earth's surface from 1902 to 1962. Hoyt's report (1979a) discusses a lack of consistency in the APO solar constant measurements resulting from the lack of a common signal between stations or between measurement methods. When the overall data set was considered, there was no evidence for cyclic variations or any long-term trend in the solar constant greater than a few tenths of a percent. Overall, the solar constant appeared to be constant to within about 0.1% over the period 1923 to 1954.

Hoyt (1979b) examined the pyrheliometric and circumsolar sky radiation measurements of the APO, especially those for Mt. Montezuma, Chile, and Table Mountain, Calif., for volcanic effects. Paluweh (8°19' S, 121°42' W), which erupted in 1928, was found to have a dust veil index of 100. Quizapu (35°39' S, 70°46' W), which erupted in 1932, had a dust veil index of 35. Both volcanic eruptions were identified in the APO record and were thought to be climatologically significant.

Using the pyrheliometric measurements of the APO, the relative atmospheric transmission was calculated at four locations during the period 1923 to 1957. Decreases in atmospheric transmission caused by three major volcanic eruptions are evident in the Mt. Montezuma, Chile, records. For those volcanic eruptions in the tropics, the transmission also decreases at Table Mountain, Calif.

A persistent annual cycle in apparent atmospheric transmission found in the APO data set was thought to be caused by variations in total precipitable water and aerosol loading. No long-term trend in total precipitable water was found at the APO sites although there is a large year-to-year variability.

4.12 Solar Variability and Climate

Hoyt (1978) made a simple model of the time variation of the solar constant, assuming that sunspots block radiation and faculae add to the solar constant. In this model an 11-yr cycle appears after 1940 but never exceeds 0.075%. The results of the model demonstrate that the physical mechanism of perturbations to the solar constant by active features on the Sun is probably not a significant source of climatic variation.

Hoyt (1979c) described sunspot structure by taking the ratio of the area of the umbra to that of the penumbra. The time dependence of this umbral/penumbral ratio is similar to the record of Northern Hemisphere surface temperature anomalies. On a year-to-year basis the correlation is 0.57, which is significant at better than the 0.01% level. The umbral/penumbral ratio can be used as a measure of convective flux in the Sun and hence solar luminosity. Using theoretical models for sunspot structure and convection, one can deduce that the observed changes in the umbral/penumbral ratio over the last century correspond to changes in the solar constant of 0.3 to 0.4%.

4.13 Trends in Atmospheric Transmission in the United States

The pyreheliometric measurements at three locations in the United States were examined to determine if there were trends in atmospheric transmission (Hoyt et al., 1979). Although the radiation values at Madison, Wis., were depressed in the 1940's because of local pollution, no strong evidence of other anthropogenic aerosol pollution was seen at Madison, Albuquerque, N. M., or Blue Hill, Mass., from 1940 to 1977. There is a suggestion of increased aerosol pollution for the three stations, but the decrease in atmospheric transmission is rather small. The radiation records give evidence for the eruptions of Agung, Awu, and Fuego. The eruption of Agung increases the optical depth by about 0.035 several months after its eruption. By 1965 the atmospheric transmission returned to normal.

5. COOPERATIVE PROGRAMS

5.1 Aerosol Climatology of the South Pole

A. Hogan, S. Barnard, and J. Samson

State University of New York at Albany
Albany, NY 12222

Cooperative aerosol measurements by Atmospheric Sciences Research Center (ASRC), GMCC, and other observers began at the old Pole station in January 1974. ASRC provided a Pollak counter to standardize the GMCC G.E. condensation nucleus counter; in return, GMCC agreed to make and log two readings of outside aerosol concentration with the Pollak counter each day for ASRC. One observation is made at about the time of the radiosonde ascent; the second is made when convenient, at least 8 h removed. Wind direction and velocity, temperature, barometric pressure, and local weather are noted at the observation time. In 1976, the output of the electrolytic water vapor detector was added to the ICDAS record. Several sizing techniques have been employed over the years, including the Rich diffuser-denuder, the Sinclair diffusion battery, and the Spurny Nuclepore method.

The Pollak counter was calibrated just before shipment to Antarctica in fall 1973. One month later, the ASRC standard was found to agree well with the Minnesota standard, and one year later it agreed well with several other instruments at NCAR. Although the instrument has not been recalibrated since it was shipped to the Pole, an identical instrument was recently recovered from 6-yr field service in Hawaii and was found to repeat its initial calibration. The instrument at Antarctica has performed reliably with only routine maintenance and inspection. A 2-mo period of data (July to August 1975), suspect because of an inlet leak discovered later, is the only flaw in the record.

The Pollak counter and the water vapor detector are exposed through the large GMCC metal inlet stack in the CAF. This exposure has proved to be excellent; a few instances of station contamination do occur each year, but are easily predictable from the meteorological record. No corrections or deletions have been applied to the reported data.

5.1.1 Results of Experiments

Seasonal Variation in Total Aerosol Concentration

A very large seasonal trend in aerosol concentration was readily apparent from initial observations. An extensive series of measurements was made during September-October to identify trends in aerosol concentration accompanying the reappearance of the Sun. Several periods of increased aerosol concentration appeared after sunrise, and summer minima did not approach winter (darkness) minima. We hypothesized that these aerosol events could be the result of photochemical aerosol production or enhanced mixing of the lower layers accompanying the weakening of the winter inversion. Since that time we have attempted in several experiments to produce aerosol particles from vapors in Antarctic air. We have not been able to produce particles during day or night by using ultraviolet light or strong oxidant vapors (iodine). We can, however, produce particles in summer with terpene (limonene from orange peel) vapors. These experiments indicate that enhanced summer aerosol concentrations result from enhanced mixing rather than photochemical production of aerosol.

Figure 55.--Mean values of temperature, wind speed, water vapor, mixing ratio, and Aitken nucleus concentrations observed concurrently at South Pole during the sunlit months, Oct - Mar. Frequency of wind direction occurrence is shown with the origin of the graph superimposed on the station location on the map.

Meteorological Variation in Aerosol Concentrations

Surface winds at the South Pole are predominantly from the northeast quadrant (north being defined here as the Greenwich Meridian). Storm winds are generally from the northwest, and bright clear days occur with winds from east to southeast. The camp is south of the CAF, but winds from this direction occur less than five times per year.

Previous experiments showed that the greatest concentrations of larger particles arrive with moist storm winds from the northwest. Great concentrations of very small particles occur in strong subsidence following frontal passage.

An attempt was made to stratify the 4 years of summer and winter data by wind direction. The variations in aerosol concentration, water vapor mixing ratio, temperature, and wind speed are shown in figs. 55 and 56, plotted as a function of wind direction by 20° increments. Wind direction is most frequently from the northeast quadrant as previously reported, with only 17% of winter winds and 18%

Figure 56.--Similar to fig. 55 but for the winter months, Apr - Sep.

of summer winds from outside this sector. The 010° to 030° sector is favored (21% of total) in winter, but all sectors of the northeast quadrant receive equal fractions of the total winds during summer. The fastest (15 kt mean speed) winter winds are also from the 010° to 039° sector.

The temperature wheels show a smooth decrease in temperature with increasing easterly component of wind in winter and a less marked decrease in summer. Most striking is the decrease in water vapor mixing ratio as the wind vector swings from northwest to southeast.

The number of aerosol particles is also at a maximum with winds from the northwest in winter and summer. A very strong decrease in aerosol concentration occurs with increasing eastward wind component in winter, but mean concentrations are more equally distributed from north to southeast in summer.

We propose a relatively simple explanation for these phenomena. When strong high pressure is present over east Antarctica, a blocking of circulation occurs which prevents air from the Weddell Sea area from reaching the Polar Plateau. When a high is centered between the Weddell Sea and the Polar Plateau (i.e., north of the station) a very short path from open water to Pole is available, and warm moisture- and aerosol-laden air reaches the station. As the high

Table 24.--Number of observations (N) and monthly mean aerosol concentrations ($\bar{Z}$ cm^{-3}) at Amundsen-Scott South Pole Station

Month	Old Pole 1974		CAF #1 1975		CAF #1 1976		CAF #2 1977		CAF #2 1978	
	N	$\bar{Z}$ cm^{-3}	N	$\bar{Z}$ cm^{-3}	N	$\bar{Z}$ cm^{-3}	N	$\bar{Z}$ cm^{-3}	N	$\bar{Z}$ cm^{-3}
Jan			25	103	43	138	48	119	62	254
Feb	6	85	56	109	42	226	48	159	56	188
Mar	22	349	91	119	72	140	62	120	84	121
Apr	22	109	85	47	56	57	54	44	102	30
May	4	29	61	24	60	49	62	31	93	20
Jun	13	29	57	13	58	M*	59	22	90	7
Jul	49	23	59	12	61	M*	62	15	93	10
Aug	19	53	63	16	62	15	62	16	91	9
Sep	94	48	57	36	83	37	60	43	90	27
Oct	56	117	40	99	61	124	62	178	93	79
Nov	23	159	25	254	55	364	56	169	80	172
Dec	1	89	41	131	32	121	57	161	53	154
Mean		82*		68		M*		88		76

*M = missing concentration.

center is displaced eastward the trajectory from open water increases, and more heat and water vapor are lost to the ice cap before the air arrives at the Pole. The discrepancy in rate of decrease in temperature and water vapor with respect to aerosol concentration indicates that at low concentrations aerosol is removed quite slowly as it approaches its end-point concentration.

Trends in Antarctic Aerosol Concentration

The monthly mean concentrations of aerosol observed at South Pole are tabulated in table 24. There is no discernible trend in either summer or winter concentrations. November has the highest mean concentration in nearly every case, and June, July, August, and early September are repeatedly quite low.

5.1.2 Conclusions

Aerosol data for 5 years from South Pole show a distinct seasonal trend but no secular trend. There is a slight tendency for aerosol concentrations to decrease with increasing easterly component of surface winds. These findings should be evaluated in future searches for secular trends.

Aerosol concentrations appear to decrease at a less rapid rate than water vapor and air temperature with increasing path length from open water. This rapidly decreasing rate in aerosol concentrations can be interpreted as an end point in aerosol removal mechanisms. The aerosol concentrations measured under these conditions are assumed to be asymptotically approaching a minimal level in the Arctic.

5.2 Chemistry of Antarctic Aerosols at the South Pole

William H. Zoller

University of Maryland
College Park, MD 20742

Atmospheric particulate material has been collected at the South Pole for four austral summer seasons and two winters since 1970. With R. A. Duce of the University of Rhode Island, we have tried to identify the sources of Antarctic aerosols by their chemical composition. During the austral summers the samples were collected at the remote site 5 km northeast of the South Pole Station to minimize contamination from the station.

The first summer samples were collected in November and December 1970, as part of Operation Deep Freeze (DF 71), upwind of the old Pole station, and the findings have been published by Zoller et al. (1974). Samples that were collected during DF 72 to 74 were badly contaminated by construction. During December 1974 and January 1975, a very good set of samples was collected at the new site (5-km altitude) as reported by Maenhaut and Zoller (1977) and Maenhaut et al. (1979a, 1979b). Additional austral summer samples were collected during DF 76,78 and 79 at the remote site and at the CAF during DF 78 and 79. The samples for DF 76 and 78 have been analyzed so that data are now available for four summer seasons.

Severe weather conditions preclude the use of the remote site after the temperature drops below -45°C. For this reason, the overwinter samples have been collected at the CAF with the help of the winter-over NOAA personnel present. Samples for winter 1975 were collected by G. Engeman and S. Kott at the temporary under-snow facility. These samples suffered some contamination but yielded usable data for many elements. The winter 1976 samples were collected by V. Szwarc and J. Jordan at the same facility after modifications to the sampling system. C. McGregor overwintered in 1978 and collected samples at the new CAF; these are being analyzed.

The samples are collected by pulling large volumes of air through filters with a vacuum pump. Care is taken to minimize contamination, and a wind-directional controller is used to turn the pumps off if the wind direction changes so that the station could contaminate the samples. Each sample returned is counted with γ-ray detectors to measure natural radioactivity, such as ^{7}Be, and fission products from nuclear tests (Maenhaut et al., 1979b). These radionuclides are good tracers of different air masses and transport phenomena. Neutron activation analysis and atomic absorption are used to measure as many trace elements as possible on each sample. (For details of the analytical work on the samples and blanks, see Maenhaut and Zoller, 1977, and Maenhaut et al. 1979a.)

The results of the chemical analyses are interpreted by comparing the elemental distributions patterns of the two dominant sources of atmospheric particulate material in remote areas. To identify elements associated with each source and estimate the relative importance of each to the South Pole aerosol burden, the marker elements Al and Na were chosen to represent the crustal and oceanic material. By comparing them with the composition of average crustal material (Taylor, 1964) and of sea salt (Brewer, 1975), the observed elements are divided into the following three groups (table 25): crustal weathering, sea salt, and enriched or volatile elements. The elements with essentially the same distribution pattern as average crustal material are probably of crustal origin.

Table 25.--Elements observed at South Pole (DF 75)

Crustal components:	Al, Sc, V, Fe, Mn, Th, Ti, La, Sm, Eu, Ce, Lu, Hf, Co, Rb, Ta, Cs, Ba, (Mg, Ca, K, Cr)*
Sea salt:	Na, (Cl, I, Mg, Ca, K)
Volatile elements:	I, Br, Cl, S, Se, Cd, Ag, As, Au, Pb, Sb, W, In, Cu, Zn (Cr)

*Elements in parentheses have components from more than one source.

Very little of the sodium is of crustal origin, and its most probable source is the ocean.

Other elements also have a significant oceanic component (table 25). The last group of elements is enriched in the South Polar aerosol far more than would be expected if their source were crustal weathering or sea salt. The source of those elements is unclear, and has been discussed at length in the literature (Zoller et al., 1974; Maenhaut et al., 1979a; Duce et al., 1975). The sulfur (as sulfate) is the most abundant element present. From the data from DF 75, it accounted for approximately 90% of the mass of the measured components whereas the crustal material and sea salt accounted for 4% and 5%, respectively. The sulfate is believed to be transported to the Pole through the lower stratosphere, since it correlates well with ^{7}Be, which is of stratospheric origin (Maenhaut et al., 1979a).

In this report, the results of the analyses of samples from four summer seasons and two over-winter periods are compared for the crustal and marine sources. The mass of crustal components has been calculated for each sample by assuming that all Sc, Al, and V arise primarily from the Earth's crust. The sea salt components were calculated by assuming that all Na not accounted for by the crustal component originated from airborne sea salt. Figure 57 shows the masses of the crustal and marine components for sampling periods. Table 26 gives the average mass loadings of crustal material and sea salt for each of the six sampling periods as well as the ^{7}Be concentration. The most striking observation is that during the winter season the crustal component drops to about one fourth of its summer value, whereas the sea salt component increases to about 20 times its summer value.

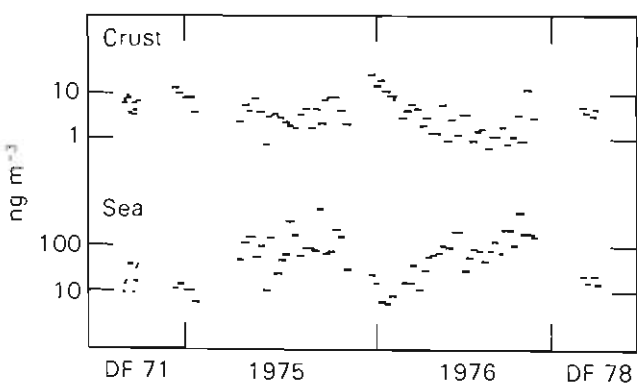

Figure 57.--Aerosol mass determinations for crustal and sea salt aerosol classifications at SPO. Samples are taken by high-volume filter sampling at the surface. Note annual variation in both aerosol classifications.

Table 26.--Mass of atmospheric components and ^{7}Be at SPO

	Crust (ng m^{-3})	Sea (ng m^{-3})	^{7}Be (fCi m^{-3})
DF 71	6.3±2.0	7.1±4.0	
DF 75	9.1±3.6	3.1±0.9	198±24
DF 76	15±8	3.1±2.3	215±30
DF 78	4.1±0.9	5.4±1.1	205±50
Av. summer	8.6	4.7	206
1975	3.1±1.3	96±43	69±1
1976	1.7±1.0	100±60	66±16
Av. winter	2.2	100	68

These observations must reflect a seasonal difference in transport of atmospheric particulates to the South Pole. Sulfate follows the crustal component, but the decrease during the winter is not as large, being only a factor of 2 or 3, which is similar to the change in ^{7}Be. These results suggest that the crustal components and ^{7}Be are involved with a transport mechanism relating to the lower stratosphere and may be indicative of long-range transport, whereas the sea salt enhancement and ^{7}Be decrease during the winter are correlated with some form of a tropospheric transport process. In the winter, severe storms surround the Antarctic continent, and probably enhance the airborne sea salt component in coastal areas. These storms could also transport the sea salt aerosols into the upper troposphere near the coast of the Weddell Sea and into the interior of the continent.

More long-term monitoring of the chemical composition is obviously needed to help evaluate both the sources and transport of atmosheric aerosols to the South Pole. The chemical compositions of the aerosols themselves identify them so that changes in concentration or composition may be related to similar changes in sources.

5.3 Individual Particle Analysis of Antarctic Aerosols

Farn Parungo

Atmospheric Physics and Chemistry Laboratory, NOAA
Boulder, CO 80303

Aerosol samples were collected on Nuclepore filters at the South Pole station during October and November 1977. The particles were analyzed with an electron microscope for their morphology, size distribution, and concentration (fig. 58). The chemical compositions of individual particles were determined with an X-ray energy spectrometer as was the frequency of elements present in the particles (fig. 59). The results provide basic information on the physical and chemical properties of Antarctic aerosols as well as their source and journey. The following origins of Antarctic aerosol particles are suggested: surrounding oceans, Antarctic mountain ranges, other continents, meteors, volcanoes (specifically Mt. Erebus), and the stratosphere (particularly for Aitken nuclei).

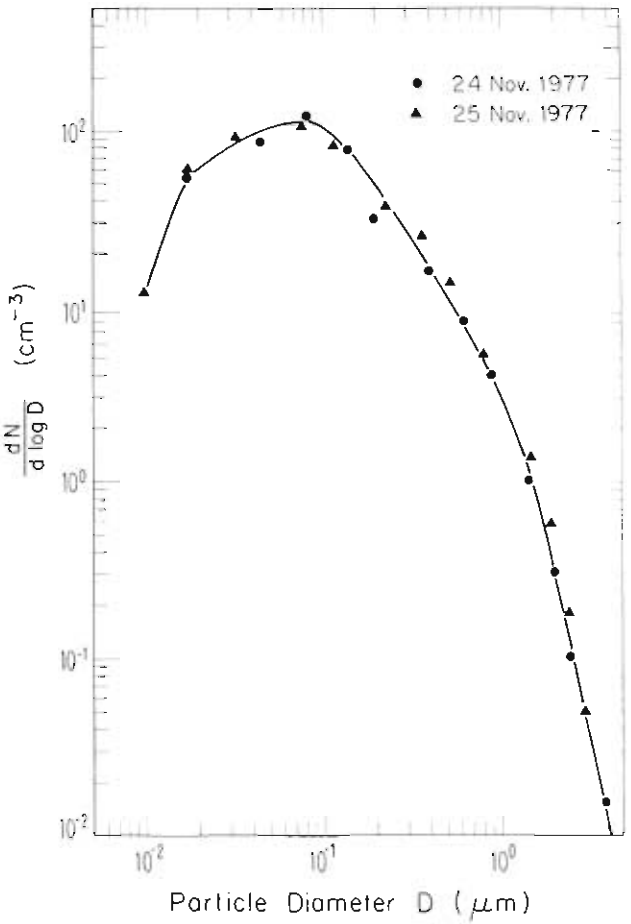

Figure 58.--Size distribution and concentration in SPO aerosol samples.

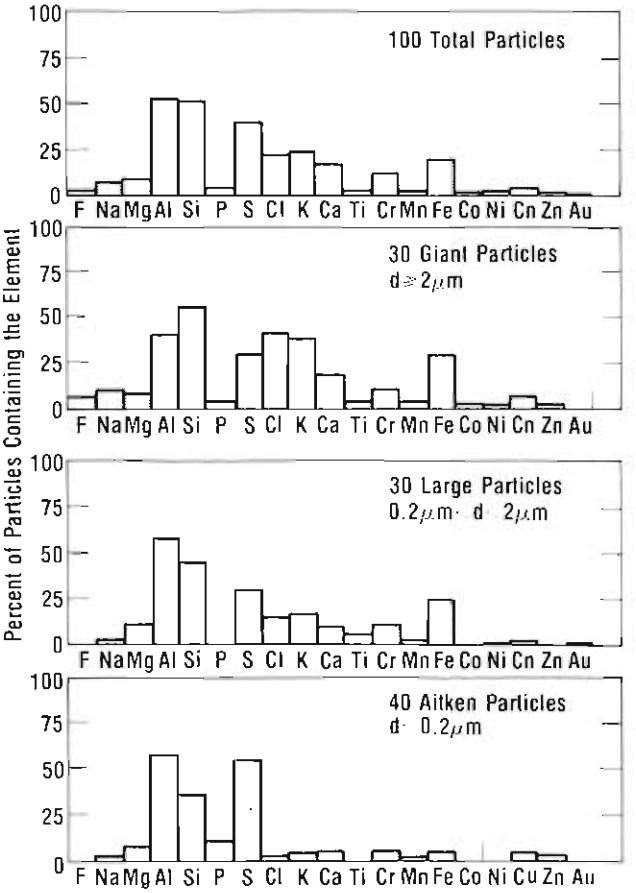

Figure 59.--Frequency of elements present in particles collected at SPO.

5.4 Monitoring of Large Atmospheric Particles at South Pole Station

J. R. Petit

Laboratoire de Glaciologie du CNRS
Grenoble, France

We are studying insoluble microparticles in the snow to determine short-term (seasonal) changes as a possible way to date ice core when other techniques, such as stable isotopes, cannot be applied. Possible correlations of microparticle content with climatic changes or volcanic events will be studied.

The seasonal changes of microparticles are not always clearly shown in the snow record, although they are generally assumed (Thompson et al., 1975). The aim of this project is to study atmospheric microparticle concentrations measured near the surface to study seasonal changes and to help evaluate the interpretation of the snow data.

To compare measurements of atmospheric aerosols with the data obtained from the snow samples (determination of particles greater than 0.8 μm) a photoelectric

particle counter (Coulter 550) was used to measure particles greater than 0.5 μm. This counter is generally used to monitor aerosol concentrations below 3,000 ℓ of air. Although calibrations are regularly made, there may be some uncertainties in the obtained absolute value; however, relative changes with time, which are the most important for our purpose, should not be affected by these uncertainties. Because of the low concentration of atmospheric particles, one measurement requires the analysis of about 10 m^3 of air, obtained by pumping for 5 hours.

The first data were obtained over a period of 3 weeks during the 1977-78 field season, by using the CAF at the South Pole Station. The measured concentrations are in the range of 400 to 2,000 particles m^{-3} STP; these values agree with the results obtained by Hogan (1977) with a similar aerosol counter (Royco). This program is being continued as a cooperative project with the NOAA/GMCC.

5.5 Chemical and Optical Properties of the Barrow Aerosol

Kenneth A. Rahn

University of Rhode Island
Kingston, RI 02881

During 1978 the joint research program on the chemical and optical properties of the Arctic aerosol by the Universities of Rhode Island (K. Rahn) and Alaska (G. Shaw) continued at Barrow. Continuous 3- to 4-day aerosol samples were taken with a high-volume filter sampler at the observatory. Trace elements such as vanadium were analyzed. In addition, techniques for determining sulfate and ^{210}Pb were developed by R. McCaffrey of URI and applied to the first 2 years of Barrow filters.

Nonmarine sulfate showed unexpectedly high monthly mean concentrations of 1 to 2 μg m^{-3} during winter, with a maximum of 2 to 2.5 μg m^{-3} in March. Individual samples varied greatly, with maxima approaching 5 μg m^{-3}. In summer, however, the concentrations were an order of magnitude lower, about 0.1 to 0.2 μg m^{-3}. This seasonal variation is very similar to that of vanadium noted in the 1977 GMCC Summary Report. Figure 60 shows the monthly mean concentrations for nonmarine sulfate and noncrustal vanadium at Barrow during 1976-77. The amplitude of the vanadium cycle is greater than that of sulfate for unknown reasons.

The high concentrations of sulfate are significant. In winter, the concentrations of sulfate in midlatitude polluted regions, such as Europe or the Northeastern United States, are about 6 μg m^{-3}, only 3 to 4 times higher than at Barrow. In contrast, vanadium is 30 to 40 times more concentrated in midlatitudes than at Barrow. Thus, sulfate is enriched relative to vanadium (and most of the other trace elements) at Barrow by an order of magnitude relative to midlatitudes. Sulfate is a major constituent of the Barrow aerosol, and its high concentration provides a clue to the explanation for the winter-long Arctic haze. As opposed to trace metals at Barrow, which are inevitably many times less concentrated than in midlatitudes, the sulfate concentration is only modestly reduced.

The most likely source of this sulfate is midlatitude pollution SO_2. Marine sulfate has already been subtracted out; it accounts for half the total sulfate in summer but only 20% in winter. Subsidence from the stratosphere can

also be eliminated because ^{7}Be and O_3 concentrations at Barrow in winter are only 1% of their stratospheric values; reducing stratospheric sulfate by this same factor yields less than 0.01 $\mu g\ m^{-3}$. Volcanism is a possible source, but it is not clear why it should produce only a winter maximum of sulfate. At this time we have no evidence that volcanoes should contribute significantly to the Barrow sulfate, although this source cannot be excluded. Biogenic sulfate should be a minimum, not a maximum during the winter, and so can be eliminated as well. Midlatitude pollution sources are sufficient to account for the sulfate at Barrow.

The ^{210}Pb data from Barrow are interesting. ^{210}Pb has been determined in filters from Barrow by the Environmental Measurements Laboratory of New York City. Their data, as well as ours, show that concentrations of ^{210}Pb at Barrow during winter are the highest of any of their sampling stations. In particular, they are about two times higher than in the Northeastern United States. During summer, however, ^{210}Pb is 10 to 15 times less concentrated in Barrow, and is lower than in the Northeast United States. This high winter concentration agrees with the behavior of sulfate and vanadium (and the Barrow aerosol in general); in fact, our data for sulfate and ^{210}Pb from the same filters show that the two have an extremely tight correlation. The high absolute values of ^{210}Pb concentration are puzzling, however, because they indicate that Barrow is twice as "continental" as the Northeast United States (^{210}Pb is derived from ^{222}Rn, which is exhumed from continents), which is clearly not the case. We feel that the great parallel between ^{210}Pb and sulfate, both of which are secondary aerosols (derived from atmospheric gases rather than being injected directly into the atmosphere as aerosol) and are much more concentrated in Barrow than expected, is no coincidence. It can be explained by continual gas-to-particle

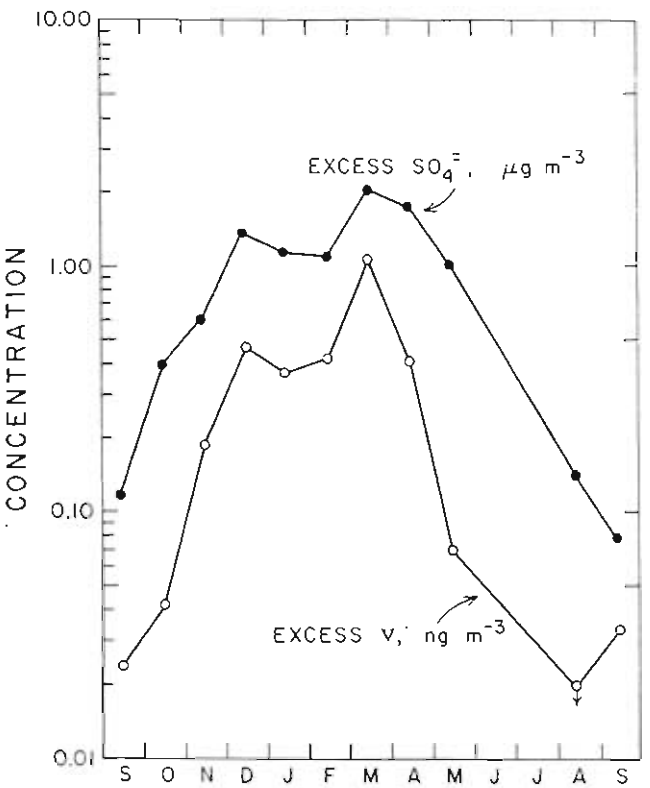

Figure 60.--Monthly mean concentrations of excess (nonmarine) sulfate and excess (noncrustal) vanadium in the surface aerosol at BRW, 1976-1977.

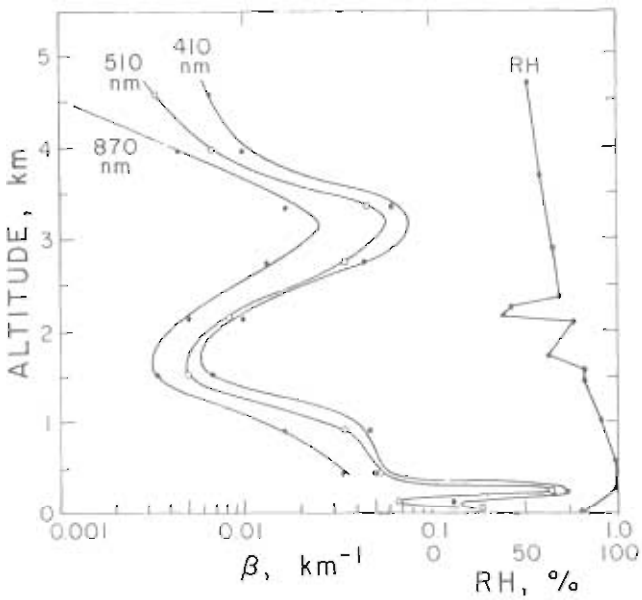

Figure 61.--Vertical profiles of optical extinction coefficient β at three wavelengths, near Barrow, Mar 31, 1978. Note general relation to relative humidity.

production in the Arctic atmosphere coupled with abnormally long residence times during winter, so that secondary products can build up to very high concentrations before being removed. We presently estimate Arctic residence times during winter to be up to an order of magnitude longer than those of midlatitudes, or 1 to 2 months or more.

Support for the midlatitude source of the Barrow aerosol, followed by long-range transport and decreasing removal rates during transport, comes from a series of calculations which show that the concentrations of V, ^{210}Pb, and sulfate at Barrow in winter are quantitatively compatible with a midlatitude source, transport times of 15 to 20 days, dilution of the basic air mass by factors of about 6 during transport, and residence times which increase from 5 to 50 days during transport.

During March and April 1978 we performed a field experiment at Barrow, part of which was a series of four aircraft flights during which vertical profiles of haze were measured with a sunphotometer. The results of one of these flights are shown in fig. 61. They are typical, and show a major low-lying haze band at about 300-m elevation and a secondary, broader band at 3000 m. Relatively clear layers are found at the surface, between the bands, and above the upper band. Our experience is that the haze layer below 1 to 2 km and the clear layer near the surface are reproducible features of the Barrow atmosphere during winter. It can also be seen from fig. 61 that maxima of haze correspond with maxima of relative humidity. This suggests that Arctic haze is largely water condensed on hygroscopic nuclei, an explanation compatible with the high sulfate concentrations in the aerosol. Microscopic inspection of haze particles impacted onto a glass slide shows that they are dominated by colorless spheres, most having a radius less than 1 μm. Our previous electron microprobe analysis of these particles has shown them to be rich in sulfur; K. Bigg of CSIRO, Australia, has demonstrated that they are made up of a mixture of ammonium sulfate and sulfuric acid.

Thus Arctic haze seems to be created in large measure by the combination of high relative humidity in the Arctic atmosphere (primarily near 1 or 2 km), high concentrations of sulfate (from midlatitude SO_2), and long residence times.

5.6 Nature of the Aerosol at Barrow

E. K. Bigg

CSIRO
Sydney, Australia

A project to collect particles at baseline air pollution monitoring stations was begun in 1975. Size distributions, chemical nature, and physical characteristics of the particles were recorded with an electron microscope. Thus aerosol properties at each site were documented as a reference against which to measure future changes and to aid interpretations of other measurements, such as back-scattered light and turbidity.

Bigg (1977) published a detailed description of the aerosol at MLO based on observations made continuously during 6 weeks in mid-1975. After another 6-wk sampling in 1976, the collectors were transferred to Barrow, Alaska, and used for 6 weeks between December 1976 and March 1977. Further continuous samples were taken from March 21, 1978, to May 25, 1978. Continuous collections have also been made at the Australian baseline station at Cape Grim, Tasmania, since April 1976, and a new sampler was installed at SPO in January 1979. In Mauna Loa and Barrow collections and during the first 2 years at Cape Grim, aerosols were impacted directly onto electron microscope grids for a few minutes every hour, the grids moving very slowly (one per 7 h) beneath the nozzle. Grids on a second turntable formed the collecting surface of an electrostatic precipitator to capture particles down to about 0.01-μm diameter. At South Pole and Cape Grim after mid-1978 reduced-pressure impactors were used to obtain the small particles.

Rahn et al. (1977) called attention to the Arctic haze, a variable but high turbidity observed in the supposedly clear Arctic regions, particularly in spring. They deduced that continental dusts from Asia were responsible for the haze. The aerosol that we collected in 1976-77 showed unequivocally that the dominant light-scattering particles were almost entirely sulfuric acid, although a fair proportion of them contained solid electron-dense inclusions. Clay particles (flat irregular plates partly transparent to electrons and stable to heat) were present but always as a minor constituent.

Figure 62 shows a typical group of particles collected on a carbon surface precoated with silicone oil at 1700 h local time on December 15, 1976. Droplet rings surrounding a central particle are typical of sulfuric acid. When collected on a calcium-fluoride-coated surface the sulfuric acid reacts to form calcium sulfate, and any insoluble inclusions are revealed (see fig. 63).

The main conclusions are as follows:

(1) Sulfuric acid was the dominant winter aerosol in 1976-77.

(2) Winter size distributions in 1976-77 were relatively constant.

(3) In spring 1978 the sulfuric acid particles contained a very variable and sometimes much greater proportion of ammonium sulfate than in winter. There were more large particles than in winter.

(4) From 10% to 20% of the acid particles contained insoluble inclusions ranging from spheres through irregular but compact forms to highly irregular chains or aggregates of small particles.

(5) Clay particles uncoated with acid were observed at irregular intervals, particularly during the spring of 1978.

(6) The most common size of particles per unit logarithmic radius interval

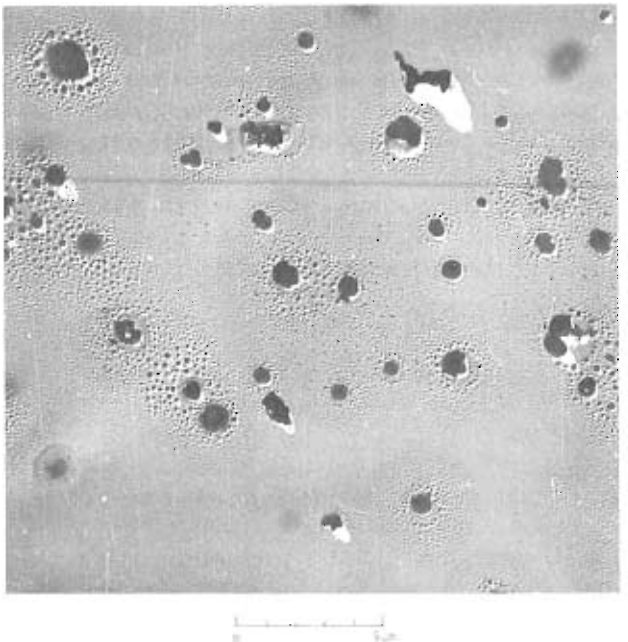

Figure 62.--Particles collected on a carbon surface at Barrow, Alaska, at 1700, Dec 15, 1976.

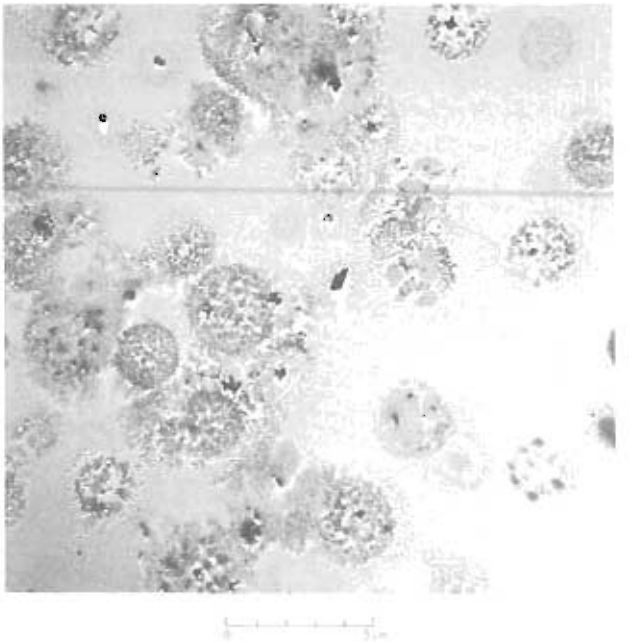

Figure 63.--Particles collected on a calcium fluoride surface at Barrow, Alaska, Jan 1977. Sulfuric acid component has reacted with the calcium fluoride. Even dark particles have an acid coating.

was between 0.1 and 0.2 μm, which is larger than at the other sites examined.

(7) Vertical soundings of the aerosol were made in June from a light aircraft by using an impactor and Aitken counter. Particle concentrations were greatly depleted below the strong temperature inversion at about 300 m.

These conclusions are not completely consistent with Rahn and Shaw's (1978) re-assessment of the origin of the Arctic haze. The fact that surface aerosol concentrations are so different from those at 300-m higher altitude suggests that vertical profiles of the aerosol at this station should form an essential part of monitoring.

5.7 Ice Nucleus Measurements

Takeshi Ohtake and Andrew Fountain

University of Alaska
Fairbanks, AL 99701

To determine the source regions and concentrations of ice nuclei in the Alaskan atmosphere, an ice nucleus observing program was set up by the Geophysical Institute, University of Alaska. For the 11 months of the project three sites were set up for data collection: Barrow (GMCC), Fairbanks, and Homer. Two temporary sites, one aboard a trans-Pacific ship and the other on Attu Island in the Aleutian Chain, were also used. At each site two filters, each sampling different volumes, were exposed simultaneously.

To estimate better any effect that condensation nuclei may have on the filter method of ice nuclei collection, the Barrow GMCC station also measured the condensation concentration during the filtering period with a G.E. condensation nucleus counter. At the Fairbanks site impactor samples were taken for later analysis in the combined X-ray energy spectrometer and scanning electron microscope. This instumentation yields a qualitative estimate of chemical composition of the ice nuclei.

Because of the close network of sites and their almost north-south alignment it is hoped that the correlation of station data and air flow trajectory will be more accurate and therefore more comparable than the large, widely spaced networks previously used in the north Pacific. The three sites also represent the three climatic zones of Alaska: the north slope, interior, and southern coast. When these stations are all subject to the same general air flow, the local climatic characteristics should appear, and it may be possible to estimate better the local effects of the ice nuclei concentration.

5.8 Multiwavelength Turbidity at Mauna Loa Observatory

Glenn E. Shaw

University of Alaska
Fairbanks, AK 99701

Multiwavelength sunphotometers were calibrated at Mauna Loa in December 1978 and in March 1979 after field work with the instruments in Antarctica. The two calibrations, separated in time by 4 months, gave calibration constants that agreed from 0.3% to 1.0%, with the largest variations occurring at the shorter wavelengths (the wavelength range sampled was $400 < \lambda < 1000$ nm). The close agreement in the calibration constants demonstrates the excellent sky conditions at the observatory; at more turbid stations one normally finds fluctuations of 10% to 20% in the Langley plot calibrations (Shaw et al., 1973) resulting from diurnal changes in aerosol concentrations. Aerosol conditions at Mauna Loa are not noticeable until midday, when aerosols are advected upslope to the observatory. All our data were taken in the morning hours.

The Mauna Loa measurements indicate that the combined upper tropospheric and stratospheric aerosol optical thickness was smaller than it was in spring 1976 and in 1977. These observations indicate that the stratosphere has recovered from volcanic perturbations created by the eruptions of Agung and Fuego. Optical attenuation at 500-nm wavelength was 1.5% to 2.0% when the Sun was near the zenith.

The same values of optical extinction (to the limits of uncertainty) were found at South Pole Station and at MLO in December 1978 and January 1979, but slightly smaller values, by about 10%, were measured from the summit of Mt. Erebus, Antarctica, in January 1979. Some measurements of turbidity (aerosol optical depth) at different station altitudes are shown in fig. 64.

Besides the optical calibrations, we also collected samples of aerosol at Mauna Loa with a Bigg impactor. The analysis of X-ray spectroscopy is not yet complete, but initial inspections indicate that a large proportion of sulfur exists in the samples taken. It is not certain if the samples were contaminated by the volcano's effluent.

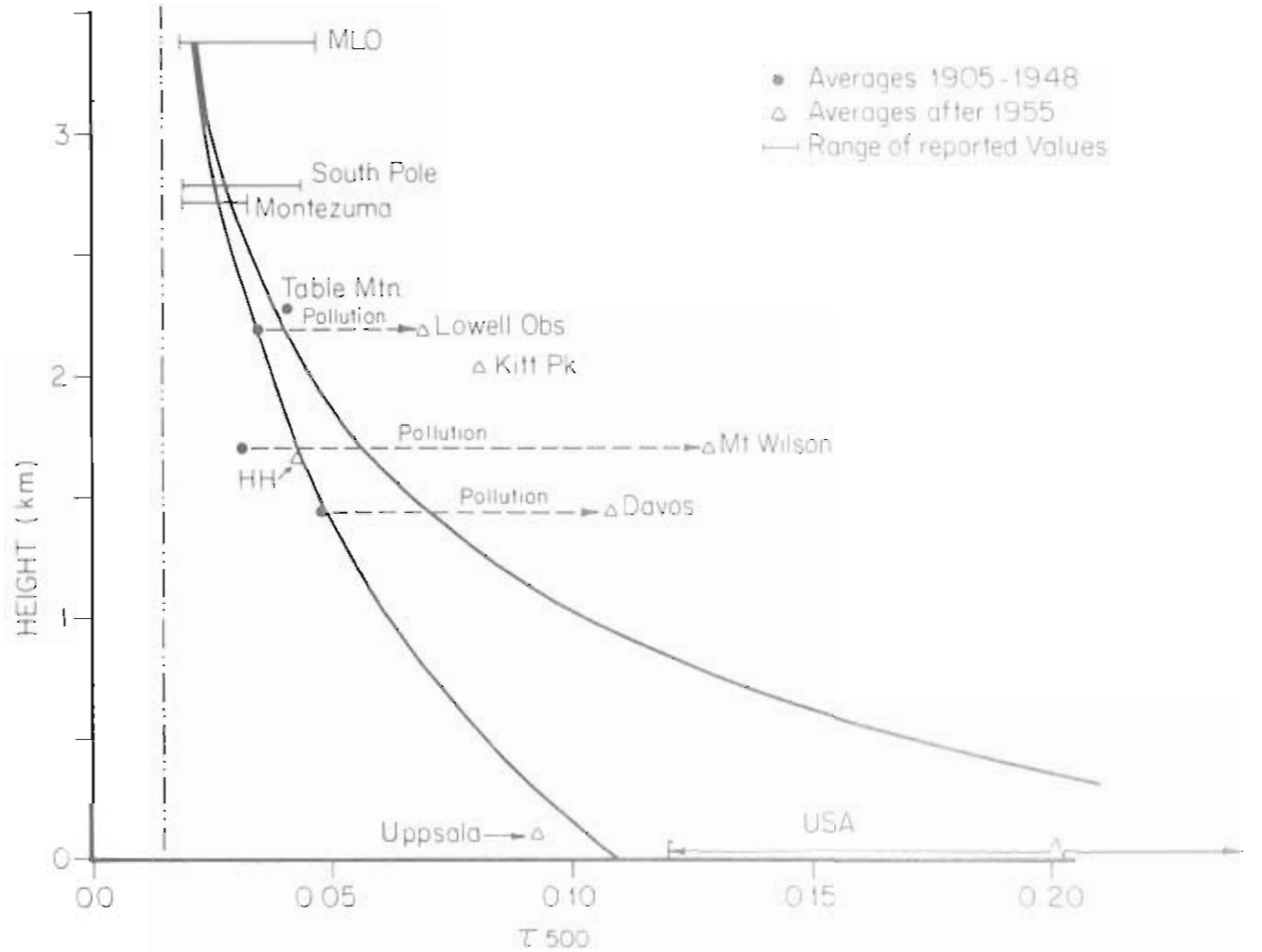

Figure 64.--Plots of turbidity at mountain observatories (τ_o at 500 nm) as a function of altitude, showing increases since 1955. Data are from Volz (1978) and Flowers et al. (1969).

5.9 Pyrheliometer Measurements at Mauna Loa Observatory

G. D. Robinson

Center for the Environment and Man
Hartford, CT 06120

We have continued work on the record of the glass filter channels of the broad-band pyrheliometer. The redundancy in the observations, provided by the overlap of the channels, allows an estimation of the systematic errors introduced by thermopile calibration errors and incorrect assumptions concerning the filter cut-off wavelengths. The method requires extrapolation to zero air mass of the difference between the measured signal and that computed for a standard particle-free atmosphere. The assumptions concerning the extraterrestrial solar spectral irradiance are given in the 1977 Summary Report. The standard atmosphere

attenuation was recomputed, using the new Fröhlich-Shaw (1978) approximation for Rayleigh scattering and the Labs-Neckel spectrum in 10-nm bands. Figure 65 shows the results of two data sets after error analysis. The method does not provide a unique analysis, and in fig. 65 all adjustments have been made by changing the relative sensitivities of the thermopiles, with no change in the assumed cut-off wavelengths. The overall average thermopile sensitivity, of course, is not changed to preserve the relation to the accepted solar constant through reference to a common substandard.

Figure 65 shows measurements on the 2 days in August 1975 discussed in the 1977 Summary Report and the average of 7 days in March and April 1974. Note that the intercept on the zero air mass axis is less than 1 W m^{-2} in all cases, indicating that the observations are compatible with the assumptions concerning solar spectral irradiance within about one-quarter percent. The slopes of the lines imply an attenuation τ_m in excess of that assumed in computation where τ (per air mass) is:

	GG22/OG1 Channel	OG1/RG8 Channel
Mar/Apr 1974	0.010	0.021
Aug 23, 1975	0.022	0.012
Aug 24, 1975	0.026	0.009

The 1975 values are of the magnitude expected for attenuation by particles, but the high value of 0.021 for the OG1/RG8 channel in 1974 relative to that for GG22/OG1 is difficult to explain, particularly as the average of 7 days, although it would be reduced to 0.005 if the assumed ozone column were increased from 0.275-cm STP to 0.325-cm STP (the τ for GG22/OG1 would be 0.008 for this ozone column). All adjusted measurements are compatible with the assumptions within 1% to 2% of the irradiance in the differential pass bands, which is better than 0.5% of the measured irradiance of the RG8 channel and less than 0.25% of the solar constant.

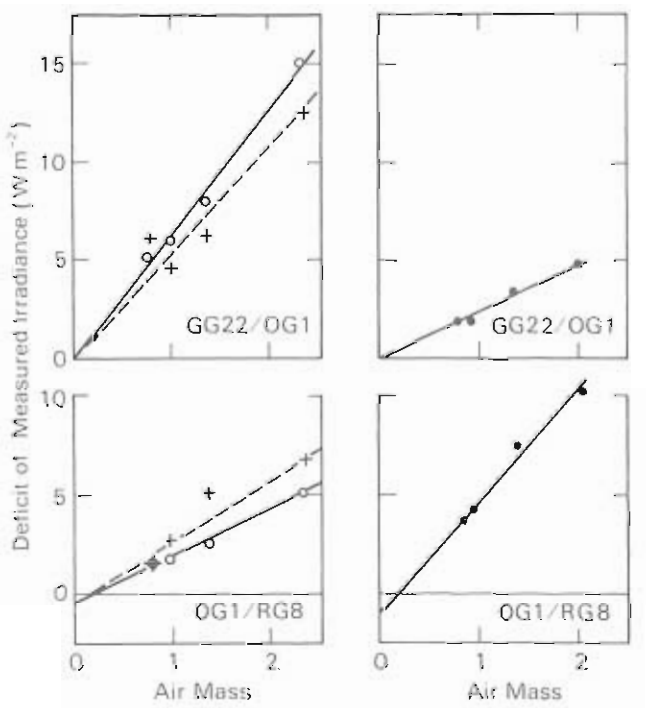

Figure 65.--Extrapolation to zero air mass of the difference between computed measured irradiance in spectral bands defined by GG22, OG1, and RG8 filters (MLO multichannel pyrheliometer). + - Aug 23, 1975; o - Aug 24, 1975; • - Mar-Apr 1974.

Because of solar tracking and atmospheric variability during the hour or more with relatively high Sun needed in the method, very few days were found on which it could be applied. The multichannel instrument has now been replaced by a hand-pointed filter wheel, but preliminary analysis indicated that the optimum performance of the multichannel pyrheliometer has not yet been matched.

5.10 Ultraviolet Erythema Global Measuring Network 1978

Daniel Berger

Temple University
Philadelphia, PA 19140

The sunburn ultraviolet meter network has operated for more than 5 years. The collected data represent the dose of sunburn effective ultraviolet radiation received on a flat detector in each half hour. Twenty-five stations are presently providing interrelatable data (see table 27). A computer compatible output has been developed and installed at three stations. Collected data are disseminated on request by NOAA, 8060 13th Street, Silver Spring, MD 20910.

Table 27.--Stations in sunburn ultraviolet meter network

Sunburn ultraviolet stations	Period in continuous operation
Bismarck, N. Dak.	Oct 1973-present
Tallahassee, Fla.	Sep 1973-present
Oakland, Calif.	Oct 1973-present
Fort Worth, Tex.	Sep 1973-present
Minneapolis, Minn.	Oct 1973-present
Des Moines, Iowa	Oct 1973-present
Albuquerque, N. Mex.	Sep 1973-present
El Paso, Tex.	Sep 1973-present
Mauna Loa, Hawaii	Dec 1973-present
Philadelphia, Pa.	Sep 1974-present
Honeybrook, Pa.	Nov 1974-present
Detroit, Mich.	Sep 1977-present
Seattle, Wash.	Sep 1977-present
Salt Lake City, Utah	Oct 1977-present
New Orleans, La.	Sep 1977-present
Atlanta, Ga.	Oct 1977-present
Tucson, Ariz.	Jun 1975-present
Belsk, Poland	May 1975-present
Warsaw, Poland	Jun 1975-Sep 1976
Aspendale (Melbourne), Australia	Jun 1974-present
Brisbane, Australia	May 1974-present
Davos, Switzerland	Oct 1974-present
Hamburg, Germany	Feb 1976-present
Panama	Nov 1978-present
Point Barrow, Alaska	Oct 1978-present
Rockville, Md.	Sep 1978-present

The network is continuing to expand. Stations in San Diego, Calif., and in New Zealand are being added. Requests from other sites are being considered.

The data have been related to biological responses and to meteorological models. A bibliography of pertinent articles can be supplied on request. A compilation and analysis of data collected in 1974, entitled "Measurements of ultraviolet radiation in the United States and comparisons with skin cancer data," was published by the Department of Health, Education, and Welfare. A multiyear analysis of data is being completed by the same organization.

5.11 Satellite-Based Estimates of Solar Radiation For the GATE Study Area

John E. Hay

CIRES, NOAA
Boulder, CO 80303

A study was made to map at appropriate time (6 h) and space (6 mi) scales the distribution of shortwave radiation incident at the sea surface for the GATE B scale study area (7°-10° N; 22°-25° W) for the study period June 28 to September 19, 1974. The data are required for such studies as investigations of the energy budget of the tropical atmosphere and the interactions between the atmosphere and the underlying ocean surface.

The only source of data with the required resolution in time and space is the Synchronous Meteorological Satellite (SMS1) located above the Equator and at 45° W during GATE. This source provided hourly values of visible (0.55- to 0.75-μm) and infrared (10.5- to 12.6-μm) spectral data at 2-mi and 4-mi resolutions, respectively. The research project attempted to derive a relation between the satellite observations and the solar radiation at the surface, the latter data coming from measurements by one Canadian and four U.S. ships.

A parameterization relating satellite-observed visible reflectivity and atmospheric shortwave transmissivity has been developed using the radiation data from the four U.S. ships. Examples are shown as figs. 66 and 67. Verification of the technique by using the Canadian radiation data shows that hourly shortwave radiation can be estimated to ±22% with a marked improvement for daily time periods to ±8%. Systematic errors over longer time periods (typically 20 days) reduce to less than 2%. These results compare very favorably to those of Davies and Uboegbulem (1979), who used a semi-empirical radiative transfer model and conventionally observed cloud and upper air data to calculate shortwave radiation. They found that even for 5-day running means the differences were still as large as 10% to 15%, this relatively poor performance being attributed to problems in characterizing the cloud (particularly cumulonimbus) conditions.

The satellite data base and the parameterization are currently being used to map the distribution of solar radiation for the GATE B scale array and to investigate the impact of areal averaging and navigation errors on the accuracy of the calculated radiation values.

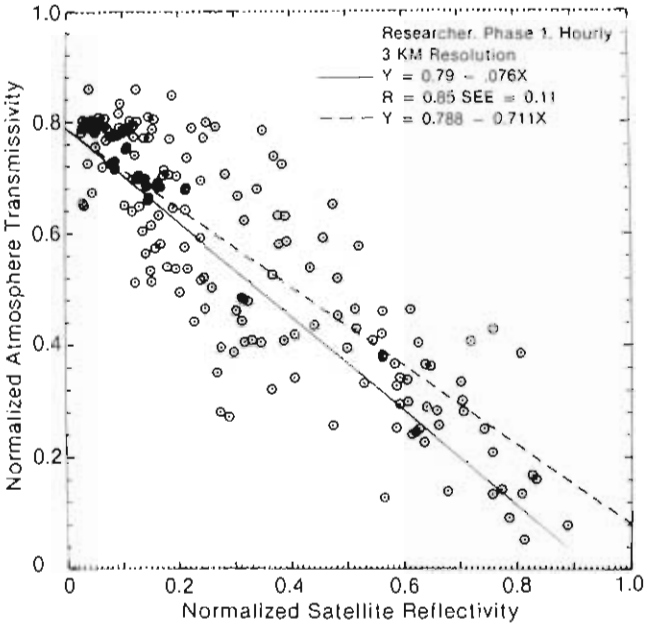

Figure 66.--Relationship between normalized hourly values of satellite reflectivity and atmospheric transmissivity for Researcher during Phase 1 (Jun 28 to Jul 16, 1974) of GATE. Solid line is best fit for plotted data points. Dashed line is best fit for all ship/all phase data.

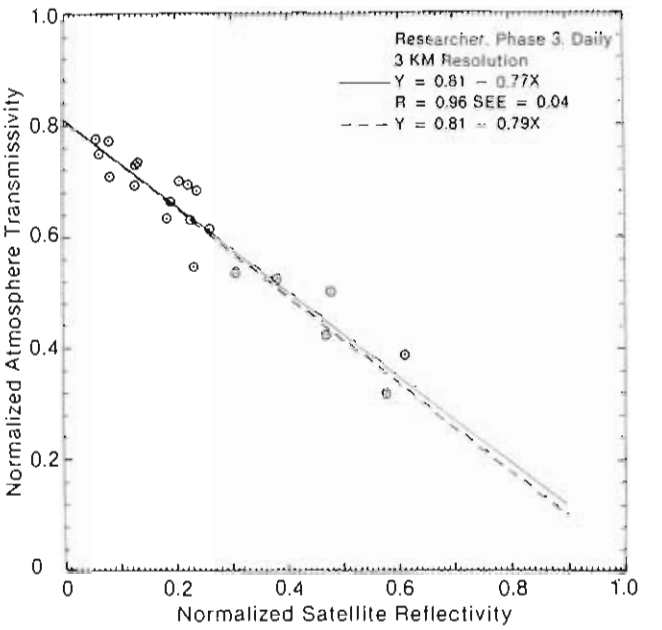

Figure 67.--As for fig. 66, but for daily values for Researcher during Phase 3 (Aug 30 to Sep 19, 1974).

5.12 Solar Radiation Fluxes at the Surface for the Continent of Africa

Jerome K. Nimira

CIRES, NOAA
Boulder, CO 80303

Monthly climatological solar radiation fluxes at the surface for the continent of Africa between latitude 30° N and 30° S were estimated by using Sadler's (1968) satellite-derived cloud data and other relevant climatological parameters. Two basic approaches were employed in the estimation of solar radiation. One method was a semi-empirical transfer method and the other involved the linear regression method that uses cloud data and observed solar radiation. In the latter, the regression equation was developed for conditions over Swan Island. If this technique is valid for conditions over Africa, differences in the optically active atmospheric constituents over the island and any location over the continent had to be accounted for.

The study data were climatological: January, April, July, and October monthly mean values of precipitable water, carbon dioxide, sunshine hours, total

ozone amount, and mean annual surface albedo. The satellite-derived cloud data were mean values for each month. The spatial data point resolution was 2.5° latitude by 2.5° longitude.

The performance of the models was judged by comparing estimated solar fluxes to observed values at 10 stations chosen from various climatic regimes over Africa. The results show that estimated and observed solar radiation fluxes on long monthly bases disagree to within less than ±20%. The semitransfer method is better than the regression method because the percentage deviation of estimates from observed mean monthly global solar radiation for the 10 stations is generally less than ±15%.

Figure 68 shows typical monthly deviation from annual mean for observed and estimated solar radiation and table 28 gives the other statistics.

In summary, the results show that by using mean monthly satellite-derived cloud data and other relevant climatological parameters, a good simulatation for the climatology of solar radiation fluxes for Africa can be obtained. This technique is useful for many parts of Africa where solar radiation observations are nonexistent or just beginning.

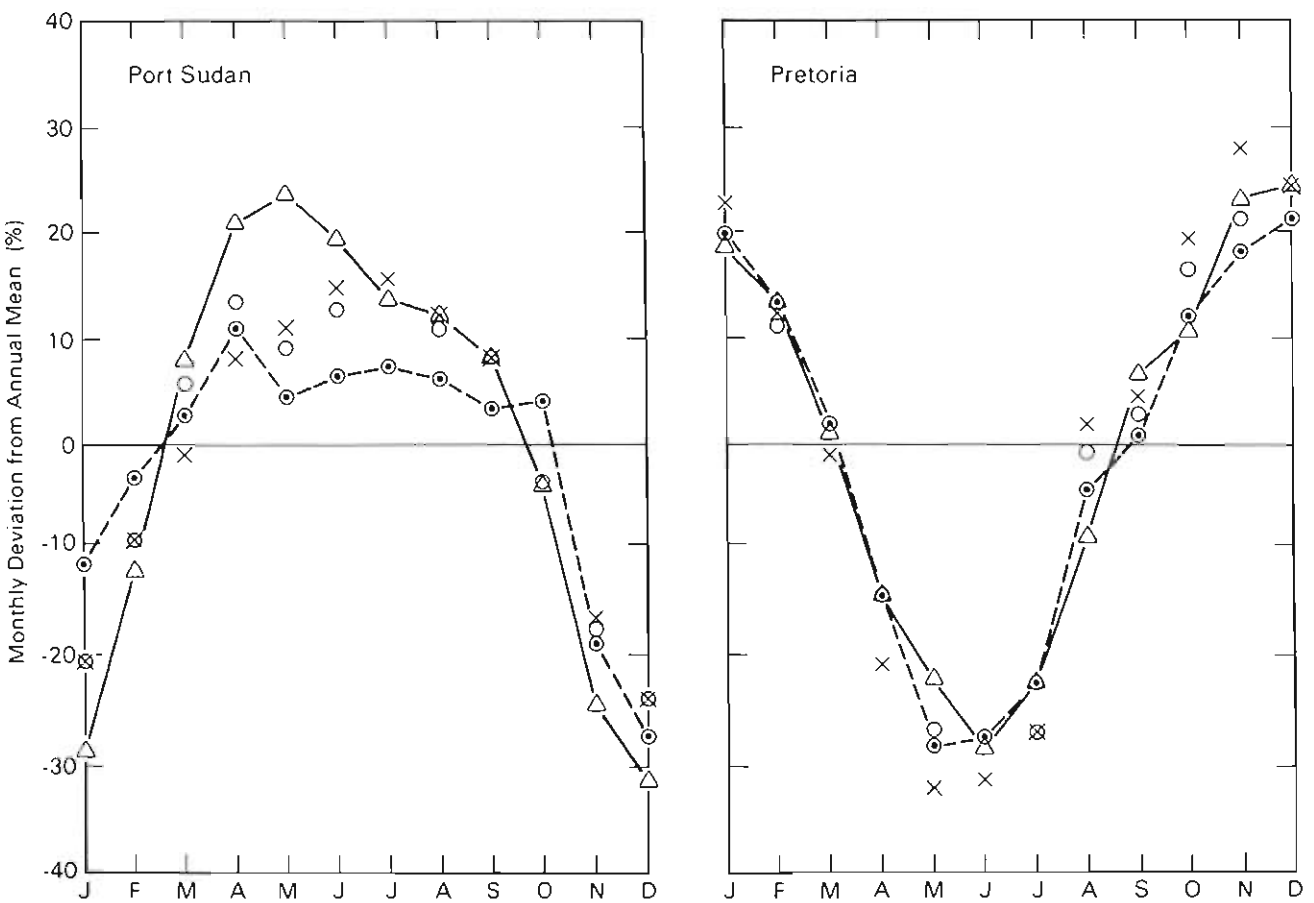

Figure 68.--Monthly deviation of estimated global solar radiation from annual mean (%). Δ - observed, X - regression, O - semitransfer with cloud only, and ⊙ - semitransfer with cloud and sunshine hours.

Table 28.--Characteristics of observed and estimated solar radiation

Station	Standard error estimate*			Standard deviation*				Variability*			
	R	ST-C	ST-CS	R	ST-C	ST-CS	Obs.	R	ST-C	ST-CS	Obs.
Dakar	33	25	19	20	26	22	30	.09	.12	.09	.12
Accra	26	16	20	19	20	15	24	.09	.10	.07	.12
Kinshasa	33	39	20	15	12	20	23	.08	.06	.11	.13
Dundo	20	21	6	14	20	17	11	.07	.10	.08	.06
Port Sudan	23	17	19	35	33	20	46	.14	.13	.08	.19
Pretoria	20	16	29	46	41	38	41	.22	.19	.18	.18
Gulu	25	15	20	21	9	15	15	.09	.04	.07	.07
Tabora	21	23	14	12	7	11	10	.05	.03	.05	.04
Nairobi	29	25	16	13	24	18	39	.06	.11	.08	.17
Lumbo	34	24	24	27	28	32	34	.13	.13	.14	.15

*R = regression method; ST-C = radiative transfer method, clouds only; ST-CS = radiative transfer method, clouds and sunshine.

5.13 Monitoring the Spectral Quality of Solar Radiation

B. Goldberg

Smithsonian Institution
Rockville, MD 20852

In 1978 data collected in 1976 and 1977 with Eppley precision pyranometers were analyzed and published (Klein and Goldberg, 1978a). From this analysis an apparent, temporary drop in UV radiation was found in Panama and Rockville, Md., but not in Barrow (fig. 69). The cause of this phenomenon is not yet known.

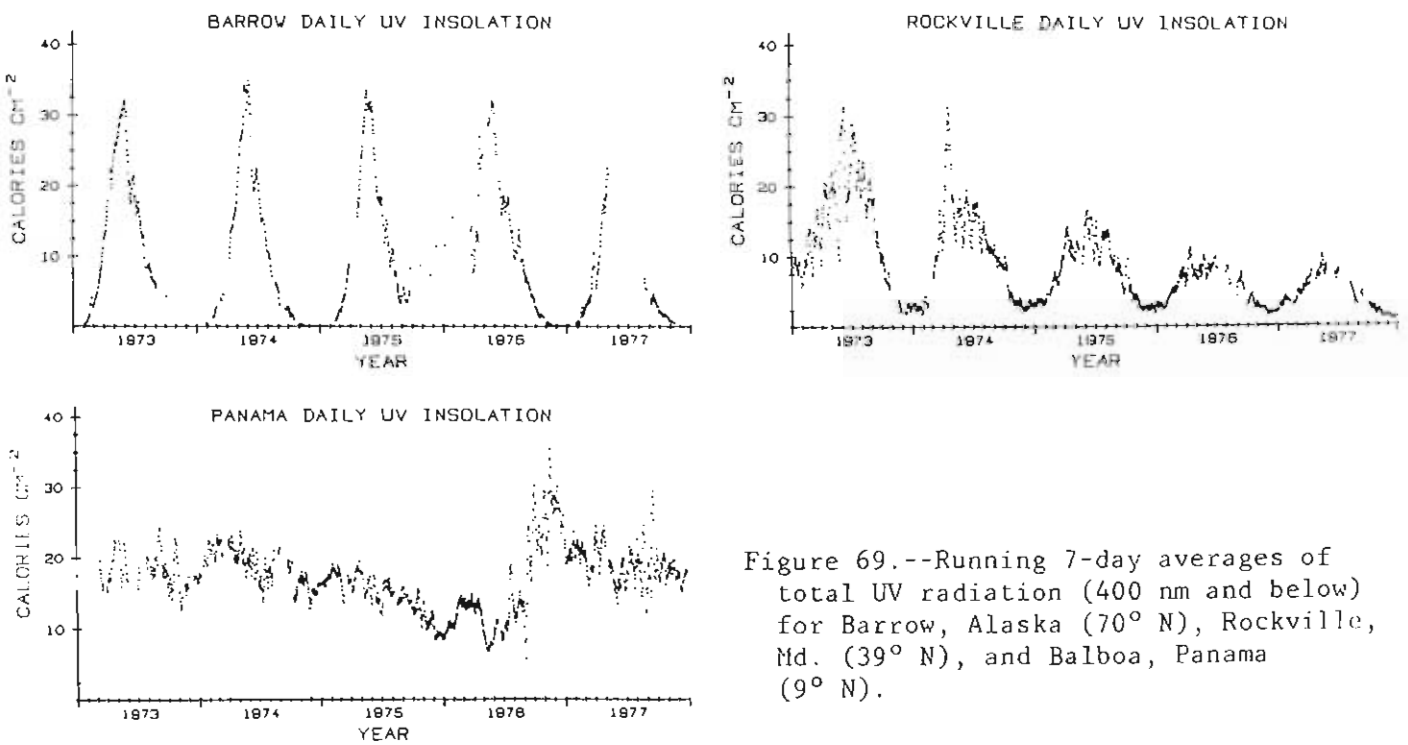

Figure 69.--Running 7-day averages of total UV radiation (400 nm and below) for Barrow, Alaska (70° N), Rockville, Md. (39° N), and Balboa, Panama (9° N).

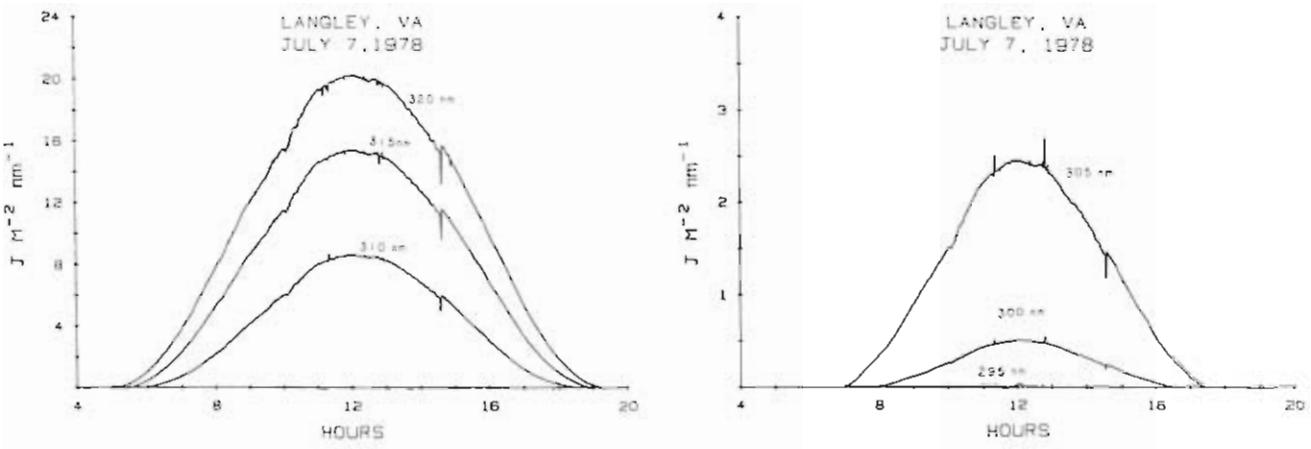

Figure 70.--Integrated values of UVB in 5-nm bands centered at given wavelengths. Values were obtained from 1-min integrations by using a filter-wheel radiometer developed by Smithsonian Radiation Biology Laboratory.

The major area of work by the Radiation Biology Laboratory in 1978 was in UVB (erythemal UV) area of the solar spectrum. Klein and Goldberg (1978b) report on much of this work. A new instrument, called an integrating, scanning radiometer, was put into the field and compared with an older sampling unit. A very good correlation was found between the two units. Figures 70 and 71 show the good agreement between the two units on a clear day. A description of the new instrument is being prepared for publication.

The two sites where the two units were used are approximately 150 air miles apart. The Langley site shows two "glitches" on the 305-nm and 300-nm curves. These would normally be removed in processing, but none of these data has been filtered. Each band is nominally 5 nm wide.

A simple model was constructed to allow computation of spectral irradiances in 100-nm bands (Klein and Goldberg, 1978b).

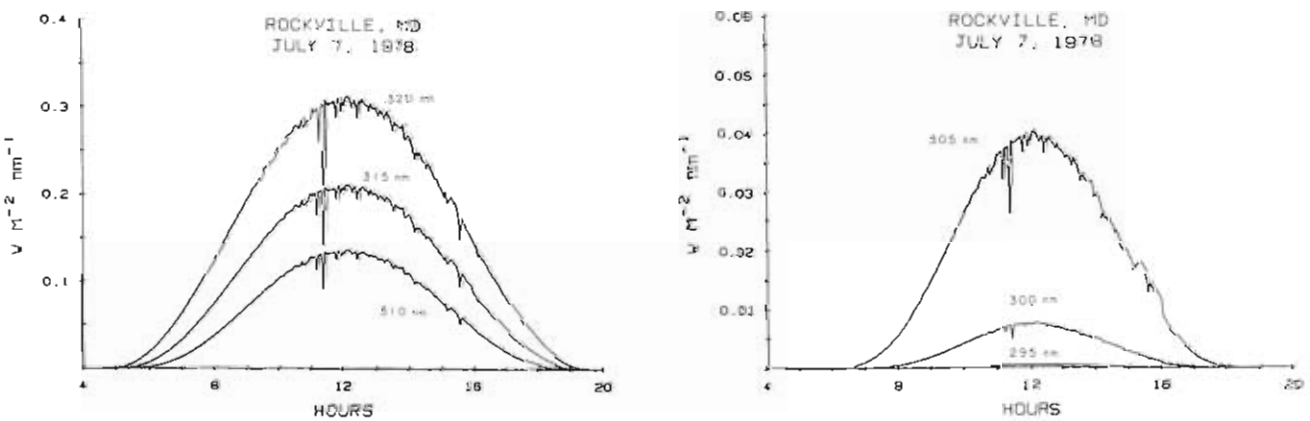

Figure 71.--Values of UVB obtained by a sampling unit on a fairly clear day in 5-nm bands centered at given wavelengths. Each point on the curve is an instantaneous value.

5.14 Nuclear Fallout and High-Volume Aerosol Collections

Herbert W. Feely

Environmental Measurements Laboratory
U.S. Department of Energy, New York, NY 10014

Precipitation samples, which are analyzed for ^{90}Sr fallout from atmospheric tests of nuclear weapons, are collected in plastic buckets at the Mauna Loa and Samoa Observatories on a monthly basis. They are currently combined into quarterly composites and are analyzed together with samples from about 70 stations in other parts of the world. An article by Feely et al. (1978) includes an interpretation of recent results.

High-volume filter samplers, which sample air at about 1 m^3 min^{-1}, are operated for EML at all four GMCC observatories. These are part of a network of about 20 samplers operated for EML, mainly in the Western Hemisphere. Monthly composites of the filter samples are analyzed routinely by gamma spectrometry for ^{7}Be, ^{95}Zr, ^{137}Cs, and ^{144}Ce. Until mid-1976 they were also routinely analyzed radiochemically for ^{210}Pb, ^{90}Sr, and $^{239,240}Pu$. Results are reported quarterly.

Table 29 summarizes quarterly mean concentrations of the various radionuclides measured in surface air filters for 1977 and 1978. The cosmic-ray product, ^{7}Be, is usually high in concentration at the Mauna Loa Observatory throughout the year. This station appears to represent better the air of the upper troposphere than does the EML continental station at Chacaltaya, Bolivia, even though the elevation of the latter (5220 m) is higher. Concentrations of ^{7}Be at the South Pole Observatory typically show a summer maximum and winter minimum. Evidently, air from the high troposphere carrying ^{7}Be takes longer to reach the surface layer during winter than it does during summer. This argues against a conclusion, based on observations of the seasonal variations in concentrations of surface level ozone at the South Pole, that attributes high wintertime ozone concentrations to rapid movement of air to the surface from the polar stratosphere or upper troposphere.

The artificial radionuclides from nuclear weapons tests, which are currently measured in the filters, are the fission products ^{95}Zr, ^{137}Cs, and ^{144}Ce. At Mauna Loa Observatory high concentrations of ^{95}Zr were found throughout 1977, and high concentrations of ^{137}Cs and ^{144}Ce persisted through the first half of 1978 as a result of fallout from the November 17, 1976, Chinese nuclear test which had a yield of 4 megatons. Lower concentrations of these radionuclides were found at Barrow Observatory during this period, and negligible amounts of the radioactive debris from this Chinese test reached the stations in the Southern Hemisphere. Rather high concentrations of fresh fission products were sampled at Mauna Loa Observatory during September 1977 immediately following the Chinese low-yield nuclear test of September 17, 1977. Concentrations fell back to their earlier levels quickly, however, as this fresh debris was diluted by mixing within the troposphere.

Table 29.--Quarterly mean concentrations of radionuclides in surface air filter samples collected at GMCC observatories, 1977 to 1978

	1977 quarters				1978 quarters			
	1	2	3	4	1	2	3	4
^{7}Be (fCi m^{-3})								
BRW	88	54	34	62	66	56	26	48
MLO	241	147	-	203	194	197	149	175
SMO	57	78	99	104	-	83	92	61
SPO	184	138	122	125	118	141	114	192
^{95}Zr (fCi m^{-3})								
BRW	1.2	6.2	8.7	5.3	1.7	1.7	<0.5	<0.5
MLO	39.	40.	869.	21.	1.7	1.4	<0.5	<0.5
SMO	<0.5	<0.5	0.7	<0.5	-	<0.5	<0.5	<0.5
SPO	<0.5	<0.5	<0.5	0.8	<0.5	<0.5	<0.5	<0.5
^{137}Cs (fCi m^{-3})								
BRW	0.3	0.5	0.6	1.2	1.7	2.1	0.5	0.4
MLO	1.4	2.3	7.2	2.3	3.9	4.7	1.2	0.6
SMO	0.1	0.1	0.1	0.3	-	<0.1	0.1	0.1
SPO	0.2	<0.1	0.1	0.2	0.1	0.2	0.1	0.2
^{144}Ce (fCi m^{-3})								
BRW	0.5	5.6	6.3	11.9	13.6	13.7	3.8	1.7
MLO	18.6	34.2	154.	26.7	32.4	34.0	7.2	2.7
SMO	<0.5	<0.5	1.0	0.8	-	<0.5	0.5	<0.5
SPO	<0.5	<0.5	<0.5	<0.5	<0.5	<0.5	<0.5	<0.5

5.15 Measurement of SO_2 and TSP at Mauna Loa Observatory

Richard Sasaki, Mavis Kadooka, and Wilfred Ching

Department of Health, State of Hawaii
Honolulu, HI 96801

A cooperative program with NOAA at the Mauna Loa Observatory was initiated by EPA to measure sulfur dioxide and total suspended particulates. In 1976 when the NASN program was closed by EPA, an agreement was reached to continue monitoring these parameters because of the interest to NOAA and the Air Program of the State of Hawaii.

A major reason to obtain data from Mauna Loa Observatory was to determine if a clear background for total suspended particulates existed within the State

of Hawaii to use as a standard against the continental SLAMS and NAMS site. The background level for total suspended particulates at Mauna Loa will be computed when valid data are obtained for three years. Monitoring for total suspended particulates will be continued for an indefinite period to determine any long-term trend.

Measurement of SO_2 of MLO will determine two parameters: the concentration of SO_2 at that altitude and the increase of SO_2 due to volcanic activity. Final computation and assessment of these parameters will be accomplished early this fall.

5.16 Precipitation Chemistry at Samoa and Mauna Loa

Donald C. Bogen and Stuart J. Nagourney

Environmental Measurements Laboratory
U.S. Department of Energy, New York, NY 10014

Monthly samples of wet, dry, and total deposition are collected at SMO and MLO. The samples are sent to the Environmental Measurements Laboratory for physical and chemical measurements.

Table 30.--Chemical analyses of total, wet, and dry deposition at American Samoa, April 1977 through March 1978

	Total collector		Wet collector		Dry collector	
	Mean	Range	Mean	Range	Mean	Range
Volume (ℓ)	6.30	0-12.14	8.67	1.64-14.00	-	-
pH	6.21	5.75-6.70	6.00	5.55-6.51	-	-
Conductivity ($\mu S\ cm^{-1}$)	48.1	21-295	26.6	11.8-67.7	-	-
Cl^- ($mg\ mo^{-1}$)	108	78-208	45	25-85	59	20-99
SO_4^{-2} ($mg\ mo^{-1}$)	18	10.7-32	7.3	3.7-12.5	8.2	3.0-13.0
NO_3^- ($mg\ mo^{-1}$)	1.16	ND*-3.9	ND*	ND*	0.23	ND*-1.47
Na^+ ($mg\ mo^{-1}$)	63	43-125	27	16-48	32	11-49
Mg^{+2} ($mg\ mo^{-1}$)	7.9	5.1-15.9	3.3	2.0-6.4	4.2	1.4-6.4
Ca^{+2} ($mg\ mo^{-1}$)	3.5	2.4-6.5	1.5	0.9-3.4	1.8	0.5-2.3
K^+ ($mg\ mo^{-1}$)	3.2	1.8-7.0	1.1	0.7-2.0	1.5	0.6-2.5
$\frac{\text{Total cations}}{\text{Total anions}}$	1.07 ± 0.09		1.10 ± 0.08		1.01 ± 0.06	

*ND - uot detectable.

Table 31.--Chemical analyses of total, wet, and dry deposition at Mauna Loa, April 1976 through March 1978

	Total collector		Wet collector		Dry collector	
	Mean	Range	Mean	Range	Mean	Range
Volume (ℓ)	0.18	0-2.56	1.07	0-7.50	-	-
pH	5.55	4.91-6.06	5.84	4.76-6.60	-	-
Conductivity ($\mu S\ cm^{-1}$)	10.6	5.6-23.4	6.4	2.8-15.5	-	-
Cl^- ($mg\ mo^{-1}$)	0.11	0.01-0.38	0.10	ND*-0.33	0.06	0.02-0.21
SO_4^{-2} ($mg\ mo^{-1}$)	0.81	0.04-5.48	0.64	0.01-4.13	0.26	0.03-0.80
NO_3^- ($mg\ mo^{-1}$)	0.10	ND*-0.49	0.10	ND*-0.48	0.06	ND*-0.40
Na^+ ($mg\ mo^{-1}$)	0.14	0.02-0.31	0.18	0.01-1.01	0.10	0.02-0.24
Mg^{+2} ($mg\ mo^{-1}$)	0.04	ND*-0.14	0.03	ND*-0.10	0.02	ND*-0.05
Ca^{+2} ($mg\ mo^{-1}$)	0.09	ND*-0.24	0.10	ND*-0.46	0.07	ND*-0.22
K^+ ($mg\ mo^{-1}$)	0.04	ND*-0.10	0.04	ND*-0.37	0.02	ND*-0.17

ND* - not detectable.

The average monthly deposition value and range of results at Samoa for the period April 1977 to March 1978 are presented in table 30. The concentration ratios of various anions and cations to sodium support the observation that sea spray is the principal constituent of these deposition samples.

The monthly mean deposition values and the range of results at Mauna Loa for the first 2 years of the program (April 1976 to March 1978) are presented in table 31.

5.17 Precipitation Chemistry at Mauna Loa Observatory

Richard J. Thompson and Ross Highsmith

Environmental Monitoring and Support Laboratory
U.S. Environmental Protection Agency
Research Triangle Park, NC 27709

During 1978, monthly wet precipitation samples were collected at the Mauna Loa Observatory by using a MISCO Model 93 wet-only precipitation collector. Monthly samples were forwarded to the ACB/EMSL for physical/ chemical analysis. Results of analyses on representative samples collected at the Mauna Loa Observatory are presented in table 32. All analyses were performed under acceptable quality control.

Table 32.--Physical/chemical analysis of representative 1978 monthly wet precipitation samples at MLO

Month 1978	Rainfall MLO (rain gauge)	Volume MLO (mℓ)	Volume ACB/EMSL (mℓ)	pH (pH)	Cond. ($\mu S\ cm^{-1}$)	Acidity ($\mu eq\ \ell^{-1}$)	SO_4 ($mgSO_4\ \ell^{-1}$)	NO_3 ($mgNO_3\ \ell^{-1}$)	NH_4 ($mgNa\ \ell^{-1}$)	CL ($mgCl\ \ell^{-1}$)	CA ($mgCa\ \ell^{-1}$)	K ($mgK\ \ell^{-1}$)	Ma ($mgMg\ \ell^{-1}$)	Na ($mgNa\ \ell^{-1}$)
Feb	0.00	0	0	-	-	-	-	-	-	-	-	-	-	
Apr	1.15	0	0	-	-	-	-	-	-	-	-	-	-	
Jun	1.27	50	40	4.63	13.6	69.0	2.03	.9	.3	.36	.25	<.13	.08	.35
Aug	2.50	50	0	-	-	-	-	-	-	-	-	-	-	-
Oct	6.25	225	215	4.70	7.1	39.0	.61	.1	<.1	.25	.09	<.13	.02	<.11
Dec	.52	0	0	-	-	-	-	-	-	-	-	-	-	-

5.18 Barrow Precipitation Data

G. P. Claggett

Soil Conservation Service
U.S. Department of Agriculture
Anchorage, AK 99504

The Soil Conservation Service maintains the network of Wyoming shielded precipitation gauges across the North Slope of Alaska which is funded by the U.S. Army Cold Regions Research and Engineering Laboratory. This network allows more accurate winter precipitation data to be collected in the Arctic, where snow precipitation in treeless regions has been notoriously difficult to measure.

Before 1975, the National Weather Service obtained the only routine precipitation data on the North Slope at Barrow (since 1919) and Barter Island (since 1950). The NWS standard 8-in rain gauge is used at these two coastal stations, sometimes wind shielded and sometimes not. An unshielded gauge is estimated to catch one-third of the precipitation. The addition of a standard Alter wind shield increases the catch to about two-thirds of the total. Use of the more elaborate wind shielding developed in Wyoming by Rechard and Larsen in 1971 increases the catch to almost 100%.

The network of Wyoming shielded precipitation gauges across Alaska's North Slope now numbers 11 sites (table 33).

Table 33.--Sites of Wyoming shielded precipitation gauges

Site	Latitude	Longitude	Activated
Barrow	71°20'N	156°40'W	9/75
Meade River	70°29'N	157°25'W	12/75
Barter Island	70°08'N	143°37'W	9/75
Prudhoe Bay	70°15'N	148°30'W	9/76
Jago River	69°42'N	143°36'W	10/76
Kavik River	69°30'N	147°00'W	10/76
Toolik River	68°37'N	149°26'W	9/76
Sagwon	69°26'N	148°34'W	11/76
Chandalar Shelf	68°05'N	149°29'W	9/77
Antigun Pass	68°08'N	149°35'W	9/77
Antigun Camp	68°10'N	149°26'W	6/78

5.19 Boron in the Marine Atmosphere: Distribution, Sources, and Fluxes

Robert A. Duce

University of Rhode Island
Kingston, RI 02881

As part of an URI program, air and rainwater samples were collected at the Samoa facility. Four air samples and six rain samples were collected by T. Fogg from August 18 to September 3, 1978. Using impregnated filters to trap the gaseous, inorganic boron, we found that the concentrations were in the range of 10 ng m^{-3}. Although we experienced some difficulties with this technique, it probably represents a lower limit on the boron concentrations. Particulate boron collected by Nuclepore filters was in the range around 1 ng m^{-3}. The rain samples have not yet been analyzed.

5.20 Variability of Atmospheric Carbon Dioxide Concentration

G. I. Pearman

CSIRO
Mordialloc, Australia

During a 1-yr visit by G. Pearman to the GMCC laboratory in Boulder, two studies were made on aspects of the annual cycle of CO_2.

Using the 21-yr CO_2 record obtained at MLO by C. D. Keeling, we attempted to ascertain whether the amplitude of the annual cycle of concentration had changed over the period. The magnitude of the annual variation in CO_2 concentration appears to have increased by about 3% each year. Also the time of year when the concentration (due to respiratory activity) increases takes place a week or two earlier now than 10 to 20 years ago. These observations imply that significant changes have occurred in the activity of the Northern Hemisphere nontropical biosphere.

Variations in CO_2 concentration at Mauna Loa, which occur on time scales of 10 to 20 days, were examined in some detail. Attempts were made to establish relationships between the 600-mb to 700-mb meteorology, as indicated by the Hilo radiosonde data, and these fluctuations in CO_2 concentrations. Although relationships were found, they did not explain the 10- to 20-day variability. It was concluded that a much more extensive analysis of these events and the meteorology is required.

In a second study, we used a 2-D computer model to simulate the global mixing of the atmosphere. By using iterative approximations the model established zonally averaged monthly surface carbon fluxes that were consistent with the observed annual variation of atmospheric CO_2 concentration at each GMCC and other CO_2 monitoring stations.

Attempts were made in a third study to examine the time and space variations of CO_2 concentration observed by aircraft sampling over the Australia-New Zealand region during the past 6 years. Although not complete, these studies have shown clearly the relationship between CO_2 concentration variations and atmospheric stability that occurs at the subsidence inversion and tropopause levels in the atmosphere.

5.21 Carbon Monoxide Monitoring

Wolfgang Seiler

Max-Planck Institute for Chemistry
Mainz, Germany

The air monitoring program of the Max-Planck Institute (MPI) in cooperation with NOAA is continuing to provide baseline measurements of the background CO mixing ratios in the upper and lower troposphere of the Northern Hemisphere. The CO instrument was installed at MLO in 1973 and replaced by an improved model in March 1975. Seiler (1976) gives details of the instrumentation. The instrument monitors automatically and continuously and has a lower detection limit of 0.1 ppb. The response time is approximately 15 s, so short-term fluctuations of the CO mixing ratios can be observed. The calibration control is performed automatically once every 3 h, using two CO calibration standards of 60 and 120 ppb, representative of the range of the CO values found in unpolluted Northern Hemisphere air. The CO instrument had been maintained twice by MPI employees during the last 4 years and was found to work satisfactorily. During these occasions samples of the calibration standards were taken and compared in the laboratory with primary standards available in the MPI.

The CO instrument has been operating continuously since 1975 except for several months during the second half of 1977 when the instrument was moved into the main building, and subsequently the automatic calibration failed. The CO data exhibit considerable variation with a time period on the order of 4 to 5 days, probably as a result of synoptic scale meteorological influences. The variability is most pronounced during the late winter and spring when the CO mixing ratios rise to concentrations of 350 ppb. Short-term fluctuations within time scales of several minutes to one hour were not observed, indicating that the CO record at MLO is not influenced by local anthropogenic and natural CO sources. Exceptions are automobiles passing the station and brush fires.

There seems to exist a slight diurnal variation of the CO mixing ratios with maximum values during the early morning. This cycle is most probably caused by the change of the local wind regimes with upslope and downslope wind during daytime and nighttime, respectively. This diurnal variation would indicate somewhat higher CO mixing ratios in the lower troposphere below the trade wind inversion relative to the upper troposphere.

Similar observations during measurements on the Tenerife Island have been reported by this author. Most interesting is the seasonal variation of the CO mixing ratios with minimum values (60 to 80 ppb) during spring. Several factors probably contribute to the observed variation of CO. First, enhanced concentrations of the hydroxyl radical (OH) during the summer could be responsible for the lower CO concentrations during the late summer and autumn since reaction with OH is believed to be the primary loss mechanism of CO in the atmosphere. Second, a seasonal variation in the prevailing wind patterns, associated with the meridional movement of the ITCZ, could strongly influence the observed seasonal variation.

The data base is not yet sufficient to make any statements about a possible increase of the CO mixing ratios in the Northern Hemisphere, resulting from anthropogenic activities.

5.22 Stratospheric Nitrogen Dioxide Program

W. Henderson and J. F. Noxon

Aeronomy Laboratory, NOAA
Boulder, CO 80303

Automated instruments for measuring stratospheric NO_2 have been operating at Barrow, Mauna Loa, and Samoa, and we are now completing analysis of the 4-yr period of data. The preliminary results confirm and extend the patterns established by brief spot checks with airborne equipment, but also provide useful continuous monitoring which, particularly at Barrow, has been invaluable in studying transport in the stratosphere. The first phase of the program is complete, and we plan to terminate operations with the present equipment. We plan further measurements with redesigned instruments that will concentrate on the Arctic and include Barrow as a site.

5.23 Total Ozone Measurements and TIROS-N

J. Miller and W. Planet

National Environmental Satellite Service, NOAA
Washington, D.C. 20233

The National Environmental Satellite Service has received total ozone records from 11 Dobson stations either operated directly by the GMCC or associated with it. The data records begin in November 1978 and will continue through the operational lifetime of the TIROS-N series of operational environmental satellites.

The infrared sounder (HIRS/s) on TIROS-N has spectral channels whose measured radiances can be correlated with the amount of total ozone. A multi-channel regression scheme has been established whereby total ozone on a global scale can be deduced from the infrared measurements. To establish and upgrade the individual regression coefficients, coincident Dobson measurements and satellite observations are required. When a statistically significant data base of coincident measurements is obtained, the regression coefficients will be generated and implemented in the TIROS-N data processing system. Regression coefficients are latitudinally stratified and will be changed seasonally.

5.24 Barrow Magnetic Observatory

John B. Townshend

U.S. Geological Survey
Fairbanks, AL 99701

The Barrow Magnetic Observatory is located at the northern tip of Alaska about 500 mi (804 km) north of Fairbanks and about 200 mi (322 km) west of Prudhoe Bay, site of the North Slope oil fields. Its geographic coordinates are latitude 71.32° N and longitude 156.62° W.

The observatory, part of the U.S. Geological Survey's Branch of Electromagnetism and Geomagnetism, is used to produce accurate and comprehensive geomagnetic data. It was started in May 1949 as a manned station. In May 1975 a digital and analog fluxgate and proton magnetometer system was installed which includes the following instruments: fluxgate magnetometer (H, D, & Z), proton recording base magnetometer (F), data logger, tape transport (7 track/556 characters per in), analog recorder (4 pen), battery system (4 ea. 6-V batteries 100 amp), battery charger, and d.c./a.c. inverter. The digital tape and analog recording paper are sufficient for the station to operate unattended for up to 7 weeks without major service. The station is operated by the U.S. Geological Survey College Observatory at Fairbanks, and one of the staff visits the station periodically (about every seven weeks) to change tapes, make absolute and scale value observations, and service equipment. NOAA Geophysical Monitoring for Climatic Change personnel at Barrow check the recording equipment weekly and advise the College Observatory staff of obvious problems.

5.25 South Pole Riometer

H. J. A. Chivers

University of California-San Diego
La Jolla, CA 92093

Riometers have been operated continuously at South Pole throughout the year as part of a cooperative program between NOAA and the University of California at San Diego. The absorption measurements are related to the precipitation of charged particles into the ionosphere above the station. The South Pole combines the advantages of an excellent geomagnetic location for detecting particle precipitation and an unvarying cosmic radio noise background. Records of excellent quality have been gathered for 3 years and have led to an analysis of a class of absorption events ("spike" events), which precede a magnetic substorm. Using Riometers on two different frequencies (30 MHz and 51.4 MHz), we found that the spike events begin with precipitation of very energetic particles spatially confined to about 10 km in width. Within a minute or so, the spectrum softens and the precipitation pattern becomes widespread across the antenna aperture. The results of this analysis lead to a more accurate description of the precipitation process from the magnetosphere, and are important in understanding the characteristics of communications difficulties at high latitudes. The work has been expanded to include study of the interrelation between ground-level cosmic ray events and radio-wave absorption.

Original strip chart recordings from the South Pole riometers are archived in the National Geophysical and Solar-Terrestrial Data Center, NOAA, Boulder, Colo.

5.26 Antarctic Tritium

Allen S. Mason and H. Göte Östlund

University of Miami
Miami, FA 33149

The University of Miami Tritium Laboratory, sponsored by the Division of Polar Programs, NSF, installed an atmospheric tritium sampler (fig. 72) in the CAF at the Amundsen-Scott South Pole station in late 1977. In late 1978, J. Bortniak of NOAA assumed operation from S. Barnard of SUNYA and is responsible for the sampler through the 1979 austral winter.

Samples are taken of tritiated water vapor (HTO) by absorption and of tritium gas (HT) and tritiated hydrocarbons by selective oxidation and absorption. The sample traps are returned to Miami for extraction and analysis. The research objectives are elucidating the flux of HTO at the surface and determining the global backgrounds of HT and tritiated hydrocarbons. The HTO is a tracer for ordinary water vapor and will be useful in study of continental water budget. The HT and hydrocarbons are products of ongoing nuclear activities, and Antarctica is an ideal location for measuring their global backgrounds.

With the projected advent of fusion power, the world HT burden will probably increase greatly. These studies will provide a baseline for the estimation of the effects of such an increase.

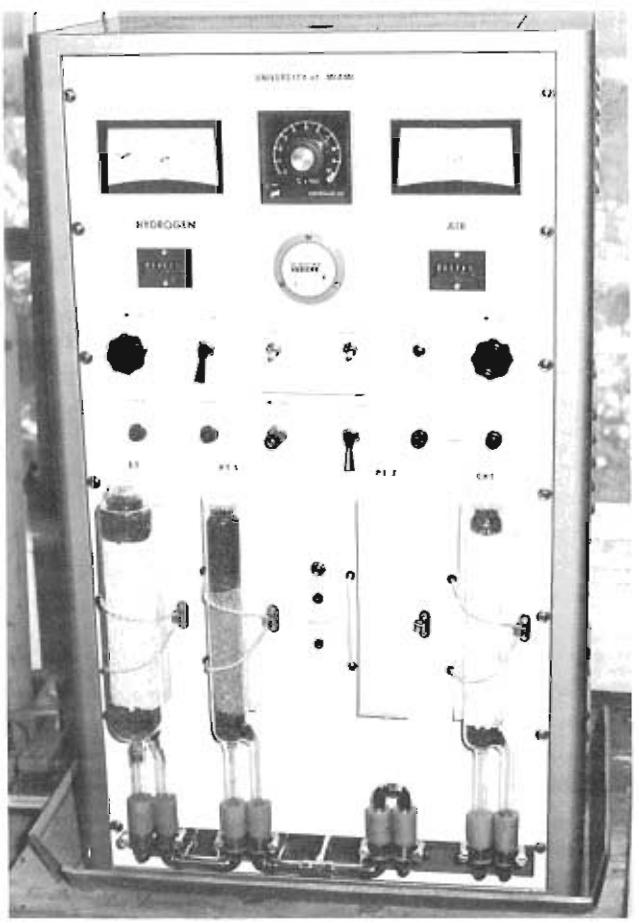

Figure 72.--Atmospheric HT/HTO/CH_3T sampler.

5.27 Atmospheric Electric Measurements at Mauna Loa Observatory

William L. Boeck

Niagara University
Niagara University, NY 14109

Donald E. Olson

University of Minnesota
Duluth, MN 55812

J. Doyne Sartor

National Center for Atmospheric Research
Boulder, CO 80303

Since 1960 W. Cobb has made intensive observations of the atmospheric electrical parameters at MLO. The observations and his results have received renewed attention in connection with solar weather interactions. Cobb (1967) reported anomalously high electric fields and conductivities at Mauna Loa after major solar flare eruptions. Other observations at high altitude observatories in the Bavarian Alps and the Colorado Rockies tend to support those of Cobb but are subject to greater contamination from local anthropogenic sources and adverse weather. A major cloud and thunderstorm mechanism receives its start from the fair weather electric field and conductivity. Stronger fair weather (globally responsive) electric fields and conductivities such as those observed on Mauna Loa favor more rapid and more intense electrification of available clouds on a worldwide scale. To substantiate these suggestions a longer period of intensive measurements is required. Since 1977 MLO personnel have helped us maintain chart recordings and inspect instruments. To ensure continuous quality data we have made periodic visits to the observatory to service instruments.

Reduction of raw data from strip chart records has continued. We have tried to update the components of the electric field mill without changing the calibration or function. Modules have been constructed to simplify the repair procedures, reduce component cost, and increase reliability.

The superposed epoch analysis method as used in solar/weather research has been analysed to improve the credibility of the results of this method.

6. INTERNATIONAL ACTIVITIES

In January 1978, K. J. Hanson traveled to the South Pole to inspect and review the GMCC program there. On the return trip he also reviewed the GMCC program at Samoa and Mauna Loa.

Under the U.S.A.-U.S.S.R. Agreement on Cooperation in the Field of Environmental Protection, Working Group VIII, J. Peterson traveled to Leningrad, Soviet Union, during August 1978. While there he consulted with Soviet scientists on their preparation for an urban-oriented aerosol experiment. They were operating two lidar systems as well as optical and paper filter aerosol samplers. J. Peterson also brought a Volz sunphotometer to Leningrad for comparisons with a similar Soviet device and for urban-rural atmospheric transparency measurements. These sunphotometer measurements are described in section 4.8.

Also under the U.S.-U.S.S.R. bilateral agreement, V. A. Kovalev and S. A. Sokolenko visited the NOAA Air Resources Laboratory, Boulder, Colo., from September 10 to October 8, 1978, to check the calibration of U.S.S.R. Dobson ozone spectrophotometer no. 108 and to modernize the electronics of the instrument. U.S. collaborators in the instrument comparisons were W. D. Komhyr and R. D. Grass of GMCC. An initial comparison of U.S.S.R. instrument no. 108 with U.S. world reference standard Dobson instrument no. 83 on September 21, 1978, showed that the two instruments yielded AD wavelength direct sun total ozone data that agreed on the average to within 0.6% for observations made within the air mass observing range of 1.3 to 3.2. A maximum difference of 1.0% in ozone data was observed within the air mass interval 1.5 to 2.0. Dobson ozone spectrophotometer no. 108 is used in the U.S.S.R. for calibrating M-83 filter ozonometers that are routinely employed for total ozone measurements at the U.S.S.R. ozone station network. Modifications to instrument no. 108 included installation of modern solid-state electronic circuitry and minor optic adjustments. A final intercomparison of instrument nos. 108 and 83, on October 6, 1978, yielded excellent data, indicating average AD, CD, A, C and D wavelength ozone value differences for the two instruments of less than 0.2% within the air mass range of 1.15 to 3.2.

During 1978 GMCC personnel continued to participate in the WMO Global Ozone Monitoring and Research Project to upgrade the quality of Dobson spectrophotometers throughout the world. Instruments upgraded by use of modern electronic circuitry and calibrated by direct comparison with world standard Dobson instrument no. 83 maintained by GMCC were nos. 52, 93 and 98 located in Manila, Philippines, Natal, Brazil, and Mexico City, Mexico, respectively. Instrument no. 93 has been loaned indefinitely to Brazil. Data from the station will be used for ground truth information to support a NASA rocket ozonesonde program.

In December 1978, K. J. Hanson traveled to Riga, Latvia, to participate in the World Meteorological Organization/United Nations Environmental Program International Symposium on Integrated Monitoring for Environmental Pollution. He presented a paper at the symposium entitled, "Comments on the Specification of Network Stations for Monitoring the Variability of Atmospheric Trace Constituents Significant for Climate."

7. PUBLICATIONS AND PRESENTATIONS BY GMCC STAFF

Berri, G. J., and J. T. Peterson. Dependence of atmospheric turbidity at Raleigh, N.C., on air mass trajectories. NOAA Tech. Memo. ERL ARL-68, 16 pp., Feb. 1978.

Bodhaine, B. A. The Mauna Loa four wavelength nephelometer: Instrument details and three years of observations. NOAA Tech. Rep. ERL 396-ARL 5, 41 pp., Apr. 1978.

Bodhaine, B. A. A possible effect of local volcanic activity at Mauna Loa Observatory. In Mauna Loa Observatory--a 20th Anniversary Report, J. M. Miller (ed.), 66-71, Sep. 1978.

DeLuisi, J. J. Use of the Dobson spectrophotometer in a variable wavelength mode as an alternative to the Umkehr measurement for observing trends in the verticle distribution of ozone. Proc. WMO Symp. on Geophys. Aspects and Consequences of Changes in Composition of the Stratosphere, Toronto, Canada, June 26-30, 1978.

DeLuisi, J. J., and J. Nimira. Preliminary comparison of satellite BUV and surface-based Umkehr observations of the vertical distribution of ozone in the upper stratosphere. J. Geophys. Res. 83(C1):379-384, Jan. 1978.

Fegley, R. W. NOAA Air Resources Laboratories Stratospheric Lidar Project--1976 Results. NOAA Tech. Rep. ERL 400-ARL 6, 13 pp., Sep. 1978.

Fegley, R. W., and C. M. Penney. An attempt to measure atmospheric ozone with ultraviolet lidar. NOAA Tech. Memo. ERL ARL-75, 20 pp., Dec. 1978.

Fegley, R. W., E. W. Barrett, and H. T. Ellis. Lidar measurements at Mauna Loa Observatory. In Mauna Loa Observatory--a 20th Anniversary Report, J. M. Miller (ed.), 59-65, Sep. 1978.

Hanson, K. J. Comments on the specification of network stations for monitoring the variability of atmospheric trace constituents significant for climate. Proc. WMO/UNEP Inter. Symp. on Integrated Monit. for Environ. Pollut., Dec. 1978.

Herbert, G. A., and B. C. Halter. Geophysical monitoring for climatic change at the South Pole, 1977. Antarct. J. U. S. 13(4):190-191, Oct. 1978.

Hoyt, D. V. An explosive volcanic eruption in the Southern Hemisphere in 1928. Nature 275(5681):630-632, Oct. 1978.

Hoyt, D. V. Interannual cloud-cover variations in the contiguous United States. J. Appl. Meteorol. 17(3):354-357, Mar. 1978.

Hoyt, D. V. A model for the calculation of solar global insolation. Solar Energy 21:27-35, July 1978.

Hoyt, D. V. Reply (to Court). Mon. Weather Rev. 106(4):572-573, Apr. 1978.

Hoyt, D. V. Variations in the solar constant measurements of the Smithsonian Astrophysical Observatory, 1923-1954. Third Conf. on Atmos. Rad., June 28-30, 1978, Davis, Calif. Preprint, A.M.S., Boston, Mass., 315-317, June 1978.

Mateer, C. L., D. F. Heath, and J. J. DeLuisi. Seasonal variation in the vertical distribution of ozone as observed with the Umkehr and BUV methods. Proc. WMO Symp. on Geophys. Aspects and Consequences of Changes in Composition of Stratosphere, Toronto, June 26-30, 1978.

Mendonca, B. G., K. J. Hanson, and J. J. DeLuisi. Secular trends in clear sky transmissions at Mauna Loa Observatory--peturbations in stratospheric aerosols. Third Conf. on Atmos. Rad., June 28-30, 1978, Davis, Calif. Preprint, A.M.S., Boston, Mass., 330-332, June 1978.

Mendonca, B. G., K. J. Hanson, and J. J. DeLuisi. Volcanically related secular trends in atmospheric transmission at Mauna Loa Observatory, Hawaii. Science 202:513-515, Nov. 1978.

Miller, J. M. The complexity of the wind patterns at Mauna Loa. In Mauna Loa Observatory--a 20th Anniversary Report, J. M. Miller (ed.), 122-128, Sep. 1978.

Miller, J. M. (ed.). Mauna Loa Observatory--a 20th Anniversary Report. NOAA/ARL, 158 pp., Sep. 1978.

Miller, J. M., and J. F. S. Chin. Short-term disturbances in the carbon dioxide record at Mauna Loa Observatory. Geophys. Res. Lett. 5(8):669-671, Aug. 1978.

Miller, J. M., and A. M. Yoshinaga. Use of a standard raingage as a precipitation chemistry collector (comments on "The effect of some meteorological parameters on the chemical composition of precipitation at the University Field Station, Trinidad, West Indies"). J. Appl. Meteorol. 17(11):1747-1748, Nov. 1978.

Miller, J. M., J. N. Galloway, and G. E. Likens. Origin of air masses producing acid precipitation at Ithaca, New York: A preliminary report. Geophys. Res. Lett. 5(9):757-760, Sep. 1978.

Peterson, J. T. (ed.). Geophysical Monitoring for Climatic Change, No. 6, Summary Report 1977. NOAA/ARL, 145 pp., Dec. 1978.

Peterson, J. T., and T. L. Stoffel. Urban-rural solar irradiance measurements at St. Louis. Third Conf. on Atmos. Rad., June 28-30, 1978, Davis, Calif. Preprint, A.M.S., Boston, Mass., 319-321, June 1978.

Peterson, J. T., E. C. Flowers, and J. H. Rudisill III. Atmospheric turbidity across the Los Angeles Basin. J. Appl. Meteorol. 17(4):428-435, Apr. 1978.

Peterson, J. T., E. C. Flowers, and J. H. Rudisill III. Urban-rural solar radiation and atmospheric turbidity measurements in the Los Angeles Basin. J. Appl. Meteorol. 17(11):1595-1609, Nov. 1978.

8. REFERENCES

Angell, J. K., and J. Korshover, 1978. Global ozone variations: An update into 1976. Mon. Weather Rev. 106:725-737.

Bigg, E. K., 1977. Some properties of the aerosol at Mauna Loa Observatory. J. Appl. Meteorol. 16:262-267.

Bodhaine, B., 1979. Aerosol monitoring at Barrow, Mauna Loa, American Samoa, and the South Pole: Instrumentation and results. Proc. WMO Tech. Conf. on Reg. and Global Obs. of Atmos. Pollut. Relative to Clim., Aug. 20-24, 1979, Boulder, Colo. (To be printed by WMO, Geneva, Switzerland.)

Brewer, P. B., 1975. Minor elements in sea water. In Chemical Oceanography, 2nd ed., vol. 1, Academic Press, New York, N. Y., 415-496.

Cobb, W. E., 1967. Evidence of a solar influence on the atmospheric electric elements at Mauna Loa Observatory. Mon. Weather Rev. 95(12):905-911.

Craig, R. A., 1976. Umkehr measurements at Tallahassee. J. Appl. Meteorol. 15:509-513.

Cunnold, D., F. Alyea, and R. Prinn, 1978. A methodology for determining the atmospheric lifetime of fluorocarbon. J. Geophys. Res. 83(C11):5493.

Dave, J. V., and P. M. Furukawa, 1966. Scattered radiation in the ozone absorption bands at selected levels of a terrestrial, Rayleigh atmosphere. Meteorol. Monogr., vol. 7, A. M. S., Boston, Mass., 353 pp.

Davies, J. A., and T. C. Ugoegbulam, 1979. Parameterization of surface incoming radiation in tropical cloudy conditions. Atmos.-Ocean 17(1):14-23.

Dixon, W. J., and F. J. Massey, Jr., 1957. Introduction to Statistical Analysis, 2nd ed., McGraw-Hill Book Co., New York, N. Y.

Duce, R. A., G. L. Hoffman, and W. H. Zoller, 1975. Atmospheric trace metals at remote Northern and Southern Hemisphere sites: pollution or natural? Science 187:59-61.

Ellis, H. T., and R. F. Pueschel, 1971. Solar radiation: Absence of air pollution trends at Mauna Loa. Science 172:845.

Feely, H. W., H. L. Volchok, E. P. Hardy, Jr., and L. E. Toonkel, 1978. Worldwide deposition of ^{90}Sr through 1976. Environ. Sci. Tech. 12:808-809.

Fegley, R. W., 1978. NOAA Air Resources Laboratories: Stratospheric lidar project, 1976 results. NOAA Tech. Rep. ERL 400-ARL 6, 9 pp., Sep. 1978.

Fegley, R. W., and C. M. Penney, 1978. An attempt to measure atmospheric ozone with ultraviolet lidar. NOAA Tech. Memo. ERL ARL-75, 20 pp., Dec. 1978.

Fegley, R. W., E. W. Barrett, and H. T. Ellis, 1978. Lidar measurements at Mauna Loa Observatory. In Mauna Loa Observatory--a 20th Anniversary Report, J. M. Miller (ed.), NOAA/ARL, U.S. Dept. Comm., Rockville, Md., 59-65.

Fegley, R. W., H. T. Ellis, and J. L. Heffter, 1979. Volcanic contributions to the stratosphere. (Accepted by J. Appl. Meteorol.)

Flowers, E. C., R. A. McCormick, and K. R. Kurfis, 1969. Atmospheric turbidity over the United States, 1961-1966. J. Appl. Meteorol. 8:955-962.

Fröhlich, C., and G. E. Shaw, 1978. Determination of Rayleigh optical depth. Pub. no. 557, World Radiation Center, Davos Dorf., Switzerland.

Goldberg, B., and W. H. Klein, 1978. A simplified model for determining the spectral quality of daylight and the availability of solar energy at any location. Proc. Int. Solar Energy Soc. Congress, New Delhi, India, Jan. 1978, 353-357.

Hogan, A. W., 1978. Atmospheric aerosol measurements. In GMCC Summary Report 1977, No. 6, J. T. Peterson (ed.), NOAA/ARL, U.S. Dept. Comm., Boulder, Colo., 109-112.

Hoyt, D. V., 1978. Variations in the solar constant caused by changes in the active features on the sun. Presented at Symp./Workshop, Solar Terrestrial Influences on Weather and Climate, Ohio State Univ., Columbus, Ohio, July 24-28.

Hoyt, D. V., 1979a. The Smithsonian Astrophysical Observatory Solar Constant Program. Rev. Geophys. Space Phys. 17(3):427-458.

Hoyt, D. V., 1979b. Pyrheliometric and circumsolar sky radiation measurements by the Smithsonian Astrophysical Observatory from 1923 to 1954. Tellus 31(3):217-229.

Hoyt, D. V., 1979c. Variations in sunspot structure and climate. Clim. Change 2:79-92.

Hoyt, D. V., C. P. Turner, and R. D. Evans, 1979. Atmospheric transmission at three locations in the United States from 1940 to 1977. (Submitted to Mon. Weather Rev.)

Hunt, W. F., 1972. The precision associated with the sampling frequency of log-normally distributed air pollution measurement. J. Air Pollut. Control Assoc. 22:687-691.

Klein, W. H., and B. Goldberg, 1978a. Solar radiation measurements 1976-1977. Smithsonian Rad. Biol. Lab., Rockville, Md., 56.

Klein, W. H., and B. Goldberg, 1978b. Monitoring UVB spectral irradiances at three latitudes. Proc. Int. Solar Energy Soc. Congress, New Delhi, India, Jan. 1978, 400-414.

Maenhaut, W., and W. H. Zoller, 1977. Determination of the chemical composition of the South Pole aerosol by instrumental neutron activation analysis. J. Radioanal. Chem. 37:637-650.

Maenhaut, W., W. H. Zoller, R. A. Duce, and J. L. Hoffman, 1979a. Concentration and size distribution of particulate trace elements in the South Polar atmosphere. J. Geophys. Res. 84:2421-2431.

Maenhaut, W., W. H. Zoller, and D. G. Coles, 1979b. Radionuclides in the South Pole atmosphere. (Accepted by J. Geophys. Res.)

Mastenbrook, H. J., 1968. Water vapor distribution in the stratosphere and high troposphere. J. Atmos. Sci. 25:299-311.

Mastenbrook, H. J., 1971. The variability of water vapor in the stratosphere. J. Atmos. Sci. 28:1495-1501.

Mastenbrook, H. J., 1973. Water vapor measurements in the lower stratosphere. Can. J. Chem. 52:1527-1530.

Mateer, C. L., 1965. On the information content of Umkehr observations. J. Atmos. Sci. 22:370-381.

Mendonca, B. G., K. J. Hanson, and J. J. DeLuisi, 1978. Volcanically related secular trends in atmospheric transmissions at Mauna Lau Observatory, Hawaii. Science 202(4367):513-515.

Miller, J. M. (ed.), 1975. Geophysical Monitoring for Climatic Change, No. 3, Summary Report 1974. NOAA/ARL, U.S. Dept. Comm., Boulder, Colo., 107 pp.

NWS, 1978. Local Climatological Data, 1978. NOAA, Nat. Climate Center, Asheville, N.C.

Oltmans, S. J., and W. D. Komhyr, 1976. Surface ozone in Antarctica. J. Geophys. Res. 81:5359-5364.

Pearman, G. I., 1977. Further studies of the comparability of baseline atmospheric carbon dioxide measurements. Tellus 29:171-181.

Peterson, J. T. (ed.), 1978. Geophysical Monitoring for Climatic Change, No. 6, Summary Report 1977. NOAA/ARL, U.S. Dept. Comm., Boulder, Colo., 145 pp.

Peterson, J. T., and V. Kovalyev, 1979. Cooperative U.S.A.-U.S.S.R. atmospheric transparency measurements. Bull. Amer. Meteorol. Soc. 60(9):1084-1085.

Peterson, J. T., and K. H. Hanson, 1978. Report on Mt. Kenya Feasibility Study. Unpublished manuscript, 21 pp.

Peterson, J. T., and T. L. Stoffel, 1979. Urban-rural solar radiation measurements in St. Louis, Missouri. NOAA Tech. Memo. ERL ARL-76, 51 pp.

Rahn, K., R. Borys, and G. E. Shaw, 1977. The Asian source of Arctic haze bands. Nature 268:713-715.

Rahn, K., and G. E. Shaw, 1978. Briefing on Arctic haze and the Arctic aerosol. Presented to Bur. of Oceans and Int. Environ. and Sci. Affairs, Dept. of State, Washington, D.C., Nov. 20, 1978.

Sadler, J. C., 1968. Average cloudiness in the tropics from satellite observations. East-West Centre Press, London, England.

Seiler, W., 1976. Carbon monoxide measurements. In GMCC Summary Report 1975, No. 4, J. A. Watkins (ed.), NOAA/ARL, U.S. Dept. Comm., Boulder, Colo., 100-105.

Shaw, G. E., J. A. Reagan, and B. M. Herman, 1973. Investigations of atmospheric extinction using direct solar radiation measurements made with a multiple wavelength photometer. J. Appl. Meteorol. 12:374-380.

Stuiver, M., 1978. Atmospheric carbon dioxide and carbon reservoir changes. Science 199:253-258.

Taylor, S. R., 1964. Abundance of chemical elements in the continental crust: A new table. Geochim. Cosmochim. Acta 28:1273.

Thompson, L. G., W. L. Hamilton, and C. Bull, 1975. Climatological implications of microparticle concentrations in the ice core from "Byrd Station," Western Australia. J. Glaciol. 14(72):433-444.

Volz, F. E., 1978. Atmospheric turbidity in Europe, 1963-1969. Environ. Res. Paper No. 631, Air Force Geophys. Lab., Hanscom AFB, Mass., 53 pp.

Wendt, J., J. Kowolski, A. M. Bass, C. Ellis, and M. Patapoff, 1979. Interagency comparison of ultraviolet photometric standards for measuring ozone cencentrations. NBS Spec. Pub., 22 pp.

Westwater, E. R., and O. N. Strand, 1968. Statistical information content of radiation measurements used in indirect sensing. J. Atmos. Sci. 25:750-758.

Zoller, W. H., E. S. Gladney, and R. A. Duce, 1974. Atmospheric concentration and sources of trace metals at the South Pole. Science 183:198-200.

9. GMCC STAFF

Director's Office

*Kirby J. Hanson, Director
*Bernard G. Mendonca, Deputy Director
Helen C. Cook, Secretary
Dale A. Gillette, CIRES
*John E. Hay, CIRES
*Jerome K. Nimira, CIRES
*Graeme I. Pearman, CIRES
Constance Shilvock, Jr. Fellow

Acquisition and Data Management Group

*Gary A. Herbert, Chief
Arija Bottomley, Clerk
Connie Carla, Secretary
*Joyce M. Harris, Computer Programmer
Lee Johnson, Computer Programmer
Milton S. Johnson, Electronic Technician
James Jordan, Electronic Engineer
Steven Waas, Jr. Fellow

Monitoring Trace Gases Group

*Walter D. Komhyr, Chief
Connie Carla, Secretary
*Robert D. Grass, Physicist
*Thomas B. Harris, Meteorological Technician
*Samuel Oltmans, Physicist
Frank Polacek III, Meteorological Technician
Thayne Thompson, Physicist
*Lee Waterman, Chemist
*Ellsworth Dutton, CIRES
Robert Evans, CIRES
Valentine Szwarc, CIRES
*William Taylor, CIRES

Aerosols and Radiation Monitoring Group

*John J. DeLuisi, Chief
*Barry A. Bodhaine, Meteorologist
*Ronald W. Fegley, Physicist
Gail M. Phillips, Secretary

Analysis and Interpretation Group

*James T. Peterson, Chief
*Douglas V. Hoyt, Physicist
Gail M. Phillips, Secretary
Cheryl Reynolds, Jr. Fellow
Thomas Stoffel, CIRES

Mauna Loa Observatory

*Kinsell L. Coulson, Director
*John F. S. Chin, Physicist
*Richard S. Cram, Meteorologist
*Howard Ellis, Physicist
*Duane Harding, Meteorologist
Judith B. Pereira, Secretary
Mamoru Shibata, Electronic Technician
*Alan M. Yoshinaga, Analytical Chemist

Barrow Observatory

*Thomas DeFoor, Lt. NOAA Corps, Station Chief
Bradley C. Halter, Electronic Technician
Steven Hill, Electronic Technician

Samoa Observatory

*Donald W. Nelson, Station Chief
Roger A. C. Williams, Electronic Technician

South Pole Observatory

*John Osborn, Lt. NOAA Corps, Station Chief
Larry Smith, Electronic Technician

---

*Contributors to Summary Report

☆ U.S. GOVERNMENT PRINTING OFFICE 1981 — 777-002/1243 Region No. 8